

RADIATION-INDUCED BYSTANDER EFFECTS IN HT-29 CELL CULTURE

By

Jennifer Bain Pafford

Thesis

Submitted to the Faculty of the
Graduate School of Vanderbilt University
in partial fulfillment of the requirements
for the degree of

MASTER OF SCIENCE

in

Physics

August, 2012

Nashville, Tennessee

Approved:

Professor Michael G. Stabin

Professor Michael L. Freeman

ACKNOWLEDGEMENTS

This work was financially supported through an education fellowship granted by the U.S. Nuclear Regulatory Commission. I would first like to acknowledge Dr. Michael Stabin, my mentor over the past four years—who saw potential in me as a lowly undergraduate student and who set a world of opportunity at my doorstep. I am greatly indebted to Dr. Michael Freeman for opening his laboratory to me and to all those working within it. Of these people, I would most like to recognize Dr. Michelle Schultz who taught me what it was to be a researcher and a scientist.

TABLE OF CONTENTS

	Page
ACKNOWLEDGEMENTS	ii
LIST OF TABLES	v
LIST OF FIGURES	vi
Chapter	
I. INTRODUCTION	1
II. LITERATURE REVIEW	4
Early medical applications and biological effects of radiation	4
Interactions of radiation with matter	8
Actions of radiation on living cells	13
Cell structure and function	16
DNA strand breaks and chromosomal aberrations	21
DNA damage and repair	26
Programmed cell death	28
Cell signaling pathways	37
Non-targeted effects of exposure to ionizing radiation	44
Mechanisms of the bystander effect	47
Expression of radiation-induced effects in biological systems	55
III. METHODS AND MATERIALS	60
Mammalian cell culture	62
<i>In vitro</i> cell survival curve	66
HT-29 cell survival curve	70
MARK I ¹³⁷ Cs irradiator	72
¹³⁷ Cs irradiator dose profile	75
Microtetrazolium (MTT) assay	78
MTT assay optimization	81
Caspase-3/7 assay	82
Positive control with staurosporine treatment	85
Caspase-3/7 assay optimization	86
Effects of radiation dose and dose rate on bystander response	87
Cell culture	87
Irradiation	89
Medium transfer	91

MTT assay	94
Caspase-3/7 assay	96
Effect of time post-irradiation of medium transfer	99
IV. RESULTS AND DISCUSSION	100
Methods of data analysis	100
Effects of radiation dose and dose rate on bystander response	100
Caspase-3/7 activation.....	105
Effect of time post-irradiation of medium transfer	109
Further research.....	111
V. CONCLUSIONS.....	113
REFERENCES	114

LIST OF TABLES

Table	Page
1. Experimental questions to define radiation-induced bystander effects	45
2. Ionization chamber measurements of ¹³⁷ Cs irradiator.....	77
3. Caspase-3/7 reagent concentration optimization.....	87
4. Dose effect study irradiation parameters.....	90
5. Dose rate effect study irradiation parameters.....	91

LIST OF FIGURES

Figure	Page
1. Pierre Curie's radium skin burn	6
2. Characteristic x-ray and Auger electron emission	9
3. Summary of x and γ -ray interactions	13
4. Direct and indirect actions of ionizing radiation	14
5. DNA structure	17
6. The eukaryotic cell cycle.....	18
7. Acquired capabilities of cancer cells.....	19
8. Single and double strand DNA breaks	21
9. Formation of a dicentric by irradiation of pre-replication chromosomes	23
10. Formation of a ring by irradiation of pre-replication chromosomes	24
11. Formation of anaphase bridge by irradiation of post-replication chromosomes.....	25
12. DNA repair pathways.....	27
13. Electron micrograph of apoptotic cell	31
14. Caspase activation pathways	32
15. p53-activating signals and downstream effects.....	34
16. Electron micrograph of mitochondria	36
17. Cell communication through electrical and chemical signaling mechanisms.....	38
18. Summary of the major cell signaling pathways	40
19. Summary of the major components in Ca ²⁺ signaling system	41
20. Mitogen-activated protein kinase (MAPK) signaling pathways	43

21.	Catalytic activity of COX-2 enzyme	49
22.	Proposed pathway for cell death–mediated tumor cell repopulation	50
23.	PGE2 synthesis.....	51
24.	Current unifying model of radiation-induced bystander signaling pathways	54
25.	Schematic of possible outcomes for irradiated or damaged cells	56
26.	Different possible extrapolations for cancer risk	58
27.	Morphology of HT-29 cells as viewed under a light microscope	64
28.	Shape of mammalian cell survival curve	70
29.	Survival curve of HT-29 cells exposed to ¹³⁷ Cs γ radiation.....	72
30.	Shepherd MARK I model 68 ¹³⁷ Cs irradiator	73
31.	Diagram of Shepherd MARK I model 68 ¹³⁷ Cs irradiator	75
32.	Ionization chamber setup for ¹³⁷ Cs dose profile measurement	76
33.	Dose profile of ¹³⁷ Cs irradiator.....	78
34.	Chemical metabolization of MTT to a formazan salt by viable cells	80
35.	MTT assay optimization.....	82
36.	CellEvent caspase-3/7 green detection reagent expression in cells	84
37.	Fluorescent excitation and emission spectra of caspase-3/7 reagent	84
38.	Staurosporine solubilization with DMSO	85
39.	Plated cells in incubator	88
40.	Experimental setup of dose rate irradiation.....	91
41.	Medium transfer workflow.....	92
42.	Experimental setup of medium transfer	93
43.	Millex-HV syringe filter.....	94

44.	MTT assay workflow	95
45.	BioTek Synergy HT multi-Mode microplate reader	96
46.	Caspase-3/7 assay workflow	97
47.	Olympus IX51 inverted fluorescence microscope	98
48.	Effect of dose on metabolic activity of HT-29 responder cells.....	101
49.	Effect of dose rate on metabolic activity of HT-29 responder cells.....	102
50.	Fluorescence analysis with ImageJ software.....	106
51.	Effect of dose on caspase-3/7 activation in HT-29 responder cells	107
52.	Effect of dose rate on caspase-3/7 activation in HT-29 responder cells	107
53.	Effect of time post-irradiation of medium transfer	110
54.	PGE2 assay principle.....	112
55.	PGE2 assay protocol	112

CHAPTER 1

INTRODUCTION

The study of radiation effects on biological systems is fundamental to the understanding and practice of health physics. Much has been established in the field of radiobiology since the discovery of radiation little more than a century ago. However, recent experimental evidence challenges the central radiobiological paradigm that the effects of radiation on a biological system occur as a direct consequence of energy deposition and damage in deoxyribonucleic acid (DNA)⁵³.

Exposure to ionizing radiation has been experimentally shown to induce an active cellular response in irradiated cells, resulting in the secretion of one or more signaling factors into the surrounding growth medium⁵. These medium-borne signals may initiate bystander responses in nearby unirradiated cells and, ultimately, alter normal cellular function in these non-targeted responder cells. The bystander effect can be stimulatory or inhibitory in nature, causing the unirradiated cell population to express increased or decreased cell proliferation rates, respectively¹⁰⁸.

National and international committees currently use a linear no-threshold (LNT) model for the estimation of health risks to exposure of ionizing radiation—stating that biological risk follows a linear relationship to radiation dose for any value of dose, no matter how small. However, bystander effects have demonstrated that cells need not even be directly irradiated in order to exhibit genomic instability—thus calling for a fundamental change in the underlying theories concerning the biological effects and

associated health risks of radiation exposure. Bystander effects have the theoretical potential to dramatically influence the shape of the dose–response curve for radiation induced carcinogenic risk, and a move away from the belief that DNA damage is the sole target of ionizing radiation would have considerable implications on radiation protection practices.

The purpose of this study is to investigate the non-targeted bystander effects in HT-29 human adenocarcinoma cells with an emphasis on their potential significance relative to current perceptions regarding the nature of biological effects of radiation exposure and the resulting health implications. Previous studies have shown that caspase 3-mediated iPLA2 activation led to increased production of arachidonic acid—whose downstream eicosanoid derivatives, such as prostaglandin E2 (PGE2), had been implicated in stimulating tumor growth¹. In one medium transfer study, Mothersill et al. reported the production of a signal by irradiated cells capable of initiating apoptosis in non-targeted bystander cell populations—indicating that apoptosis is a major mechanism of cell death due to ICCM exposure⁵⁷. Based on these findings, one aim of the current study is to examine the hypothesis that irradiated cells produce signals which are released in the medium and, subsequently, activate caspase 3 in responder cell populations—being responsible for the observance of either inhibitory or stimulatory bystander effects.

It has also been shown that alterations to cyclooxygenase-2 (COX-2) expression and the presence and concentration of its enzymatic product PGE2 are influential in the development of colorectal cancer⁸⁰. COX enzymes are utilized in the biosynthesis of prostaglandins from arachidonic acid, and earlier reports have indicated that the COX-2 signaling cascade plays a significant role in the bystander process⁷⁶. Therefore, this study

seeks to investigate the relationship between PGE2 expression and the magnitude of the elicited bystander response to determine if the COX pathway is a critical signaling link utilized in the observed bystander phenomenon induced by exposure of HT-29 cells to irradiated cell conditioned medium.

The concept of bystander effects was first proven in 1992 to be a legitimate tenet of radiobiology⁶, and while the existence of such phenomenon is incontrovertible, an understanding of the intrinsic nature of the phenomenon and its overall influence on the response of living tissues to exposure to ionizing radiation remains largely unclear. The vast majority of publications to date have reported primarily on phenomenological observations while failing to identify the underlying mechanisms at work. Thus, the current work aims to shed more light on the bystander responses elicited in HT-29 cells and to further characterize the fundamental nature of this phenomenon.

CHAPTER II

LITERATURE REVIEW

Early Medical Applications and Biological Effects of Radiation

Within a few months after Roentgen announced his discovery of x-rays in November 1895, ionizing radiation was reportedly being used in medical applications. In these early studies, experimenters observed that the passage of x-rays through living tissue induced biological changes within the subject. Initially, the low energy x-rays appeared to have a beneficial effect on many skin diseases—causing open cancers to shrink, sores to dry up, and providing relief to arthritis sufferers³¹. However, it was not long before the deleterious effects of ionizing radiation on biological systems were realized.

In February of 1896, the first diagnostic medical x-ray was reported in the *Lancet* after being used to locate a piece of a knife that had been dislodged in a sailor's back. After obtaining the x-ray images, the fragment was able to be located and removed—alleviating the sailor of paralysis. Later that year, in December of 1896, Leopold Freund, provided the world's first scientific proof of the biological effectiveness of x-rays by performing a successful fractionated radiation treatment on a young girl suffering from a large hairy nevus³.

During the first year after Roentgen's discovery, nearly 50 books and 1,000 papers had been published on x-rays³³. While many studies reported successful use of radiation in medical applications, there were also reports of deleterious effects. In one of

the first published accounts regarding the physiological effects of radiation³², John Daniel, a physicist at Vanderbilt University, described what he called the most interesting observation of his experiments with x-rays--epilation.

A month ago we were asked to undertake the location of a bullet in the head of a child that had been accidentally shot. On the 29th of February Dr. Wm. L. Dudley and I decided to make a preliminary test of photographing through the head with our rather weak apparatus before undertaking the surgical case. Accordingly Dr. Dudley, with his characteristic devotion to the cause of science, lent himself to the experiment. A plateholder containing the sensitive plate was tied to one side of his head, with a coin between the plate and his head, and the tube was set playing on the opposite side of his head. The tube was about one-half inch distant from his hair, and the exposure was one hour. The plate developed nothing; but yesterday, 21 days after the experiment, all the hair came out over the space under the X-ray discharge. The spot is now perfectly bald, being two inches in diameter. This is the size of the X-ray field close to this tube. We, and especially Dr. Dudley, shall watch with interest the ultimate effect.

Soon after Henri Becquerel's discovery of radioactivity in February 1896, experimentation began utilizing radioactive elements such as radium. Just as it had been observed with x-rays, the biological effects induced by radioactive substances on the human body were realized for both their possible harm and beneficial potential. Among the earliest recorded accounts of biological effects induced by exposure to radioactive substances were those reported independently by German scientists Friedrich Walkoff and Friedrich Giesel. Two years after the discovery of radium, Giesel conducted a self-exposure experiment to test its physiological effects on the human body. In his study published in October of 1900, he records strapping 270 mg of radium salt to his inner forearm for two hours. In the same year, Walkoff presented a general review to a photography club in Munich which contained only a few sentences in reference to his own encounter with radium.

Furthermore, radium owns astonishing physiologic properties. An exposure of the arm to two 20-minute sessions has produced an inflammation of the skin which

has now lasted already for two weeks, and exhibits the same aspect as that obtained after a long exposure to X-rays.

Further investigations into the biological effects of radium were carried out by Henri Becquerel and Pierre Curie and, in 1901, they published their results in an article titled, *Action Physiologiques des Rayons du Radium* [*Physiological Action of Radium Rays*]*—*the most extensive and detailed early report of the effects of radiation on the human body. The article begins with a summary of Giesel's experiment followed by the personal accounts of Curie and Becquerel. Although not published under her name, Marie Curie also conducted her own self-exposure experiment with radium, and her results were included in the paper. Each one reported varying degrees of erythema, inflammation, ulceration, and necrosis of the skin and concluded that the evolution of a radiation-induced lesion is dependent on the intensity of the radiation and the duration of exposure.

116 THE PHYSIOLOGICAL ACTION OF RADIO-ACTIVE SUBSTANCES

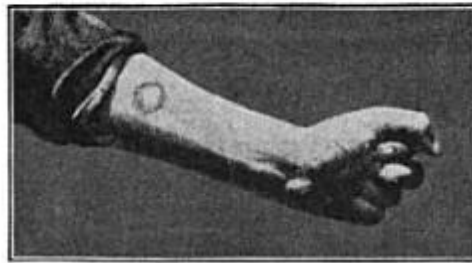


Fig. 51.

Professor Curie's arm, showing a scar resulting from a radium sore. (Through the courtesy of the Success Company.)

Figure 1^a. Pierre Curie's radium skin burn resulting from self-exposure experiment

^a Reprinted from Baskerville. ¹⁰¹. Radium and Radio-active Substances (1905).

Marie Curie later reflected on these early experiments in her biography of husband Pierre Curie.

In order to test the results that had just been announced by F. Giesel, Pierre Curie voluntarily exposed his arm to the action of radium during several hours. This resulted in a lesion resembling a burn that developed progressively and required several months to heal. Henri Becquerel had by accident a similar burn as a result of carrying in his vest pocket a glass tube containing radium salt. He came to tell us of this evil effect of radium, exclaiming in a manner at once delighted and annoyed: "I love it, but I owe it a grudge."

The medical use of radioactive elements developed much more slowly than that of external radiation sources—most likely due the limited world supply of such substances.

In 1901, Henri Alexandre Danlos and Eugene Bloch conducted the first medical application of radium by placing it in contact with a tuberculous skin lesion⁴². It was only a few years later, in 1903, before a more invasive technique of treating cancer by inserting sources of radium directly inside a tumor was suggested⁴².

Over time, it became evident that the newly discovered form of energy—ionizing radiation—could have profoundly detrimental effects on biological systems. In his presidential address to the British Association for the Advancement of Science in September of 1896, Sir Joseph Lister voiced his concern regarding the effects of radiation on biological systems³³.

It is found that if the skin is long exposed to their action it becomes very much irritated, affected with a sort of aggravated sunburn. This suggests the idea that a transmission of the rays through the human body may be not altogether a matter of indifference to internal organs.

The new technology had been, undoubtedly, hastily exploited for use in biological experiments and medical applications before a fundamental understanding of the phenomenon was acquired. In addition, after its initial discovery, a large majority of studies were conducted by people who were not scientists—most were, in some way or

another, tied to the medical field. These situations began to reflect the need for informed and standardized radiation protection practices, which Tesla addressed in his 1897 paper *On the Hurtful Actions of the Lenard and Roentgen Tubes*⁴¹.

In scientific laboratories the instruments are usually in the hands of persons skilled in their manipulation and capable of approximately estimating the magnitude of the effects, and the omission of necessary precautions is, in the present state of our knowledge, not so much to be apprehended; but the physicians, who are keenly appreciating the immense benefits derived from the proper application of the new principle, and the numerous amateurs who are fascinated by the beauty of the novel manifestations, who are all passionately bent upon experimentation in the newly opened up fields, but many of whom are naturally not armed with the special knowledge of the electrician—all of these are much in need of reliable information from experts.

Much can be said for the considerable advancements that were made in the radiation sciences during their infancy, not only in the realm of scientific research but also in its clinical application—with the twentieth century witnessing marked improvements in diagnostic medicine and the sophistication of therapies used for the cure and maintenance of patients suffering from a wide array of maladies. Though, the nature of a biological system's response to ionizing radiation exposure is, especially at the cellular level, a complex phenomenon that is still, over a century later, not completely understood—reminding us there is much we have left to learn and much we have learned that is left to review.

Interactions of Radiation with Matter

All matter is composed of atoms. The stability of an atom and, consequently, its electron configuration is determined by the number and configuration of protons and neutrons within the nucleus. The chemical properties of an atom are determined by the number and distribution of electrons within the orbital shells.

An atom emits radiation to release any extra energy it may possess following decay or some other nuclear event. In nuclear de-excitation, the jumps that release energy are made by protons or neutrons in the nucleus as they move from a higher energy level to a lower level. The photons emitted in the process are called gamma rays, which have very high energy relative to the energy of visible light. As an alternative to gamma decay, an excited nucleus in some cases may return to its ground state by giving up its excitation energy to one of the atomic electrons around it. This process is a kind of photoelectric effect in which a nuclear photon is absorbed by an atomic electron. The emitted electron has a kinetic energy equal to the lost nuclear excitation energy minus the binding energy of the electron in the atom.

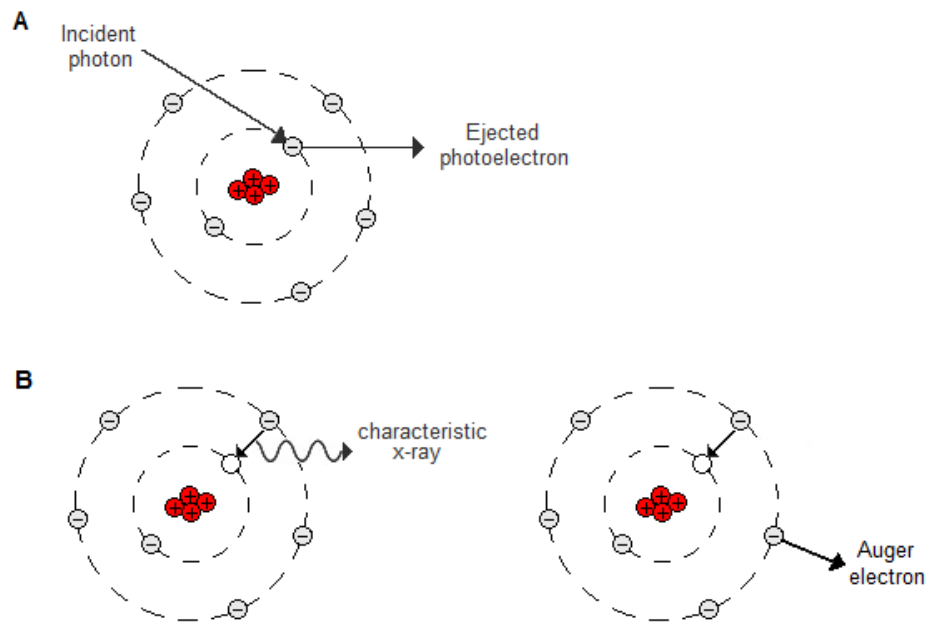


Figure 2. Characteristic x-ray and Auger electron emission

An atom's nuclear stability is dependent upon its ratio of neutrons to protons. If this ratio is too low or too high, the nucleus will eventually rearrange itself into a more stable configuration. Nuclei that tend to be least stable contain an odd number of protons and neutrons. In stable elements with a low atomic number Z , the number of neutrons is about equal to the number of protons. However as the number of protons increase, the number of neutrons also increase but at a more rapid and disproportionate rate. Nuclei that contain too many or too few neutrons are, therefore, unstable and undergo radioactive decay. Radioactive decay processes can be classified as three different types of transitions: alpha, isobaric, and isomeric. Isobaric transitions include beta emission, positron emission and electron capture. Isomeric transitions include excited state, metastable state and internal conversion processes.

All types of radiation interact with the environment in which they are released and, consequently, transfer energy to that medium. Electromagnetic radiation transports energy through space as a combination of electric and magnetic fields, behaving as both a wave and particle. The wave-particle duality of light was indirectly demonstrated by Thomas Young in 1801 with his double-slit experiment, and explained in 1905, when Albert Einstein published a paper on the photoelectric effect—in which he formulated the theory of light quanta, or photons. According to the wave theory, electromagnetic waves leave a source with their energy spread out continuously through the wave pattern. According to the quantum theory, they consist of individual photons, each small enough to be absorbed by a single electron⁷. In effect, electromagnetic radiation travels as a wave but interacts as a particle.

When an electron is ejected from an atom, the atom is left in an ionized state. Radiation of energy less than 13.6 eV is ‘nonionizing’ radiation because it cannot eject the hydrogen k-shell electron—which is the element with the smallest atomic number and, thereby, contains the most easily removed electron. If electrons are not ejected from the atom but, instead, are raised to a higher energy state through electron shell transitions, the atom is said to be in an ‘excited’ state.

Radiation interacts with matter through the transfer of energy to its surroundings. Ionizing radiation is emitted with a certain energy and with or without a charge. Charged particles such as electrons, protons, and atomic nuclei are forms of directly ionizing radiation because they can eject electrons and disrupt the atomic structure through which they pass directly causing chemical and biological changes. Uncharged electromagnetic radiations such as photons—x and γ -rays—and neutrons are said to be indirectly ionizing as they can set charged particles into motion but cannot, themselves, produce significant ionization.

When a photon impinges upon a material, there are three possible outcomes—absorption, scatter and traversal. Absorption occurs when the photon transfers its energy to the atoms in the target material through one or more interactions. Upon interaction, the incident photon may also be scattered off at an angle resulting in partial energy transfer to the material—as the scattered photon carries off the remaining energy along its redirected path. The photon may also pass through the material unscathed and without any atomic interactions along its path.

The manner in which x and γ -rays are absorbed depends upon the energy of the incident photon and the chemical composition of the absorber. There are a few possible

interaction processes—coherent (Rayleigh) scattering, photoelectric absorption, Compton (incoherent) scattering, pair production and photodisintegration. Coherent scattering is a relatively unimportant interaction mechanism as incident photons are deflected or scattered with negligible loss of energy. Consequently, little energy is deposited in the attenuating medium. Photoelectric absorption occurs when an incident photon is completely absorbed by an inner shell electron of an atom resulting in the ejection of a photoelectron followed by emission of either a characteristic x-ray or Auger electron. X and γ -rays with energies between 30 keV and 30 MeV interact in soft tissue predominantly by means of Compton scattering. During a Compton interaction, an incident photon interacts with a loosely bound electron in the attenuating medium and transfers part of its energy, resulting in the emission of a scattered photon and recoil Compton electron.

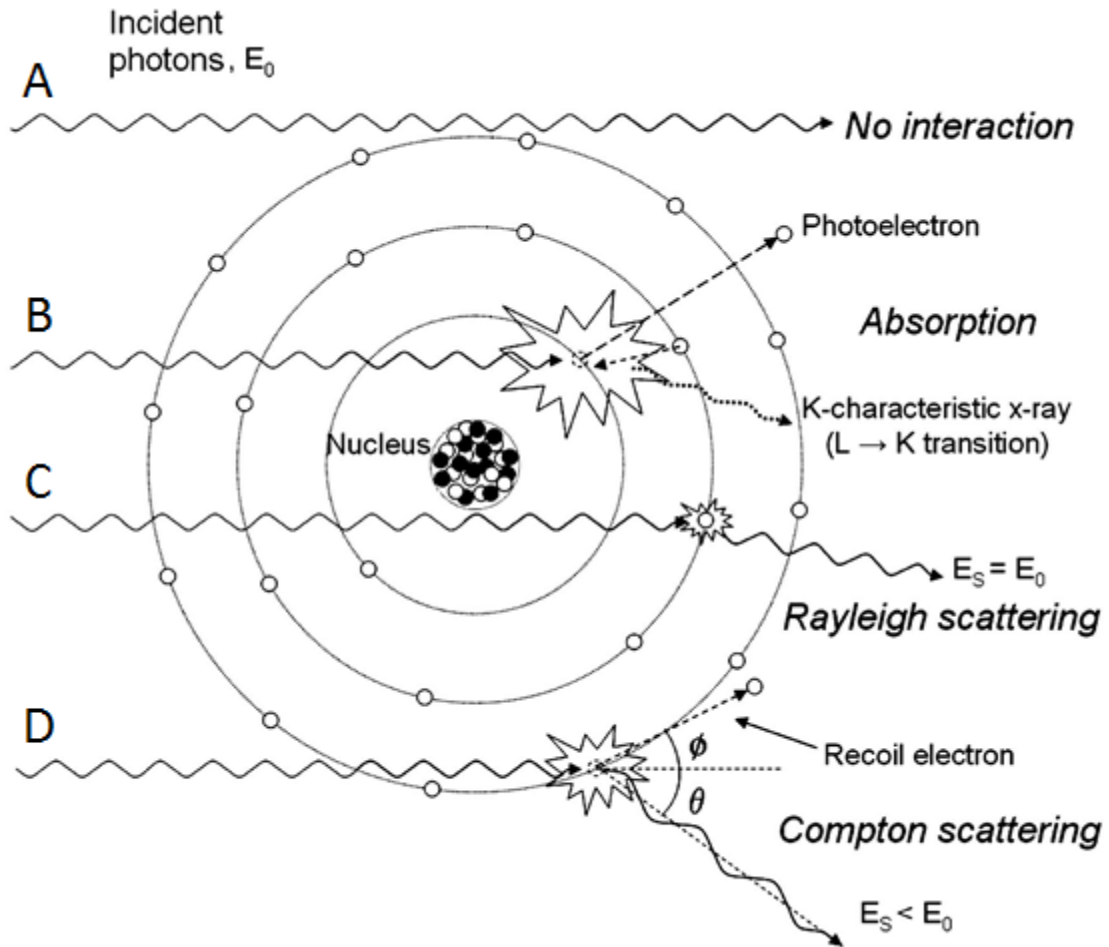


Figure 3^a. Summary of x and γ ray interactions

^a Reprinted from Seibert. ¹⁰⁹. X-ray imaging physics. *J Nucl Med Technol* (2005).

Actions of Radiation on Living Cells

The energy deposition of ionizing radiation into biological targets is defined as occurring by a direct or indirect action—not to be confused with directly and indirectly ionizing radiation. Direct action occurs when the radiation physically impinges upon the target, causing damage directly. In contrast, indirect action occurs when the radiation acts not upon the target itself but with other molecules and atoms in the cell to produce free

radicals—initiating a chain of events that ultimately leads to causing an effect within the target.

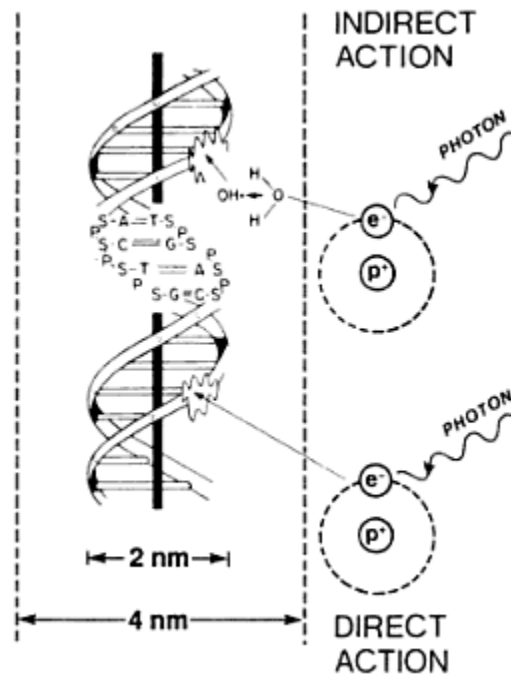


Figure 4^a. Direct and indirect actions of ionizing radiation

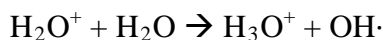
^a Reprinted from Hall. ³. Radiobiology for the Radiologist (2006).

Radiation chemistry concerns the chemical effects of radiation on matter. A large majority of these concerns, and the most relevant for this discussion, is the effect of ionizing radiation within water. This process creates several resulting molecules—radicals and reactive oxygen species—that are of a detrimental effect for biological targets such as DNA. This is accomplished via an indirect action, as the ionizing radiation doesn't directly damage the DNA itself. Because 80% of a cell is composed of water³, there exists a large probability that the majority of radiation interactions will be with

water. When cells are exposed to ionizing radiation, the atoms in the water become ionized and result in radiolysis—dissociation—of the molecule into radicals.



A free radical is a molecule with an unpaired electron in the outer shell—making it highly reactive. An ion is an atom that has lost an electron and become electrically charged. H_2O^+ is both an ion and a free radical. The primary ion radicals have a very short lifetime on the order of 10^{-10} second—decaying to form free radicals, which are not charged but have unpaired electrons³. The ion radical H_2O^+ then reacts with another water molecule producing the highly reactive hydroxyl radical $\text{OH}\cdot$.



The hydroxyl radical is a powerful oxidant and the most damaging free radical. It is highly reactive and able to diffuse short distances to reach critical targets within the cell. It is estimated that about two thirds of the DNA damage caused by sparsely ionizing, low-LET radiations—such as x and γ -rays—is caused by the hydroxyl radical³. The dissociation of water molecules result in radicals that are themselves chemically reactive—in turn recombining to produce a series of highly reactive species such as protonated superoxide (HO_2) and hydrogen peroxide (H_2O_2), which produce oxidative damage within the cell.

The molecules produced through the radiolysis of water have important roles in cell signaling, and increased levels can result in significant damage. There can be up to forty or fifty species formed during the dissociation of water. When these molecules are converted back into oxygen, the compounds formed from the preceding breakdown of the water will subsequently release great amounts of energy—which may be lethal to the cell.

From the initial absorption of the incident photon to the final observed biological effect, the steps involved in the indirect action of ionizing radiation on biological systems consist of widely varying time frames. The initial ionization may take only 10^{-15} second. This is followed by ejection of electrons and the production of primary radicals—which have a lifetime of about 10^{-10} second. In striking contrast, depending on the particular consequences involved, the period between the breakage of chemical bonds and the expression of the biologic effect may be days, months or generations. If the end point is cell killing, the biologic effect may be observed within a matter of hours to days as the damaged cell attempts to divide. If the damage is oncogenic in nature, it may be decades before the initial damage to the cell manifests in cancer³.

Cell Structure and Function

The cell is a living unit greater than the sum of its parts. Cells are the structural and functional units of all living organisms. They are the simplest collection of matter that can live. Although microscopic in size, they are dynamic and very complex. Everything an organism does occurs fundamentally at the cellular level.

Every cell has the capacity to impart the characteristics of its species—including characteristics unique to itself—on to a following generation. This particular information which is passed on from parent to progeny is stored in the cell's deoxyribonucleic acid or DNA—which, for mammalian and all other eukaryotic cells, is located in the nucleus. Nucleic acids store and process information inside cells at the molecular level. These large organic compounds are made of monomers called nucleotides. Each nucleotide is composed of a nitrogenous base, a pentose—or five-carbon sugar—and a phosphate

group. Four nitrogenous bases occur in DNA: adenine (A), guanine (G), cytosine (C), and thymine (T). Nucleotides are joined by covalent bonds between the phosphate of one nucleotide and the sugar of the next. This bonding configuration results in a backbone of repeating sugar-phosphate units. Nitrogenous bases are appendages all along the sugar-phosphate backbone. Each base is attached by a hydrogen bond to its complementary base--A-T and G-C.

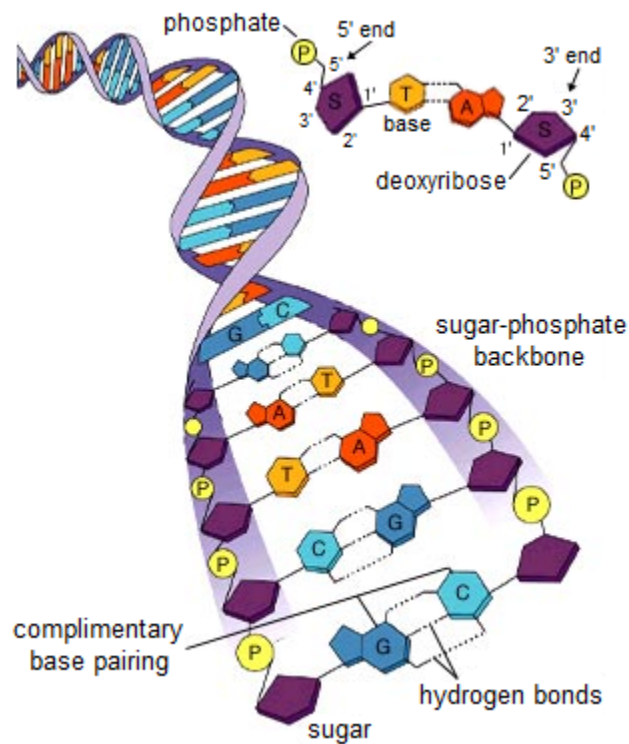


Figure 5^a. DNA structure

^a Reprinted from Essential Study Partner: General & Human Biology. ⁷⁰. McGraw-Hill (c2001).

Each functional DNA segment consisting of a sequence of nucleotides which code for a specific protein is known as a gene. Within the nucleus, DNA is organized into a fibrous material called chromatin. During cell division, the thin chromatin fibers coil up and

condense, becoming thick enough to be resolved as separate structures called chromosomes. The nucleus contains the genetic instructions required to synthesize the proteins that determine cell structure and function. While most of the genes in a eukaryotic cell are located in the nucleus, some are also in mitochondria and chloroplasts.

Mammalian cells propagate and proliferate by mitosis. The continuity of life is based on the cell division—the reproduction of cells. The division process is an integral part of the cell cycle, the life of a cell from its origin in the division of a parent cell until its own division into two. Lack of fidelity in cellular reproduction—such as in the expression of DNA and chromosome alterations—is a hallmark of cancer.

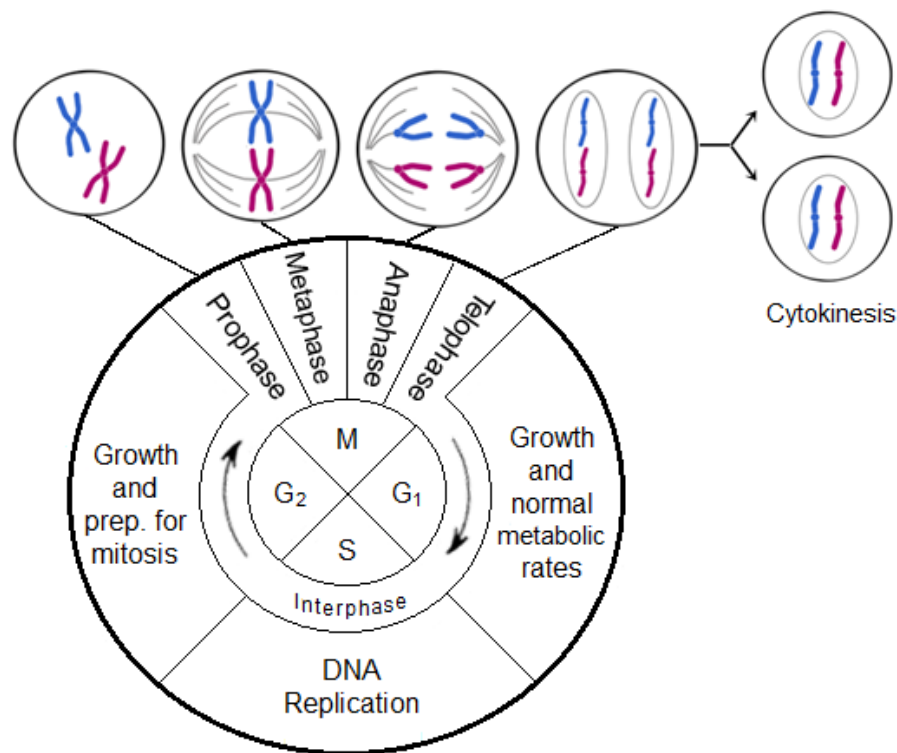


Figure 6. The eukaryotic cell cycle; stages of meiosis, mitosis and cytokinesis

Cancer is a disease of the cells. When the rate of cell division exceeds the rate of cell death, homeostasis is no longer maintained and the tissue begins to enlarge. The resulting mass produced by abnormal cell growth and division is called a neoplasm. The word tumor—often times used interchangeably with neoplasm—was derived from Latin meaning “swelling” and was originally used to describe any form of inflammation; however, it has become accepted in modern language as a synonym for neoplasm—even though, not all neoplasm form tumors, such as is the case for leukemia.

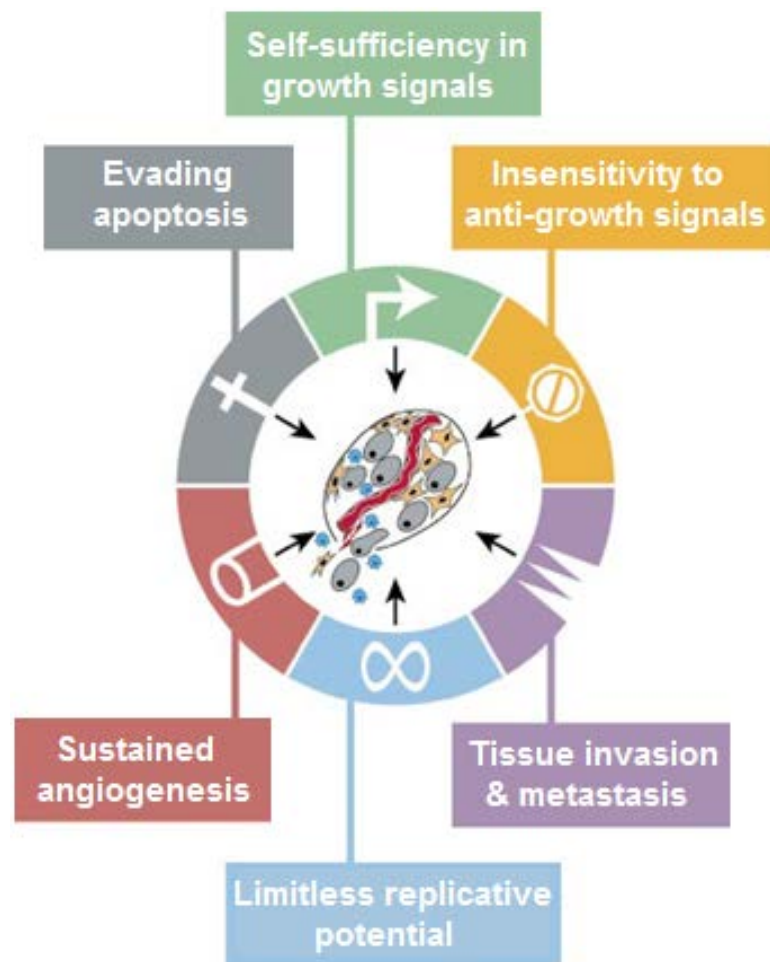


Figure 7^a. Acquired capabilities of cancer cells

^a Reprinted from Hanahan et al. ⁸⁷. The Hallmarks of Cancer. *Cell* (2000).

The formation of a tumor is a complex process that usually proceeds over a period of decades. Normal cells evolve into cells with increasingly neoplastic phenotypes through a process called tumor progression. In the United States, the risk of dying from colon cancer is as much as 1,000 times greater in a seventy-year-old man than in a ten-year-old boy⁴⁹—suggesting tumor progression is strongly related to age. While this is generally true for a large population sample, in neoplastic diseases such as colon cancer, the probability of the rate-limiting pathogenic events occurring per unit of time varies dramatically from one individual to another—being affected by hereditary disposition, diet, lifestyle and other variables which strongly influence colon cancer incidence in various human populations.

DNA Strand Breaks and Chromosomal Aberrations

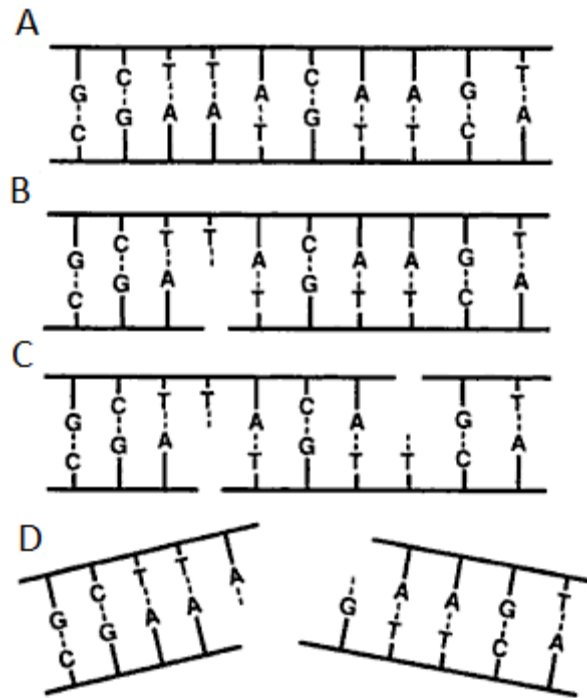


Figure 8^a. DNA strand breaks caused by ionizing radiation; A) normal DNA sequence with complementary base pairing, B) single strand break, C) double strand breaks well separated and repaired as independent breaks, D) double strand breaks in close proximity resulting in chromatin snapping in two

^a Reprinted from Hall. ³. Radiobiology for the Radiologist (2006).

It is common practice to describe chromosome aberrations according to the appearance of the damage caused by ionizing radiation at the first metaphase after exposure to radiation³. The reason is because this is the phase when the structure of the chromosomes can be viewed. The aberrations seen at metaphase are of two classes: chromosome aberrations and chromatid aberrations. Chromosome aberrations result if a cell is irradiated early in interphase, before the chromosome material has been duplicated. The break caused by the radiation for a chromosome aberration is in a single strand of

chromatin. During the DNA synthetic phase that follows, this strand of chromatin lays down an identical strand next to itself and replicates the break that has been produced. This allows for the chromosome aberration to be visible in the next mitosis.

If the dose is received later on in interphase, the aberrations are then referred to as chromatid aberrations. This is because at this point, the DNA has doubled and the chromosomes then have two strands of chromatin. Chromatid aberrations are caused by a break that occurs in a single chromatid arm after chromosome replication and leaves the opposite arm of the same chromosome undamaged.

Once breaks are produced, the created fragments behave in different ways. The breaks may rejoin back into their original configurations. This causes nothing out of the ordinary to be seen at the next mitosis. The breaks may also fail to reconstitute, and will consequently produce an aberration. This is a deletion at the next mitosis. The last way a fragment may behave is that its broken ends may reassociate and rejoin other broken or “sticky” ends. This action, therefore, will lead to chromosomes that appear to be distorted at the next mitosis.

There are three lethal aberrations. They are called the dicentric, the ring and anaphase bridge. All of these lethal aberrations lead to gross distortions that are clearly visible and morphologically distinctive. A dicentric involves an interchange between two separate chromosomes and can be replicated during the DNA synthetic phase. This results in a chromosome with two centromeres and, also, two fragments that have no centromere at all. This is quite a distorted configuration which will lead to a lethal event.

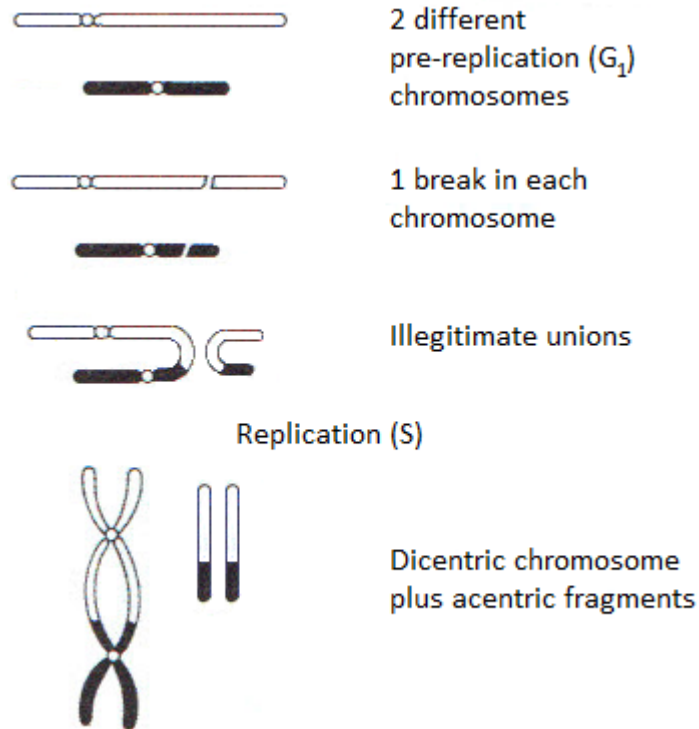


Figure 9^a. Formation of a dicentric by irradiation of pre-replication chromosomes

^a Adapted from Hall. ³. Radiobiology for the Radiologist (2006).

A ring is caused by a break in each arm of a single chromatid early on in the cell cycle. The sticky ends that are created may rejoin and form a ring and a fragment. The resulting fragments have no centromere and will most likely be lost at mitosis because they will not be pulled to either pole of the cell.

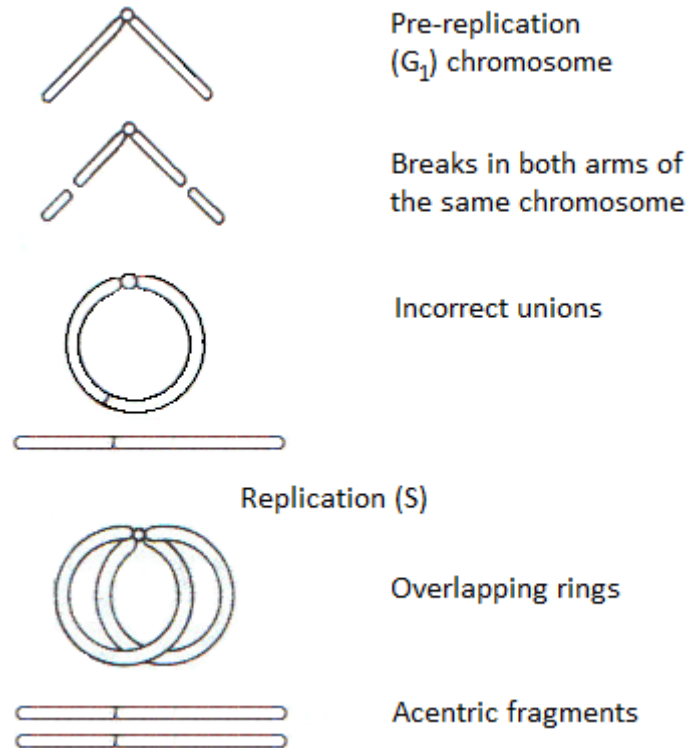


Figure 10^a. Formation of a ring by irradiation of pre-replication chromosomes

^a Adapted from Hall. ³. Radiobiology for the Radiologist (2006).

When a break occurs late in the cell cycle, an anaphase bridge may be produced. Breaks can occur in both chromatids of the same chromosome, and the sticky ends may rejoin incorrectly to form a sister union. The resulting joined fragment will most likely be lost in the first mitosis and cause a lethal event.

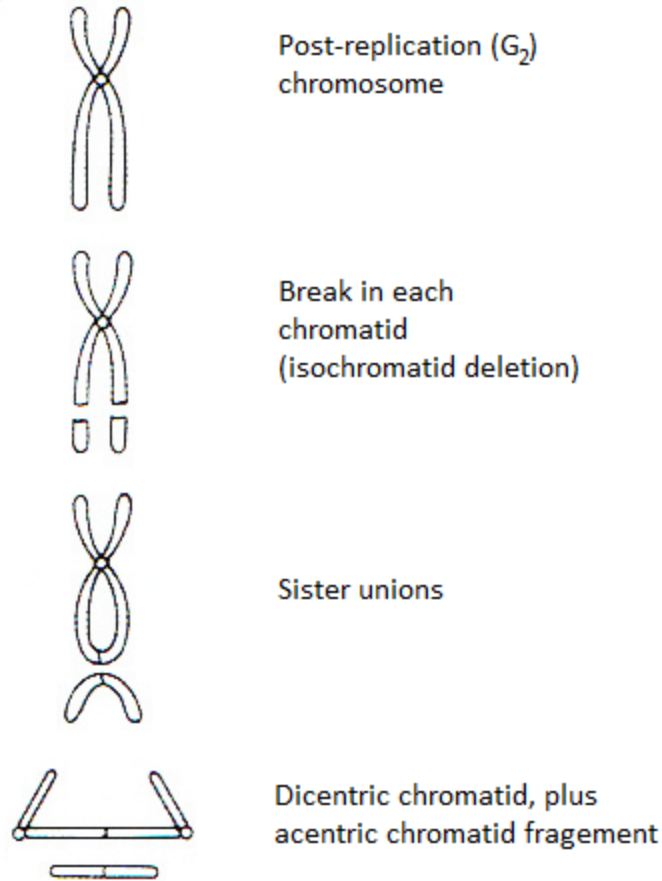


Figure 11^a. Formation of an anaphase bridge by irradiation of post-replication chromosomes

^a Adapted from Hall. ³. Radiobiology for the Radiologist (2006).

Not all chromosome changes induced by ionizing radiation are lethal. These non-lethal chromosome changes are called symmetric translocations and small deletions. A symmetric translocation involves a break in two pre-replication (G_1) chromosomes, with the broken ends being exchanged between the two chromosomes. Translocations are commonly associated with several malignancies—which are due to the resulting activation of an oncogene. Small interstitial deletions result from two breaks in the same arm of the same chromosome. This, consequently, leads to the loss of genetic information

between the two breaks. Deletions may be associated with carcinogenesis if the lost genetic material includes a tumor suppression gene.

DNA Damage and Repair

Radiation damage to mammalian cells can be operationally divided into three categories—lethal damage, potentially lethal damage (PLD) and sublethal damage (SLD)³. Lethal damage is irreversible and irreparable and, by definition, leads assuredly to cell death. Potentially lethal damage is the component of radiation damage which can be modified by post-irradiation environmental conditions. The relevance of PLD to application in radiotherapy is a matter of debate³. Sublethal damage can be repaired in a matter of hours under normal circumstances unless additional sublethal damage is accumulated—such as another dose of radiation—with which it may interact to form lethal damage. Sublethal damage is the mechanism responsible for the increase in survival observed in dose fractionation studies—when radiation exposure is separated by specified intervals of time.

Mammalian cells experience over 100,000 DNA lesions every day due to factors such as replication errors, chemical decay of their bases, attack by reactive oxygen species, or exposure to ionizing radiation³. Mutation rates are low, however, due to the development of DNA repair pathways. Those that will be discussed here are: base excision repair (BER), nucleotide excision repair (NER), DNA double-strand break repair, nonhomologous end joining (NHEJ), homologous recombination repair (HRR) and mismatch repair. The choice of repair mechanism pathway is largely determined by

the type of lesion produced; however, it is also influenced by factors such as the stage of cell cycle in which the damage is inflicted⁴⁷.

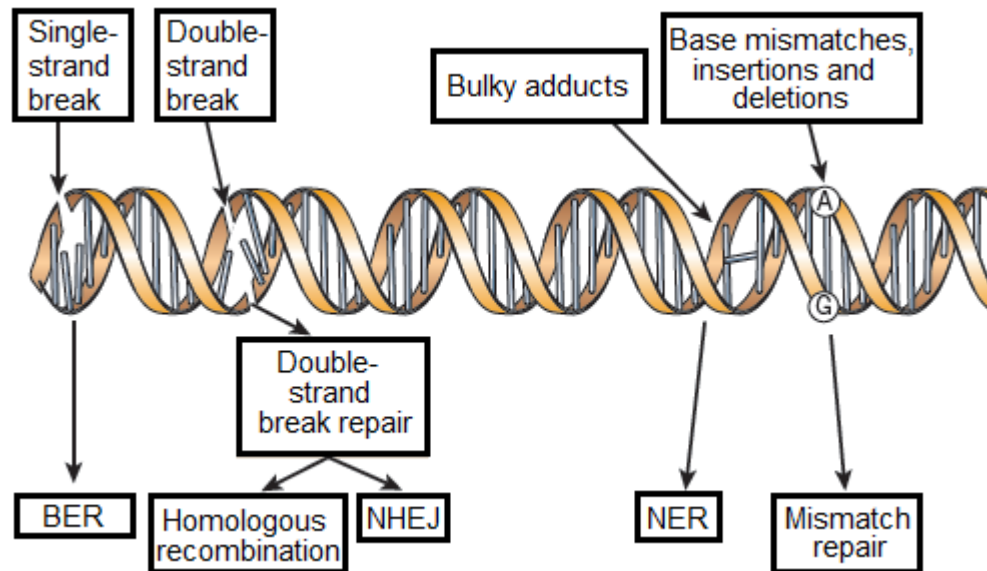


Figure 12^a. DNA repair pathways

^a Adapted from Lord et al. ⁴⁷. The DNA Damage Response and Cancer Therapy (2012).

BER is the means by which base damage is repaired. Because bases on opposite strands must be complementary, a mutation must be corrected. A single-base mutation is first removed by a glycosylase/DNA lyase that is followed by the removal of the sugar residue by an AP endonuclease. It is then replaced with the correct nucleotide by DNA polymerase β and completed by DNA mediated ligation.

NER removes bulky adducts in the DNA. The essential steps in this pathway are:

- 1) damage recognition
- 2) DNA incisions that bracket the lesion
- 3) removal of the region containing the adducts

- 4) repair synthesis to fill in the gap region
- 5) DNA ligation

DNA double-strand breaks can be repaired by two basic processes—homologous recombination repair and nonhomologous end joining. HRR requires an undamaged DNA strand as a component in the repair to be used as a template. NHEJ mediates end-to-end joining and can be divided into four basic steps:

- 1) end recognition
- 2) end processing
- 3) fill-in synthesis
- 4) ligation

Programmed Cell Death

Programmed cell death is fundamental to survival as it is responsible for the maintenance of homeostasis and other various physiological processes. Because cell death is so intimately linked to tissue homeostasis, its disruption is implicated in many pathological conditions²⁶. Programmed cell death has been recognized in cancer therapy applications as being one of the pleiotropic mechanisms of cell killing by cytotoxic agents—such as radiation exposure¹⁵. Such abnormalities in the regulation of cell death can pose serious consequences and, ultimately, result in disease states. For example, uncontrollable and unwanted cell accumulation manifests into cancer; the inability and subsequent failure to eradicate aberrant cells results in autoimmune diseases; and states of inappropriate cell loss are responsible for disorders such as heart failure, acquired immunodeficiency syndrome (AIDS), and neurodegenerative diseases²⁷.

Since it was first described over forty years ago²¹, our understanding of programmed cell death has increased dramatically. Much attention in this field of study has been devoted to one major mechanism of cell death—apoptosis. Historically, three types of cell death have been identified: apoptosis, autophagy and necrosis. Recently, however, there has been growing evidence to support the existence of a number of various cell death mechanisms. In one report, eight types of cell death were classified²⁹, while another described as many as eleven different pathways²⁸.

Apoptosis is the genetically controlled ablation of cells and is the most prevalent form of cell death²⁶. The term was first proposed in 1972 by Kerr et al.¹⁴ to describe the specific morphological changes associated with cell death as being markedly distinct from necrosis. A Greek derivation, *apoptosis* means ‘falling off’—thus, likening its physiological nature to that of petals falling from a flower or leaves dropping from a tree³.

Apoptosis is commonly referred to as ‘cell suicide’ and is a normal biological process essential for survival. In a broad sense, apoptosis is used to maintain appropriate numbers of different cell types in a wide variety of human tissues. For example, each year of our lives, the turnover of cells approximates the total number of cells present in the adult body at any one time—which is estimated to be around 3×10^{14} cells⁴⁹. While apoptosis is important for the promotion of normal physiology, it has also been shown to play an equally important role in the function of disease¹⁵ and is a well-recognized cell death mechanism occurring in cancer treatment through which cytotoxic agents kill tumor cells¹.

The purpose of subjecting a patient to radiation therapy is for tumor eradication. For this to happen, a lethal amount of damage must be incurred by the cell to ultimately result in its death—rendering the cancerous cell unable to divide and cause further growth and spread of the malignancy. Irradiated cells die by a number of different mechanisms—of which, the apoptotic process has come to be recognized as a significant mechanism employed in post-irradiation cell death²⁶.

Ionizing radiation may serve as a cytotoxic agent when incident upon a biological target. Double-strand DNA breaks induced by radiation or reactive oxygen species may lead to cell cycle arrest or apoptosis. A cell that has accumulated a large amount of DNA damage induced by radiation or reactive oxygen species—or one that no longer effectively repairs damage incurred to its DNA—can enter into one of three possible states: senescence, apoptosis, or unregulated cell division³. Senescence is defined as an irreversible state of dormancy; and unregulated cell division may potentially lead to the formation of a cancerous tumor.

If a cell becomes resolved to initiate the suicide sequence and undergo apoptosis, the subsequent cellular changes that constitute the apoptotic program will proceed according to a precisely coordinated schedule. This type of death is not a messy process in the way of cell lysis—which results in a spewing out of cellular contents into the surrounding environment and causing further potentially damaging effects. Rather, the apoptotic cell is neatly dismantled and then dissolved. One of the first actions the cell will make in this process is the termination of communication with its neighbors—evidenced by the rounding up and detaching of cells³. After rounding up and detaching, condensation of the chromatin at the nuclear membrane and fragmentation of the nucleus

occurs. The cross-linking of proteins and loss of water result in cytoplasmic condensation and cause cell shrinkage. Usually within an hour, the apoptotic cell breaks up into a number of small fragments, referred to as apoptotic bodies—membrane-bound fragmented vesicles—which are rapidly phagocytized. Thus, all traces of what had recently been a living cell are removed. Apoptosis is distinguished morphologically by the formation of crescents around the periphery of the nucleus or by clusters of spherical fragments³.

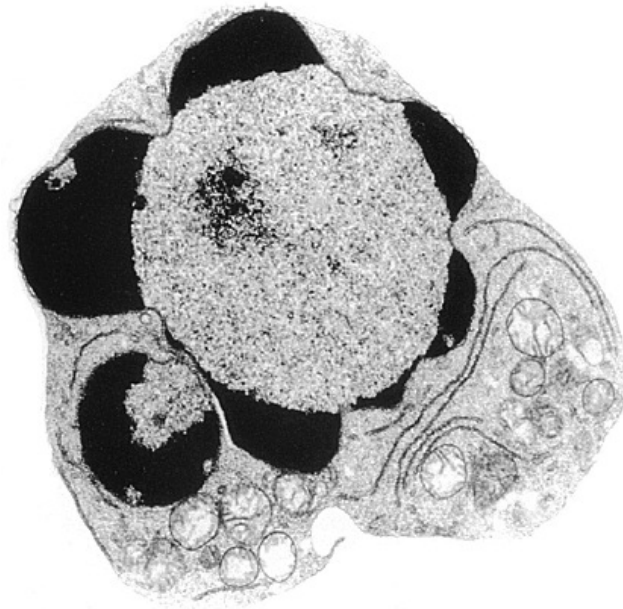


Figure 13^a. Electron micrograph of apoptotic cell; characteristic early apoptosis with compaction and segmentation of nuclear chromatin and condensation of the cytoplasm in a Burkitt's lymphoma cell 72 hours after external beam irradiation at x 6000 magnification

^a Reprinted from Illidge. ¹⁵. Radiation-induced Apoptosis. Clin Oncol (1998).

Two major pathways that mediate cell death originate from either the cell membrane or the mitochondrion. Those beginning at the membrane are initiated via death signals and receptors; with those pathways originating from within the nucleus being

signaled by DNA-damaging stresses. The signals transmitted by each respective pathway result in the activation of intracellular cysteine proteases—caspases—which cleave substrates, including themselves, at aspartic acid residues³. Members of the caspase family of proteases form the central framework of apoptosis and are involved in the initiation, execution and regulatory phases of the pathway—operating in hierarchical cascades which serve to amplify the apoptotic signal²⁶. Caspases can be broadly divided into two categories—upstream initiators and downstream effectors—based upon their cell death pathway structure and sequence.

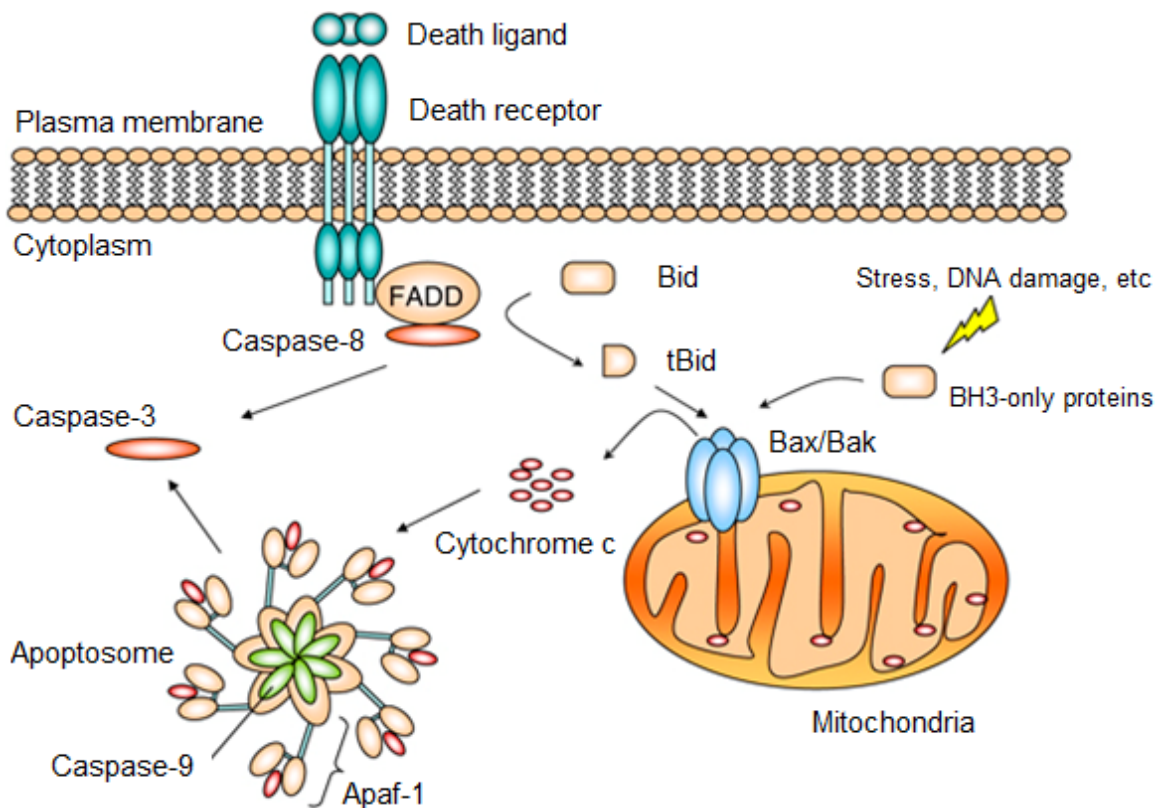


Figure 14^a. Caspase activation pathways; The extrinsic pathway is death receptor-mediated while the intrinsic pathway is internally initiated by damage, stress, etc.

^a Reprinted from Li et al. ⁷². Caspases in Apoptosis and Beyond. Oncogene (2008).

In addition to their established role in cell death, caspases have recently been reported to participate in several non-apoptotic processes by controlling events in cell proliferation and differentiation⁵⁰.

Because of its various functions, p53 has become known as the ‘guardian of the genome’. The p53 protein continuously receives signals from a diverse array of surveillance systems. If, for example, information is received indicating the presence of metabolic disorder or genetic damage within the cell, it may react by arresting the cell in its growth-and-division cycle while, at the same time, orchestrating localized responses to facilitate the repair of damage. However, under certain conditions, p53 also has the ability to provoke a response far more drastic than the reversible halting of the cell cycle. In response to massive, essentially irreparable genomic damage, anoxia—extreme oxygen deprivation—or severe signaling imbalances, p53 will trigger apoptosis⁴⁹. Upon receipt of information indicating that the metabolic derangement or damage to the genome is too severe to be corrected, p53 may emit signals to awaken the cell’s normally latent suicide program, resulting in rapid death and elimination of the cell. If a defective cell is allowed to continue growth and division, it would likely pose a threat to the organism’s overall health and viability.

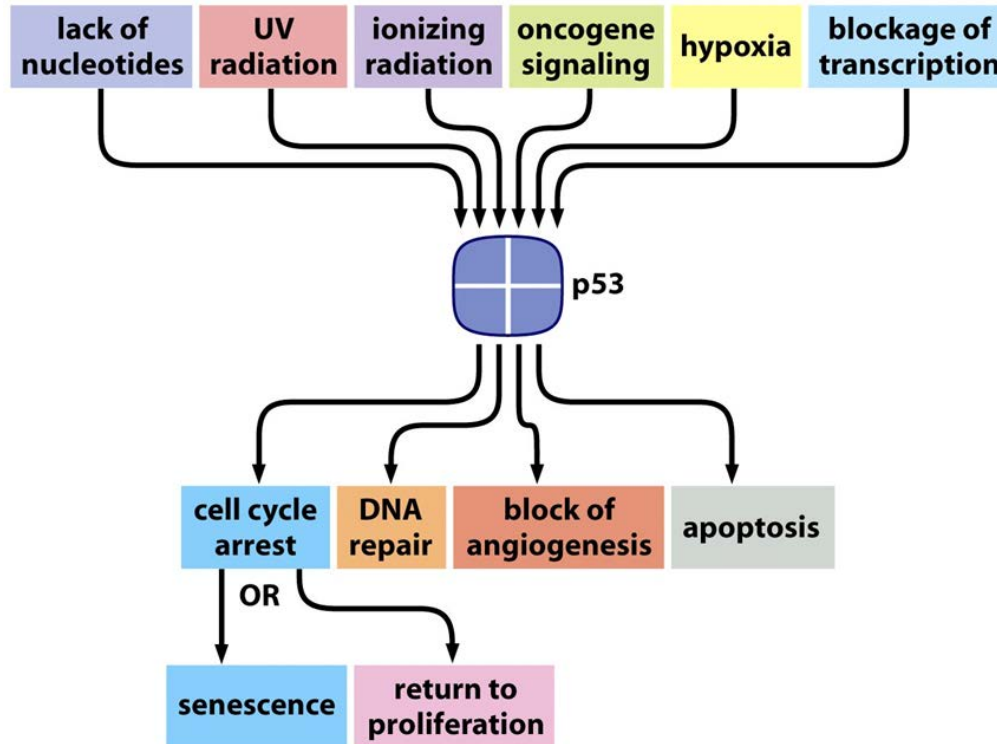


Figure 15^a. p53-activating signals and downstream effects

^a Reprinted from Weinberg. ⁴⁹. The Biology of Cancer (2007).

The p53 protein initiates apoptosis in part through its ability to promote expression of several downstream target genes that specify components of the apoptotic machinery. There is an ever-increasing list of causative agents which have been shown to induce rapid increases in p53 protein levels—ionizing radiation is one of the most effective⁴⁹.

Because of the cytostatic and pro-apoptotic powers in which p53 possesses, cancer cells must blunt or even fully eliminate p53 activity if they are to prosper—which explains the why most and, perhaps, all human tumor cells have partially or totally inactivated their p53 alarm response⁴⁹. Without p53 on duty, cancer cells are able to tolerate hypoxia, extensive damage to their genomes, and profound dysregulation of their

growth-controlling circuitry—acquiring a resistance to these normally debilitating factors, which allows them to continue on toward a highly malignant growth state.

Recent studies have reported a new role for p53 in the cytoplasm and specifically at the mitochondria, where it may function directly to initiate the caspase cascade and apoptosis by releasing cytochrome c, bypassing the need for its transcriptional activity³. In eukaryotic cells, mitochondria are organelles that convert energy into forms that cells can use for work¹³. The primary function of mitochondria is the generation of ATP by oxidative phosphorylation. Mitochondria are distributed throughout a cell's cytoplasm and have many functions including the generation of ATP, shaping and responding to Ca^{2+} signals, generation of reactive oxygen species (ROS) and, under extreme conditions, the release of factors such as cytochrome c to induce apoptosis⁶⁷.

Cytochrome c, a key player in the apoptotic program, normally resides in the space between the inner and outer mitochondrial membranes, where it functions to transfer electrons as part of oxidative phosphorylation.

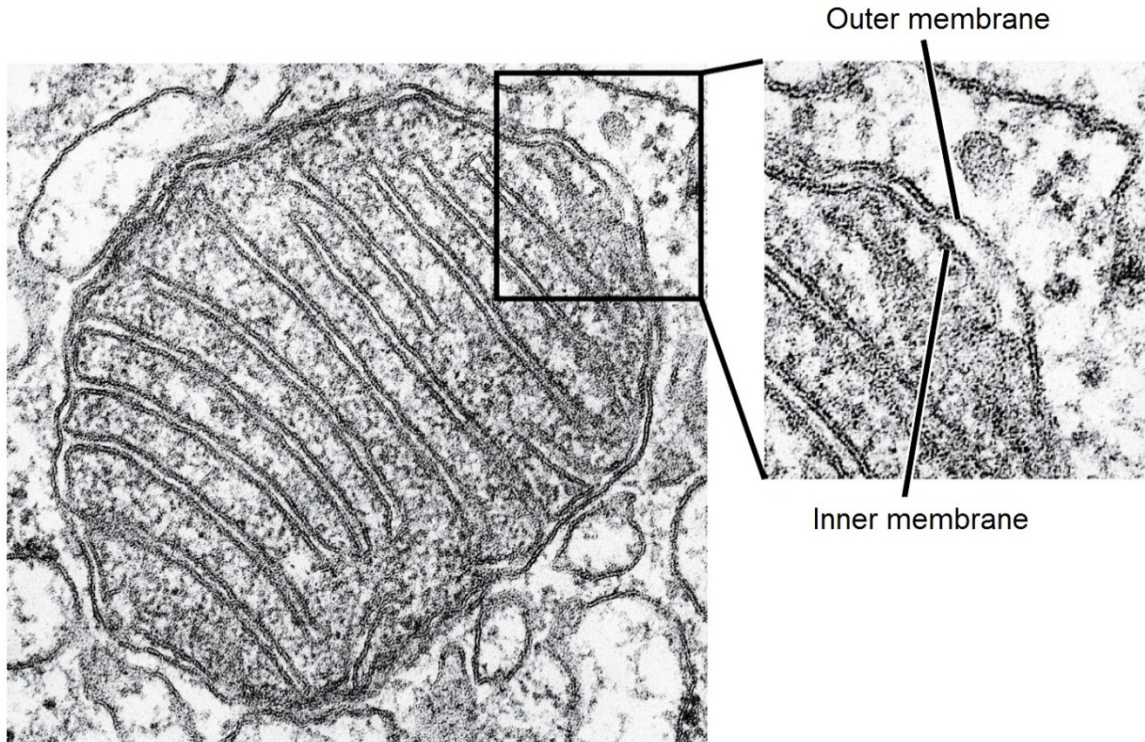


Figure 16^a. Electron micrograph of mitochondria from human liver cell; Cytochrome c is stored in the space between the inner and outermost mitochondrial membranes.

^a Reprinted from Weinberg.⁴⁹ The Biology of Cancer (2007).

When certain signals trigger the initiation of apoptosis, the outer mitochondrial membrane depolarizes, resulting in the spillage of cytochrome c out of the mitochondrion and into the surrounding cytosol—where it then associates with other proteins to trigger a cascade of events that together yield apoptotic death⁴⁹. It is interesting to consider the dual and opposing functions in which the mitochondria serves. While it serves as the cell's center of energy production, it also harbors and releases a biochemical messenger that triggers the changes that lead to cell death.

Cell Signaling Pathways

A single cell may express over 20,000 distinct proteins, many of which are actively involved in the cytoplasmic circuits and act as regulatory proteins⁶⁷. Through a complex signal processing circuitry, a cell can gather a wide variety of external signals from its environment through receptors displayed on its surface. A signaling pathway reaches from the cell surface into the nucleus—which is where processed signals are usually transmitted, providing critical input information to the central machinery that governs cell proliferation.

Cells within an organism are constantly communicating with each other by electrical and chemical signaling mechanisms. Communication through electrical signals is fast and requires the presence of gap junctions to allow information to pass directly from one cell to its neighbor. Communication through chemical signals is the most widely occurring form of information transfer between cells⁶⁷. In chemical communication, one cell releases a chemical stimulus—such as a neurotransmitter, hormone, or growth factor—which then diffuses to other cells and alters their activity. Cells are enclosed within a lipophilic plasma membrane—which forms an imposing barrier which must be crossed by all incoming signals. Target cells possess receptors capable of detecting the incoming signal and relaying the information to the appropriate internal cell signaling pathway.

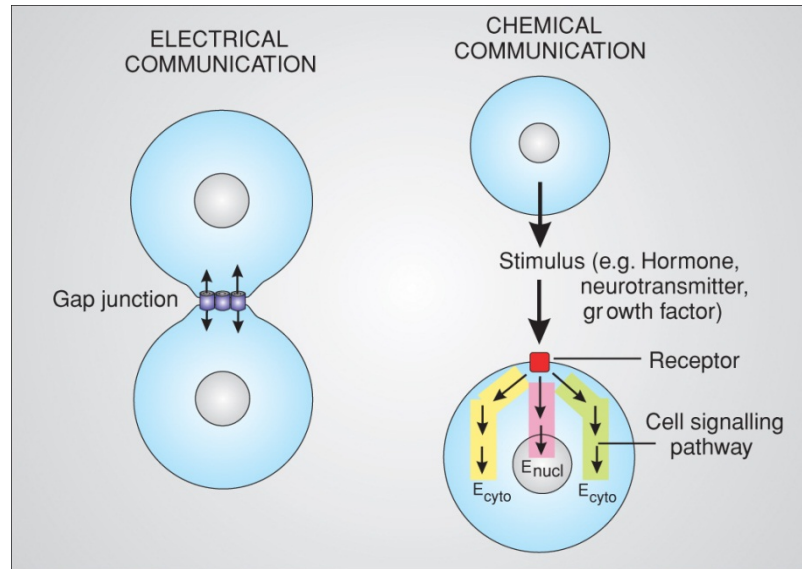


Figure 17^a. Cell communication through electrical and chemical signaling mechanisms

^a Reprinted from Berridge M. ⁶⁷. Cell Signalling Biology. Biochemical Journal Signal (c2012).

The signals passed between cells are primarily carried by proteins⁴⁹.

Consequently, signal emission requires an ability by some cells to release proteins into the extracellular environment. After the process of protein secretion, the recipient cells must be able to sense the presence of these proteins or these signaling proteins in their surroundings. The deregulation of normal signaling is central to the formation of cancer cells.

The basic concept of a cell signaling pathway concerns the mechanisms responsible for receiving external information and relaying it through internal cell signaling pathways to activate sensors and effectors which bring about a change in cellular responses. A signaling protein operating in a linear signaling cascade must be able to recognize only those signals which come from its upstream partner proteins. Likewise, it must then be able to pass them on to its intended downstream partners—all

while ignoring thousands of other proteins within the cell. Signaling mechanisms are highly integrated and act through different effectors—including muscle proteins, secretory vesicles, transcription factors, ion channels and metabolic pathways—to control the activity of cellular processes such as development, proliferation, neural signaling, stress responses and apoptosis⁶⁷. Once stimuli has reached the target cells, a diverse number of cell signaling pathways are used to control cellular activity.

Cells use a large number of clearly defined signaling pathways to regulate their activity. Each cell type has a unique repertoire of cell signaling components.

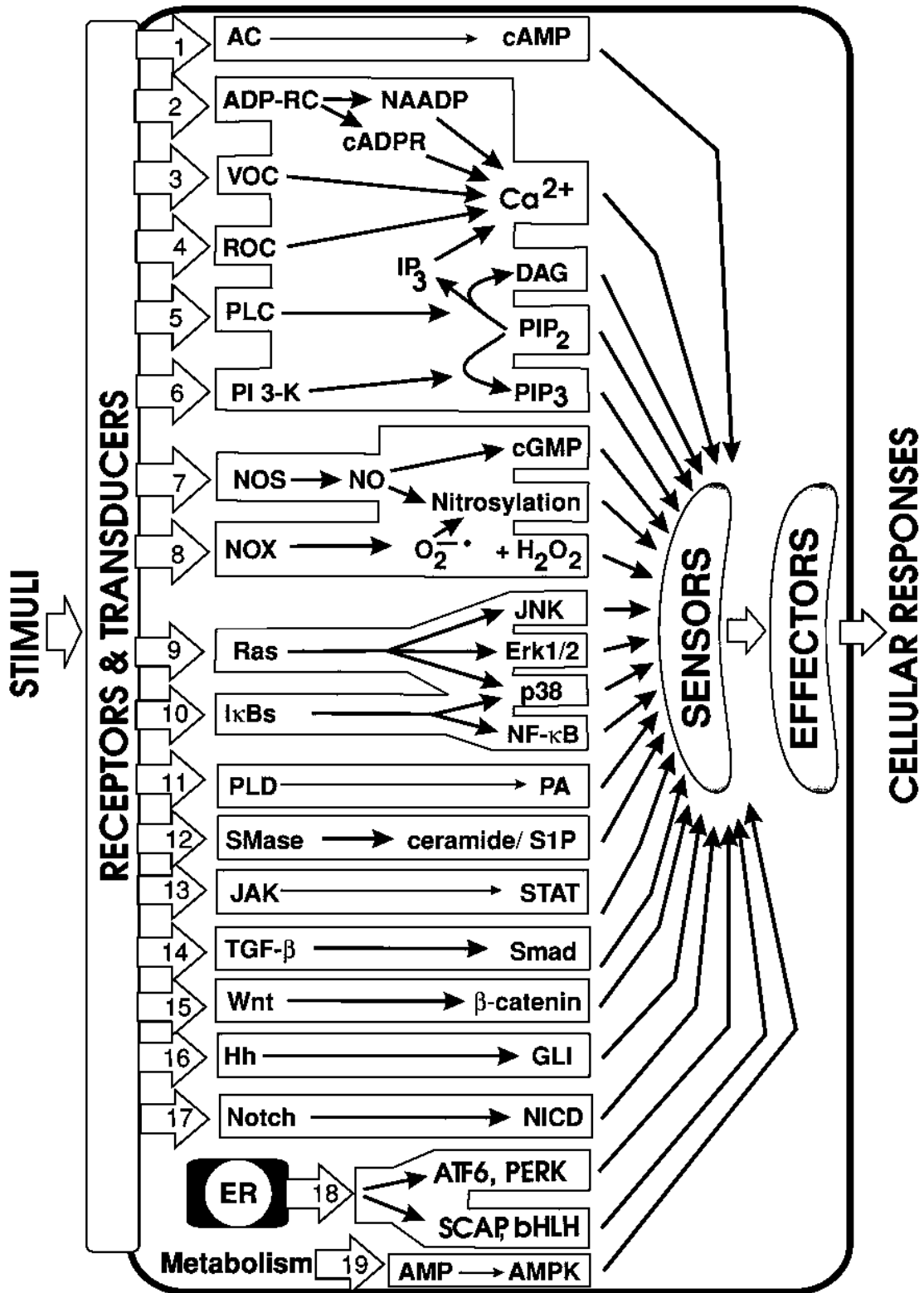


Figure 18^a. Summary of the major cell signaling pathways

^a Adapted from Berridge M. ⁶⁷. Cell Signalling Biology. Biochemical Journal Signal (c2012).

Ca²⁺ signaling is one of the major signaling systems in cells. It functions to regulate many different cellular processes throughout a cell's life history; however, increased levels of this ion can result in cell death either by apoptosis or through catastrophic necrotic changes. Levels of Ca²⁺ are low when cells are at rest, but when a stimulus arrives, there is a sudden rise in concentration—which induces changes in cellular activity. Previous studies have also shown oxidative stress and calcium signaling to be important modulators in radiation-induced bystander responses⁵³.

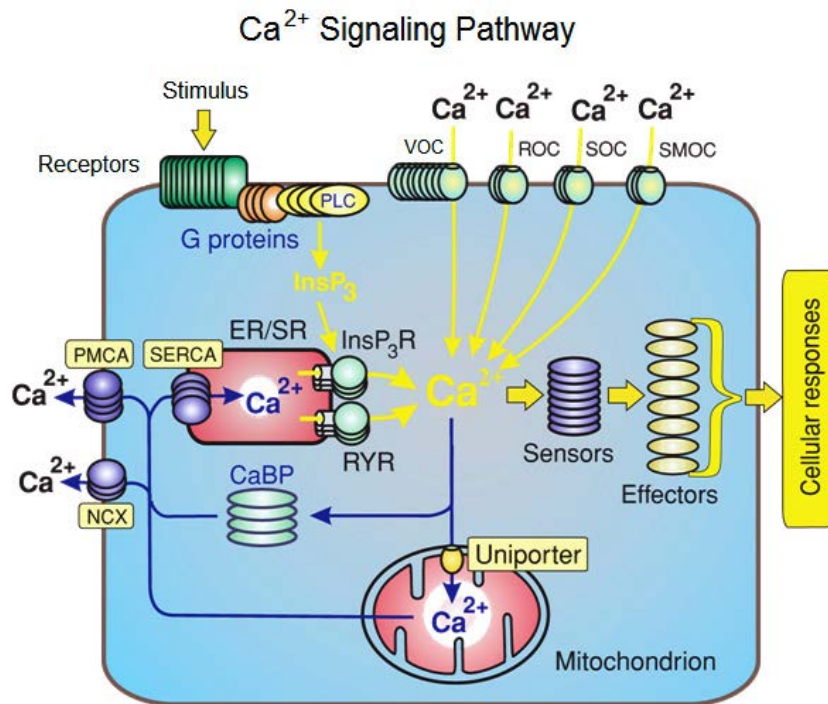


Figure 19^a. Summary of the major components in Ca²⁺ signaling system

^a Reprinted from Berridge M. ⁶⁷. Cell Signalling Biology. Biochemical Journal Signal (c2012).

The mitogen-activated protein kinase (MAPK) super-family is multi-functional and consists of separate pathways that work together to control a range of cellular

processes and have been linked to growth factor-mediated regulation of cellular events such as proliferation, senescence, differentiation and apoptosis⁵³. These different downstream effectors are activated by the final MAPK components associated with three primary sets of kinases:

1) Extracellular-signal-regulated kinase (ERK) pathway

The ERK pathway performs a number of important signaling functions—such as the control of cell proliferation—and can be activated by both protein tyrosine kinase-linked receptors (PTKRs) and by G protein-coupled receptors (GPCRs).

2) c-Jun N-terminal kinase (JNK) pathway

The JNK pathway also functions in the control of a number of cellular processes including proliferation and apoptosis. It is activated by a staggering number of mechanisms—made evident by the fact that there are thirteen MAPK kinase kinases (MAPKKKs) responsible for feeding information into the JNK pathway.

3) p38 pathway

The p38 cascade controls apoptosis and the release of cytokines by macrophages and neutrophils. This pathway can be activated by a variety of receptor mechanisms or by various environmental stresses such as osmotic, redox or radiation stress.

MAPK Signaling Pathway

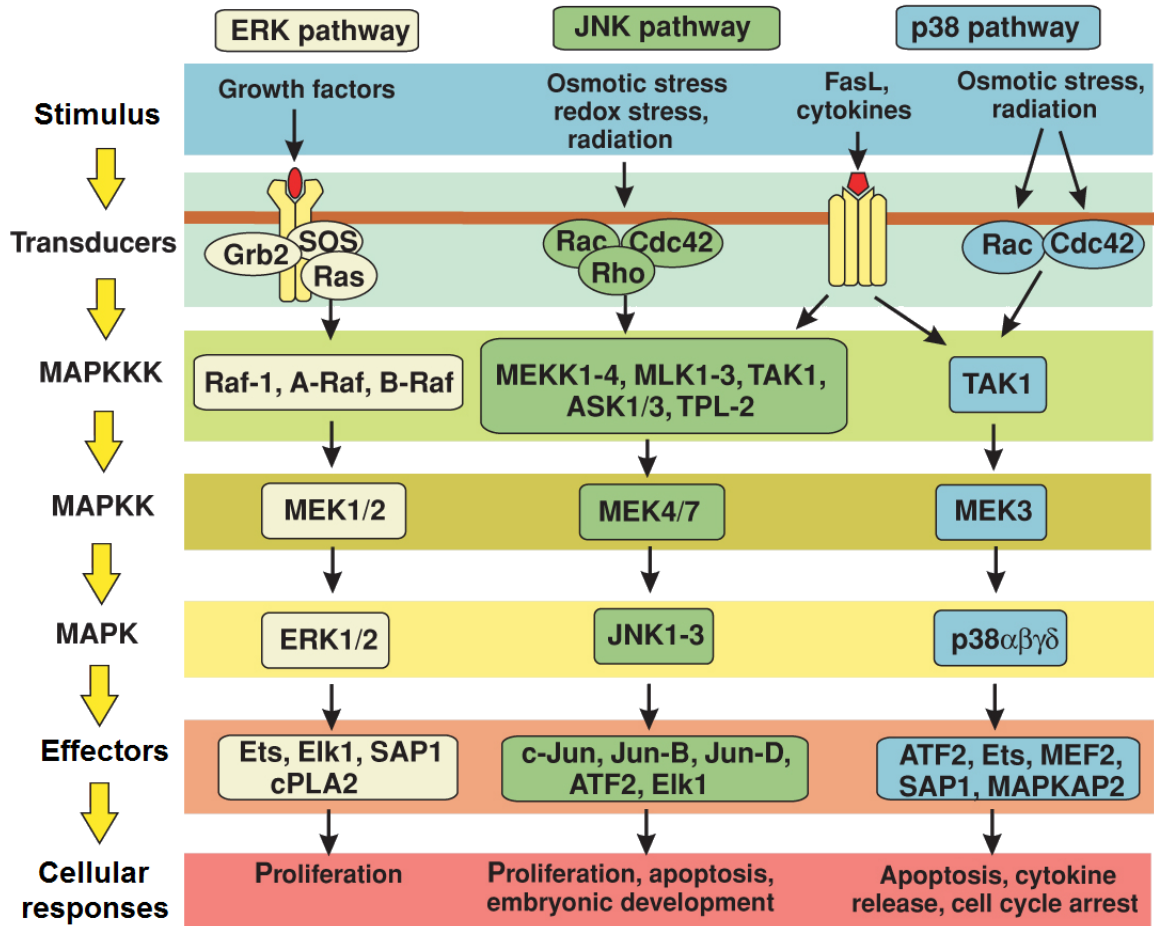


Figure 20^a. Mitogen-activated protein kinase (MAPK) signaling pathways

^a Adapted from Berridge M. ⁶⁷. Cell Signalling Biology. Biochemical Journal Signal (c2012).

Exposure of cells to ionizing radiation and other toxic stresses induces simultaneous compensatory activation of multiple MAPK pathways⁵³.

Non-Targeted Effects of Exposure to Ionizing Radiation

Radiation-induced bystander effects have been defined as responses expressed in cells that were not directly hit by radiation—receiving no exposure— but were influenced in some way or another by the direct hit received in another cell⁵⁴. Radiation-induced bystander effects, then, describe the phenomenon in which unirradiated cells manifest radiation-induced biological changes despite having been exposed to radiation. Although evidence of this phenomenon exists in the literature dating back more than forty years⁶⁵, bystander effects weren't specifically described until 1992 by Nagasawa and Little⁶. In this study, they observed results indicative of the transmission of damage to neighboring, unirradiated cells, reporting that clastogenic effects occurred in alpha-particle irradiated cells which did not receive a direct hit. By the late 1990s, this phenomenon had become widely known as the bystander effect⁵.

Over the past two decades, much work has been accomplished in this field of study. Bystander responses have been shown to include sister chromatid exchanges⁶, micronucleus formation⁵⁶, apoptosis^{57,58}, damage-inducible stress responses⁵⁹, gene mutation^{60,61}, chromosomal instability¹⁰⁵, transformation¹⁰⁶, reduction in clonogenic survival⁵, and delayed cell death¹⁰⁷—as well as stimulatory effects such as protective adaptive response and increased proliferation¹⁰⁸. Furthermore, the effect has been observed across numerous cell lines following exposure to both densely and sparsely ionizing radiations.

Bystander effects can be generally divided into four sub-categories based on experimental design and protocol:

- 1) Bystander effects after cytoplasmic irradiation

- 2) Bystander effects after exposure to low fluences of alpha particle irradiation
- 3) Bystander effects after irradiation with a charged-particle microbeam
- 4) Bystander effects after transfer of medium from irradiated cells

Table 1^a. Experimental Questions to Define Radiation-Induced Bystander Effects

Dose Dependence	<ul style="list-style-type: none"> ▪ Does the nature or magnitude of the signal produced by an irradiated cell depend on the dose received?
Signal Potency	<ul style="list-style-type: none"> ▪ How much signal is required to induce a bystander effect in any one unirradiated cell? ▪ If there is a threshold, how many cells need to be irradiated before effects begin to manifest?
Signaling Range	<ul style="list-style-type: none"> ▪ How is the bystander signal propagated and how is it attenuated? ▪ Is the signal further propagated by responding cells?
Radiation Source	<ul style="list-style-type: none"> ▪ How does the nature or magnitude of the bystander signal produced in any one cell depend on the nature of the radiation source?
Signal Timing	<ul style="list-style-type: none"> ▪ How fast are bystander signals emitted? ▪ How quickly do the signals effect a response once received? ▪ How long do the signals persist?
Cell Type	<ul style="list-style-type: none"> ▪ Are all cells capable of producing/responding to bystander signals? ▪ Does the nature or magnitude of the signal/response depend on cell type?

^a Adapted from Blyth et al. ². Radiation-induced Bystander Effects. *Radiat Res* (2011).

It has been demonstrated that bystander signals can induce proliferation or death in unrelated and unirradiated cells receiving medium from directly irradiated cultures— suggesting that an active cellular response in exposed cell populations is responsible for

the secretion of signaling factors upon irradiation⁵. In vitro experiments have further shown that untargeted cells do not need to be present at the time of exposure—with medium transfer studies demonstrating clear evidence of the production of a signaling factor which does not require gap junction-mediated communication from cell to cell⁶⁶.

A dependence on cell number present at the time of irradiation and the magnitude of the bystander response induced in non-targeted populations has also been demonstrated⁷³—further suggesting the production of soluble factor(s) by the exposed cells. Experiments by Mothersill and Seymour⁷⁸ showing suppression of bystander signal production by low temperature suggest that the bystander effect is energy-dependent. They further concluded that a key factor in determining the bystander response in non-targeted cell populations depended on the cell's ability to produce ATP as an energy source for repair, repopulation or programmed cell death⁷⁷.

It has been further demonstrated that signal generation from irradiated cells is a distinct process, controlled independently from that of the signal response⁷⁷, and not all cells have the ability to produce such a signal⁷⁴. Different effects are observed in different cell types and depend on the type of cell producing the bystander signal after irradiation and the type of cell receiving the bystander signal. Consequently, models or tissues consisting of multiple cell lines may present a more complicated bystander scenario—where some cell types have the ability to produce a bystander signal while others are unable to respond, giving the illusion that no bystander signal was produced. Likewise, some cells could have an increased responsiveness to signals secreted by a particular cell line relative to others. A wide range of communication and interaction capabilities undoubtedly exist within multi-cellular systems—and certainly between cancerous and

non-cancerous cells. An understanding of these cellular relationships would clearly have importance in radiotherapy applications—especially in the determination of factors controlling normal tissue response to treatment.

Research has shown that irradiated cells communicate with non-irradiated cells through secreted factors and/or gap junctional intercellular communication—resulting in the unexposed cells to exhibit functional changes⁵³. While irrefutable evidence of the bystander effect exists in the literature, an understanding of their mechanisms is only beginning to emerge. It has been suggested that the bystander signal is a small protein molecule that occurs as an early signal transduction event following exposure to ionizing radiation⁷³. Roles for reactive oxygen species have also been reported⁵³.

Mechanisms of the Bystander Effect

Following exposure to ICCM, both intracellular and extracellular signals responsible for determining whether a cell will live or die are altered. A previous study reports that mitochondria play a major role in this process and that the MAPK family of proteins is also involved in determining proliferation or apoptosis in damaged cells⁷⁹. The MAPK (mitogen-activated protein kinase) superfamily of signaling pathways are linked to growth factor-mediated regulation of diverse cellular events such as proliferation, senescence, differentiation and apoptosis⁷⁸. Exposure of cells to ionizing radiation and other toxic stresses induces simultaneous compensatory activation of multiple MAPK pathways. These signals play critical roles in controlling cell survival after radiation exposure⁷⁸.

Calcium has also proven to be an important signaling molecule in bystander responses⁵³. Changes in intracellular calcium modulate cell functions such as secretion, enzyme activation and cell cycle regulation. One study found that a requirement for bystander-induced apoptosis was calcium influx from voltage-dependent calcium channels—and, to a lesser extent, from intracellular stores⁵³.

In a recent study, Huang et al. reasoned that among the many cellular processes activated or deactivated in dying cells, the factors and processes directly responsible for cell death are most likely to be involved in regulating the growth-promoting properties of dying cells¹. In their study, an immunoblot of irradiated cells showed that caspases 3 and 9 and the downstream cytochrome c were activated; whereas, caspase 8 was not. Western blot showed iPLA2 was activated in a caspase-3 dependent manner. The results of this previous study indicate dying tumor cells use the apoptotic process to generate and release potent growth-stimulating signals to stimulate the repopulation of tumors undergoing radiotherapy¹. They also reported—for the first time—that activated caspase 3, a key executioner in apoptosis, is involved in the stimulation of cell growth. One downstream effector that caspase 3 regulates is prostaglandin E2 (PGE2), which can potentially stimulate growth of surviving tumor cells. In addition, earlier reports have shown that caspase 3-mediated iPLA2 activation led to increased production of arachidonic acid, whose downstream eicosanoid derivatives such as PGE2 had been implicated in stimulating tumor growth.

The production of prostaglandins begins with the liberation of arachidonic acid from membrane phospholipids by phospholipase A2 in response to inflammatory stimuli. The cyclooxygenases enzymes COX-1 and COX-2 then convert arachidonic acid to

prostaglandin H₂. COX-1 is expressed constitutively and acts to maintain homeostatic function such as mucus secretion, whereas COX-2 is induced in response to inflammatory stimuli. Further downstream, cell-specific prostaglandin synthases convert PGH₂ into a series of prostaglandins including PGI₂, PGF₂, PGD₂ and PGE₂. Prostaglandin E₂ (PGE₂) is produced by several cell types including macrophages, fibroblasts and some malignant cells and exerts its actions through four receptors—EP1, EP2, EP3 and EP4⁸⁴.

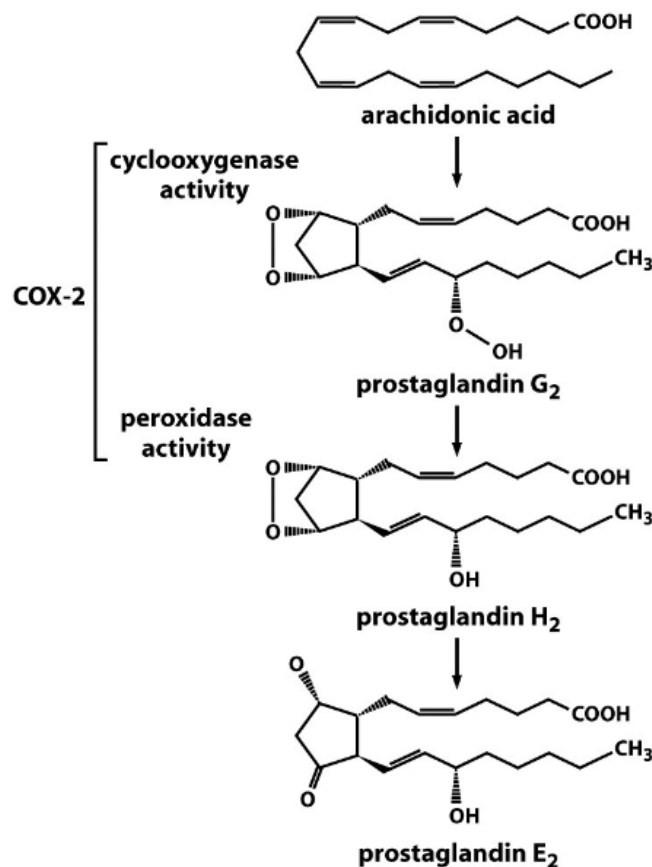


Figure 21^a. Catalytic activity of COX-2 enzyme; PGE₂ is a primary product of arachidonic metabolism and is synthesized *de novo* by three enzymatic steps via the cyclooxygenase (COX) pathways. PGE₂ assay is well suited for detecting compounds that modulate COX-2 enzymes.

^a Reprinted from Weinberg.⁴⁹ The Biology of Cancer (2007).

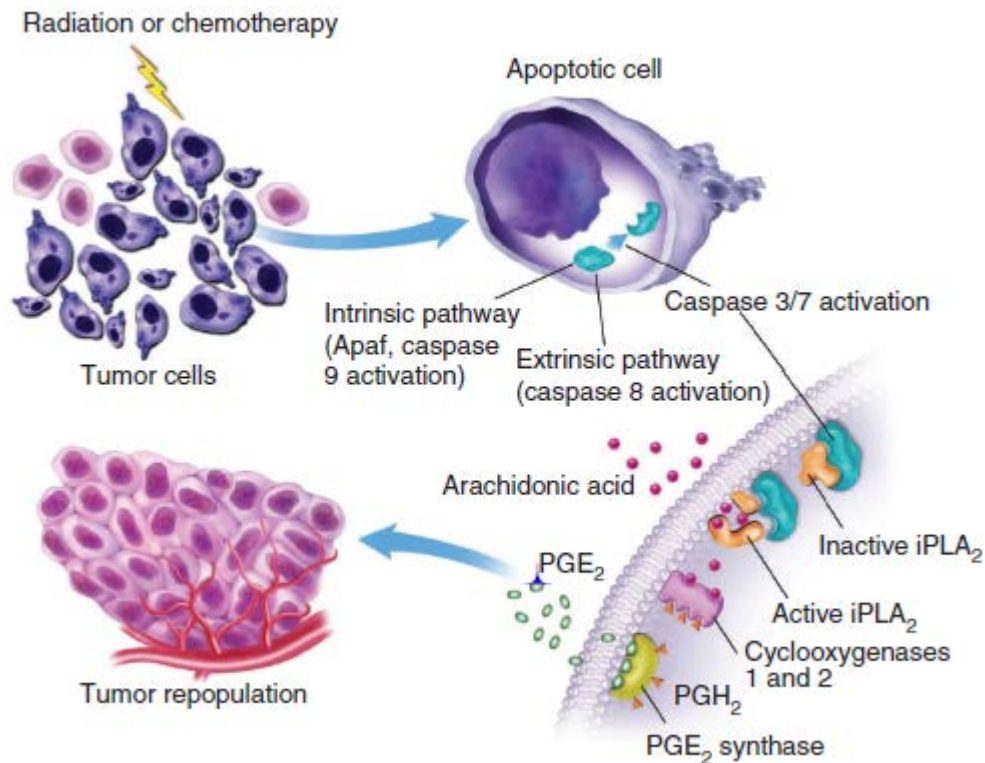


Figure 22^a. Proposed pathway for cell death–mediated tumor cell repopulation

^a Reprinted from Huang et al. ¹. Caspase 3–mediated stimulation of tumor cell repopulation during cancer radiotherapy. *Nat Med* (2011).

In a medium transfer bystander study, Mothersill et al. reported the production of a signal by irradiated cells capable of initiating apoptosis in non-targeted bystander cell populations⁵⁷—indicating that apoptosis is a major mechanism of cell death due to ICCM exposure⁷⁷.

It has been shown that alterations to cyclooxygenase-2 (COX-2) expression and the presence and concentration of its enzymatic product prostaglandin E2 (PGE2) have influential roles in the development of colorectal cancer⁸⁰. Recent studies have further identified important components in the process of cellular adaptation within hostile

microenvironmental conditions. A delicate interplay exists between COX-2, hypoxia-inducible factor 1 and dynamic switches in β -catenin function that are responsible for fine-tuning the signaling networks to meet the ever-changing demands of a tumor⁸⁰.

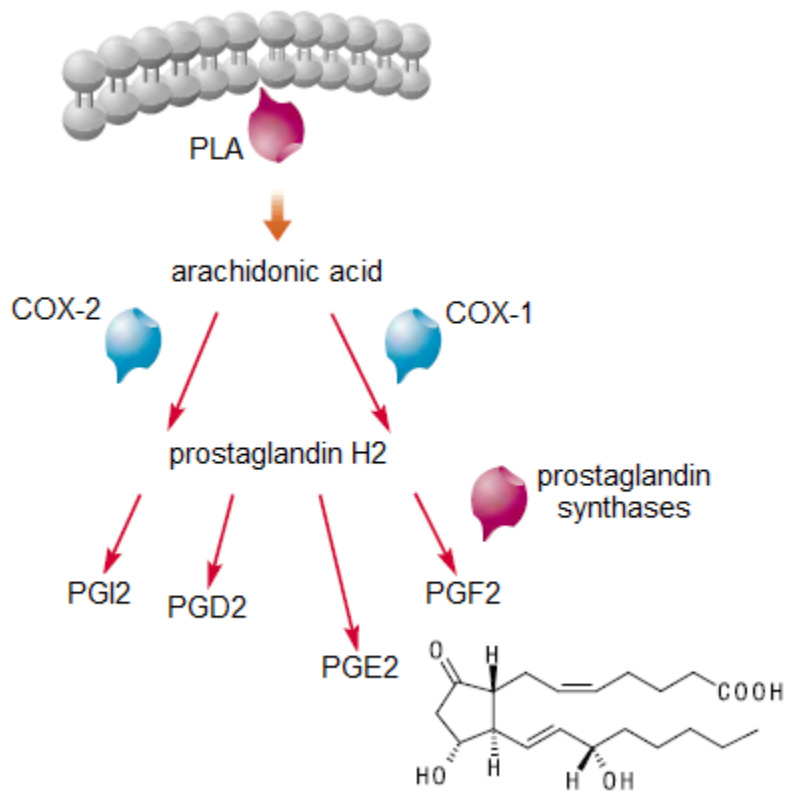


Figure 23^a. PGE2 synthesis

^a Adapted from HTRF Product and Services Catalog: Prostaglandin E2 Assay. ⁸⁴. Cisbio (c2009).

The cyclooxygenase-2 (COX-2) signaling cascade plays a significant role in the bystander process and is essential in mediating cellular inflammatory responses⁷⁶. COX enzymes play key roles in the biosynthesis of prostaglandins from arachidonic acid following its release from the plasma membrane by the action of phospholipase-A2. One of the most crucial events in the COX-2 cascade, is the activation of the mitogen-activated protein kinase (MAPK) signaling pathway. COX-2 is an inducible enzyme that

produces prostaglandins in inflammatory and tumorigenic environments. The COX-2-related pathway has been identified for the past several years as being the critical signaling link of the bystander phenomenon⁷⁶. However, a recent investigation of global gene expression in directly irradiated and bystander cells has also reported transcription factor NF- κ B as a dominant signaling hub in bystander response⁸².

COX-2 and its derived prostaglandin E2 (PGE2) have been shown to stimulate the growth of cancer cells and promote tumor angiogenesis⁸⁵, and COX-2 has repeatedly demonstrated pro-tumorigenic effects in the colorectum, which has been attributed to its PGE2 production. Increased levels of PGE2 have been reported both in human colorectal adenomas as well as carcinomas⁸⁰. Much evidence exists indicating the important tumor-promoting role of COX-2 in the process of tumorigenesis. However, there have been cases when the COX-2/PGE2 pathway has produced unexpected and counterintuitive results by acting in a tumor-suppressive manner. It is believed the reason for such opposing results can be related back to the level of PGE2 present in the cellular environment. It has been shown that the growth rate of human colorectal adenoma cells is actually stimulated by low concentrations of PGE2 and growth inhibited at high PGE2 concentrations⁸¹.

Normal cells in a multicellular organism are controlled by the coordinated regulation of complex signaling pathways—transforming signals from growth factors and cytokines into decisions that ultimately decide the cell's fate. Tumor cells acquire the ability to evade apoptosis through a variety of mechanisms. Usually, such changes within a cell result in an impaired ability to engage the intrinsic cell death machinery, or the mitochondrial pathway of apoptosis. COX-2 is typically over-expressed in colorectal

cancer cells, while PGE2 exerts pleiotropic effects in colorectal tumors—promoting proliferation, survival, angiogenesis, migration and invasion. While the exact mechanism by which the COX-2/PGE2 pathway suppresses apoptosis is not fully clear, it has been shown to increase the expression of BCL-2 via activation of the Ras-MAPK/ERK pathway. Under conditions of hypoxia—a situation typically conducive to cell death—PGE2 has been observed to promote cell survival in colorectal tumor cells by the stimulation of the Ras-MAPK signaling pathway⁸³.

COX-2-derived PGE2 can activate pro-survival pathways including the PI3K/AKT pathway⁸⁰, ERK signaling, cyclic adenosine monophosphate (cAMP)/protein kinase A signaling, and activation of epidermal growth factor receptor (EGFR) signaling. It has also been found to attenuate radiation-induced apoptosis in colorectal cancer cells by the activation of EGFR/AKT signaling and a mechanism that prevents the translocation of pro-apoptotic Bax to the mitochondria.

Angiogenic factors are also produced. In the case of colorectal cancer, over-expression of COX-2 induces the production of such angiogenic factors as vascular endothelial growth factor (VEGF) and basic fibroblast growth factor, which are instrumental in stimulating the formation of new blood vessels. COX-2-derived PGE2 also contributes to the pro-angiogenic effects of COX-2 over-expression, and has been reported to stimulate VEGF expression in colon cancer cells through the activation of HIF-1, a key regulator of VEGF expression⁸⁰. Adding to the countless roles of the COX-2/PGE2 pathway in tumorigenesis, PGE2 also has the ability to suppress immune responses, thereby allowing tumor cells to escape immunosurveillance. The gene function of p53 is not necessary for the bystander effect to occur, as experiments with

cells lacking normal p53 function—such as Chinese hamster ovary cells—have shown a large bystander response⁷⁶.

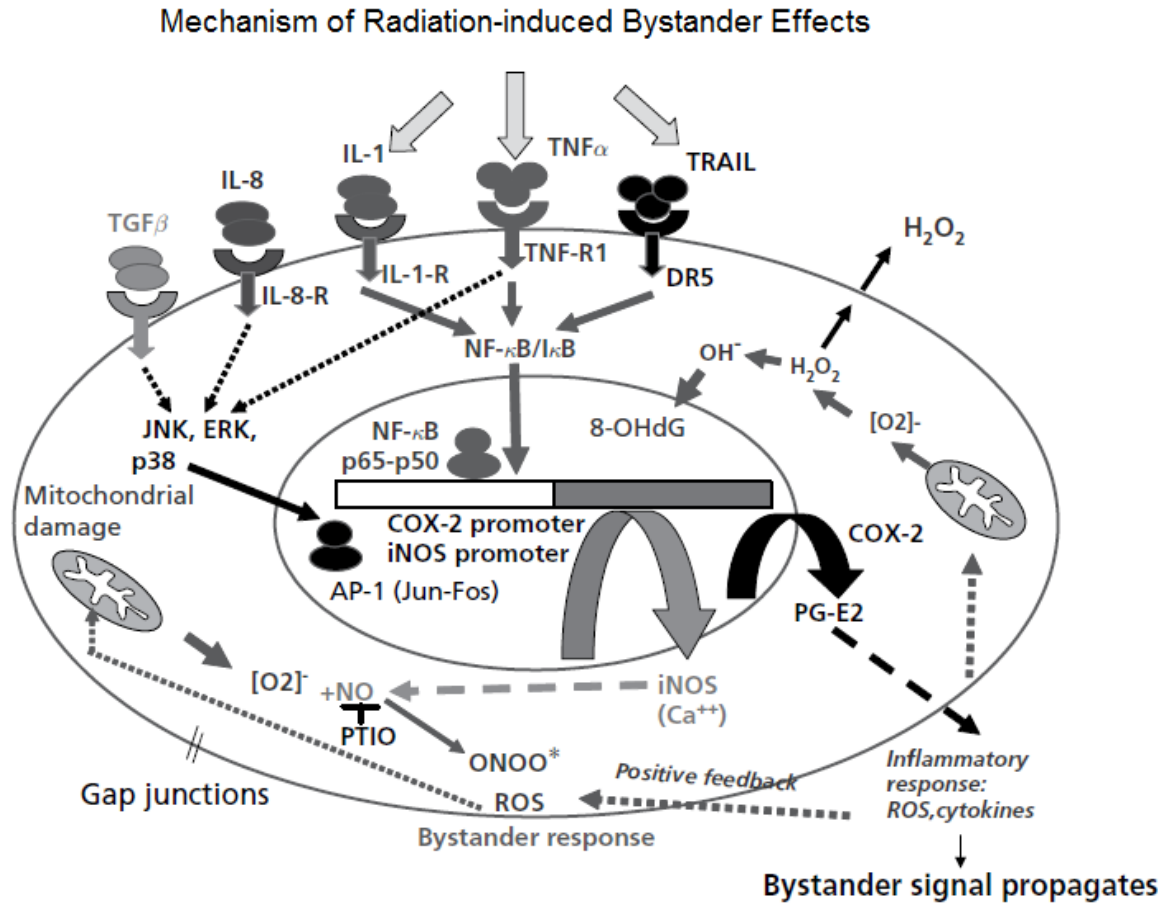


Figure 24^a. Current unifying model of radiation-induced bystander effect signaling pathways

^a Reprinted from Hei et al.⁷⁵. Mechanism of radiation-induced bystander effects: a unifying model. *J Pharm Pharmacol* (2008).

A number of variables define human radiation exposure such as dose, dose rate, radiation quality, exposed tissue type and volume, and dose distribution. The extent to which these variables have the potential to induce bystander effects in humans is not yet known.

Expression of Radiation-Induced Effects in Biological Systems

The nature of a biological system's response to exposure of ionizing radiation is, especially at the cellular level, a complex phenomenon that is still not well understood. If cellular damage is induced by radiation and is not adequately repaired, the cell may be prevented from surviving and reproducing or it may result in a viable cell that has been modified by suffering a change or mutation³. When cells are exposed to ionizing radiation the fundamental interaction between radiation and the atoms or molecules of the cells occurs initially with the manifestation of any possible biological damage to cellular functions being subsequently expressed. Irradiation of a cell can result in a number of possible outcomes and are classified as follows:

- No effect
- Division delay
- Apoptosis
- Mitotic death
- Genomic instability
- Mutation
- Transformation
- Adaptive response
- Bystander effect

Following exposure to a cytotoxic agent—whether it be through direct irradiation or bystander signals—a cell population faces a number of different possible consequences. This stands in opposition to the classically accepted DNA damage target theory, which summarizes the subsequent reaction of an irradiated group of cells as

adhering to an initiation, promotion and progression model. An alternative model has been proposed outlining the stages of induction, fixation and expression in the evolution of a cancer where tissue processes can influence the outcome both before and after DNA damage⁵⁵.

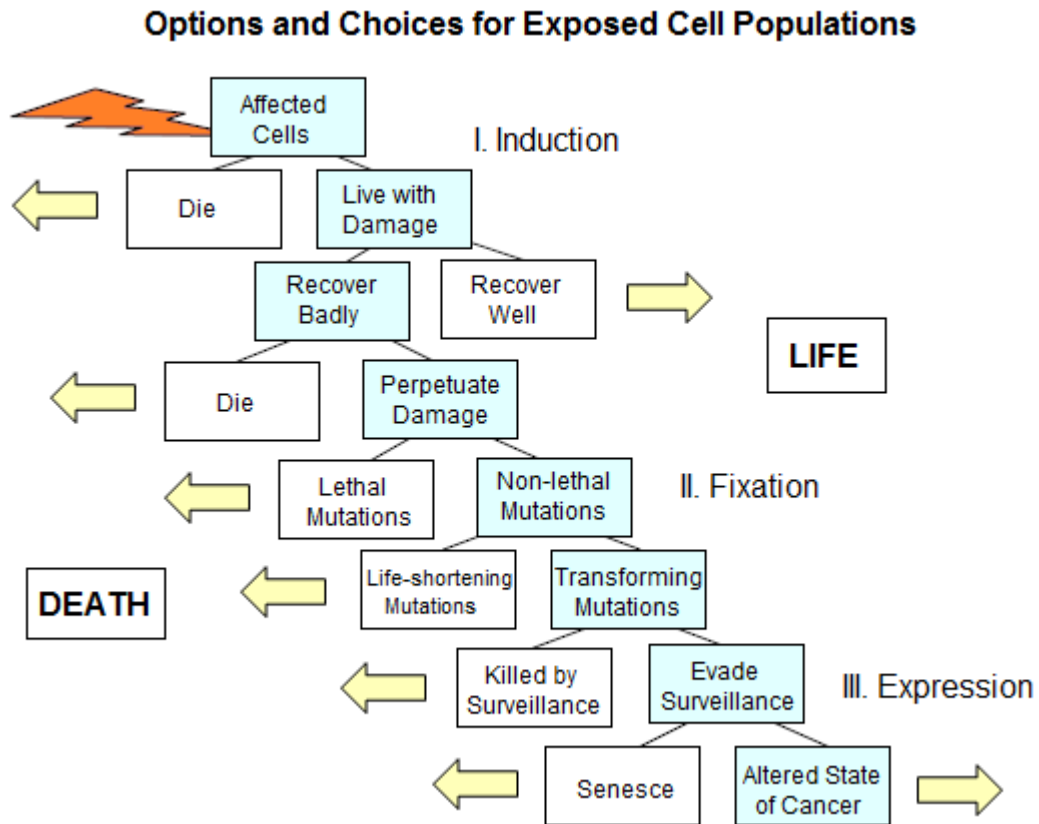


Figure 25^a. Schematic representation of possible outcomes for irradiated or damaged cells

^a Adapted from Mothersill et al. ⁵⁵. Radiation-induced Bystander Effects. *Oncogene* (2003).

The period of time between the occurrence of radiation-induced damage on the cellular level and the expression of the biologic effect in the tissue/organ level may be days, months, years or even generations apart. If the end point is cell killing, the biologic

effect may manifest within a matter of hours as the damaged cell attempts to divide. If the damage is oncogenic in nature, it may be decades before any recognition of cancer³.

Radiation-related effects as observed in humans on the macroscopic level are often divided into two broad categories—stochastic and deterministic. Deterministic effects are acute in nature and are generally observed soon after radiation exposure. Late effects of radiation exposure are stochastic in nature and, consequently, their expression is probabilistic—such as the induction of cancer.

Most environmental protection legislation is based on models that extrapolate predictions of potential health effects of low doses of radiation from high dose level data. This is particularly true in the field of radiation protection, where regulations are based on the extrapolation of cancer incidence rates from data acquired from the Japanese atomic bomb survivors to arrive at predicted cancer incidences for populations exposed to very low or chronic doses of radiation⁶². The Linear No-Threshold (LNT) model assumes that radiation-induced cancer risk possesses an intrinsic linear relationship to the dose of radiation. However, bystander effects have been experimentally shown to be independent of dose, negating any possibility of a simple linear relationship between the amount of radiation received by a biological system and the probability of cancer. It has been proposed, rather, that outcome is determined by the overall response to a signal or signal cascade generated as a consequence of radiation exposure to the system⁵⁵.

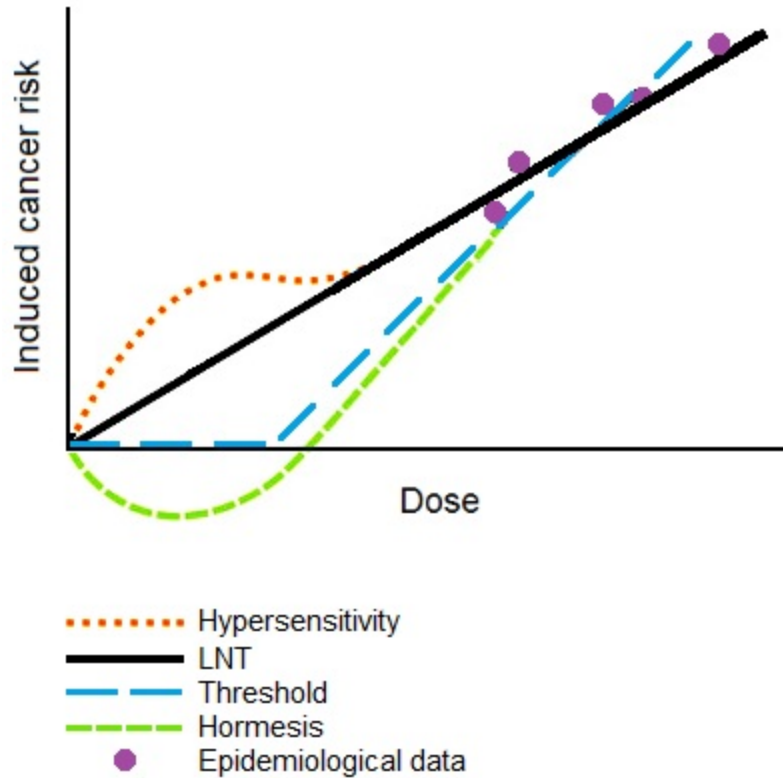


Figure 26^a. Different possible extrapolations for cancer risk

^a Adapted from Stabin. ⁵². Radiation Protection and Dosimetry (2007).

Although the LNT theory is endorsed by such influential bodies as the International Commission on Radiological Protection (ICRP), many studies have resulted in data suggesting otherwise. Such alternative reports indicate levels of no-effect and the idea that a threshold exists at which a response changes abruptly from tolerable to toxic⁶². The most controversial issue with the LNT model is, perhaps, that it denies the possibility of any beneficial effects of radiation. Contrary to this tenet of LNT theory, there has been experimental evidence of a phenomenon in which exposure to low doses of ionizing radiation has a beneficial effect—hormesis—resulting in less cancer induction or other deleterious effects in systems receiving low doses than in those deprived of radiation

exposure. Organisms show a great ability to adapt, as demonstrated experimentally by the many instances of induced resistance—with exposures to low doses of radiation providing protective resistance at higher doses⁶³.

Low-dose radiation induces DNA repair mechanisms responsible for the induction of cytogenic adaptive response and also stimulates the activities of oxidative radical scavengers to minimize the indirect damaging effects of subsequent ionizing radiation⁶⁴. An adaptive response is triggered by the release of certain proteins responsible for cell signaling. Consequently, there must be production of extracellular factors which transmit signals with the ability to produce these cellular responses. Because protein synthesis is required to initiate the cytogenic response, the metabolic state of the cells at the time of irradiation is an important factor in the production of an adaptive response at low-dose exposures.

CHAPTER III

METHODS AND MATERIALS

Several preliminary studies were performed before the primary experiments could be carried out. Many basic laboratory techniques and procedures were first established such as cell culture, optimization studies for the MTT and caspase 3 assays—including standardization of the medium transfer technique—and basic operation of laboratory equipment such as the ^{137}Cs irradiator and multi-mode microplate reader. Also, an HT-29 cell survival curve was generated and plotted against a range of radiation doses—which required determination of the plating efficiency by means of clonogenic assay and cell staining. In addition to basic operation of the ^{137}Cs irradiator, a comprehensive study was done in order to characterize the dose rate profile inside the irradiation cavity—a requirement to accurately calculate exposure times and source-to-flask distances of irradiated cell cultures. This evaluation was performed using an ionization chamber. After the preliminary studies were completed, the primary experiments could begin.

HT-29 human colon adenocarcinoma cells were externally irradiated with ^{137}Cs γ -rays to investigate the effects of dose and dose rate to irradiated cell cultures on the metabolic activity of unirradiated responder cells by means of medium transfer. The ICCM from flasks of irradiated cell cultures was collected six hours after irradiation, filtered, and transferred to unirradiated responder cells in order to isolate the effect of soluble factors secreted by the dying cells. The cells receiving the irradiated conditioned medium (ICCM) are called responder cells, as it is by assessing the reactions of these cells in which the bystander effect is measured. Medium transfer experiments rule out

oxidative damage or any other possible effects of radiation on the target cell and provide clear evidence for the presence of radiation-induced factors secreted by the irradiated sample. Medium transfer experiments do pose some limitations which are important to consider—the signal must be diffusible, able to pass through the filter unaltered, and to persist in its original state during the collection and transfer processes. Though, it has been reported in previous medium transfer studies^{5,91} that the bystander factor does have the ability to pass through a 0.22 µm filter, is present in the irradiated cell culture medium as early as one hour following irradiation, and persists for several hours thereafter.

A microtetrazolium (MTT) colorimetric assay was used to assess the metabolic reaction of responder cell populations to growth factors and external stimuli present in the medium of irradiated cells. The MTT assay is read by a spectrometer and the results are quantified in units of absorbance—serving as the endpoint in this study by which the magnitude of the bystander effect is assessed. The use of MTT assay was preferred in this study rather than the traditional clonogenic assay technique because the clonogenic assay is dependent on colony formation and, consequently, is reliant upon those cells which have maintained reproductive integrity—usually measured with a week or two following the irradiation event. This is an important factor to consider when studying the early responses of medium-borne bystander signals because cells which have lost their reproductive potential either immediately following irradiation or within a few subsequent cell divisions are still, at that time, viable, but will not be accounted for in a clonogenic assay²². Although these cells are headed toward eventual cell death, they will remain metabolically active during the early response time frame in which bystander

effects are elicited in the responder cells. Therefore, because the MTT assay measures metabolically active cells, it was the preferred method for this study.

To investigate the mechanism by which the bystander response is elicited in the non-targeted population, a fluorescent assay was performed to detect caspase 3 activation—which has recently been shown to be a key regulator of growth-promoting signals generated from dying cells¹. This procedure was performed in parallel to the MTT assay, providing direct correlation between the level of caspase 3 activation to the early metabolic responses observed in the unirradiated responder cells induced by medium-borne signaling factors present in the ICCM.

Mammalian Cell Culture

Mammalian cell culture refers to the removal of cells from an animal to, subsequently, be grown in a favorable artificial environment. The technique of using cultured cells to study radiation effects was developed in 1957 by Theodore Puck and his colleagues at the University of Colorado¹⁶. This method allows for quantitative assessment of cultured mammalian cells through controlled laboratory conditions in which the effects of various agents on cell survival may be studied.

Originally, a tissue specimen is taken directly from a tumor and disaggregated enzymatically with the use of trypsin before cultivation into what is referred to as the primary cell culture. Once the primary culture cells reach confluence, they are transferred, or passaged, to a new vessel to allow for continued growth, resulting in subcultured cells. After the first subculture, the primary culture becomes known as the cell line. Single-cell suspensions used in radiobiological experiments are commonly

derived from an established cell line. Each time that a cell line is subcultured it will grow back to confluence, requiring routine maintenance to prevent the cell density from increasing beyond the physical capacity of the vessel and the nutritional capacity of the growth medium.

Normal cell lines are genetically determined to divide a limited number of times before losing their ability to proliferate—an event referred to as ‘senescence’. However, some cell lines—such as those that are cancerous—become immortal through a process called transformation. Transformation can be a spontaneous event, or it may be induced chemically or virally. After having undergone this process, the cells possess the ability to divide indefinitely and are defined as a continuous cell line.

If these cells are seeded into a culture dish containing a suitable complex growth medium and maintained at 37°C under aseptic conditions, they provide for a continually replenished stock supply of cells from which to furnish laboratory experiments. Most cells are adherent and attach to the surface of the vessel in which they are cultured, while others grow suspended in the culture medium. Immediately after reseeding, or passaging, cells enter what is known as the ‘lag period’, which is marked by a lack of growth. This time frame is relatively short and allows cells to recover from the process of trypsinization and replantation—enabling them to reenter the cell cycle. Once the cell cycle is resumed, exponential cell growth marks the period known as the ‘log phase’. During this time, the cell population doubles over a definable period. The doubling time is characteristic to each cell type and provides a quantitative unit by which to assess cell growth³.

This study was conducted using HT-29 cells. The HT-29 cell line was originally isolated by Fogh and Trempe¹⁷ and established in 1964 from a forty-four year-old Caucasian woman with colorectal adenocarcinoma¹⁸. HT-29 cells are anchorage-dependent and grow adherently in cell culture, forming a monolayer. The doubling time of HT-29 cells has been observed to be between eighteen and twenty-four hours.

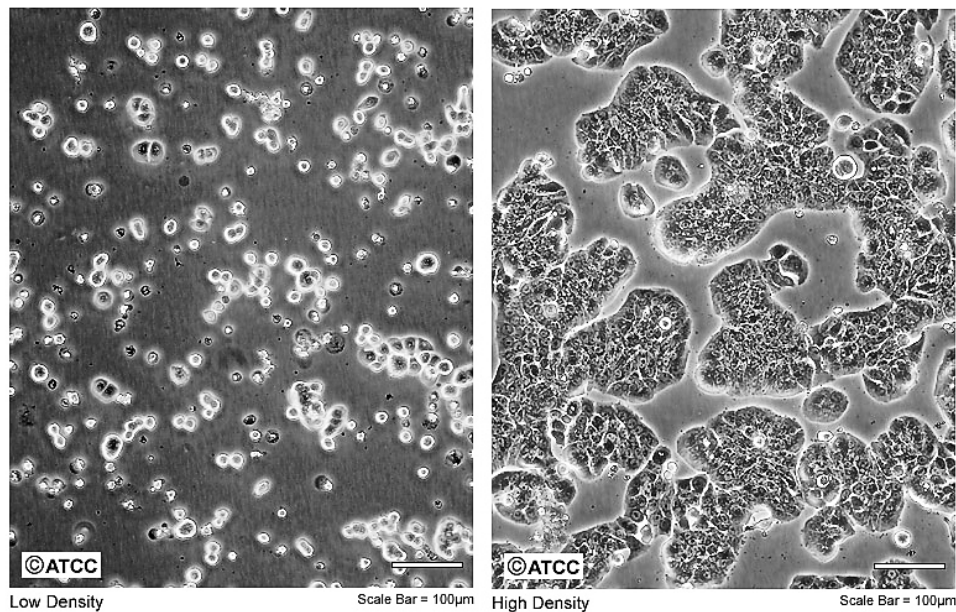


Figure 27^a. Morphology of HT-29 cells as viewed under a light microscope

^a Reprinted from ATCC product catalog: HT-29 cell line. ¹⁸. American Type Culture Collection (2012).

HT-29 cells were obtained from the American Tissue Culture Collection (ATCC). Reagents used for cell culture were obtained from Gibco-Life Technologies. All cell culture was performed in a class two laminar flow cabinet. Stocks were maintained in T75 flasks in 20 mL medium. The cell line was adapted to grow in Dulbecco's Modified Eagle Medium: Nutrient Mixture F-12 (DMEM: F-12) containing 10% fetal bovine serum.

Cell Culture Protocol

1. Aspirate medium from the cell monolayer

2. Add 10 mL PBS; tilt flask and wash over cells

To avoid dislodging cells, pipette the saline onto a wall of the culture flask—not directly over the cells themselves.

3. Aspirate the PBS

4. Repeat steps 2 and 3

5. Add 3 mL trypsin; tilt flask and cover cells completely

Leave trypsin on the cells for only 10-30 seconds,

6. Aspirate the trypsin

7. Incubate the cells for 3-5 minutes at 37°C

Observe the cells both macroscopically and microscopically for evidence of the monolayer being released from the flask surface

8. Add 10-20 mL fresh growth medium and pipette vigorously to break cell clumps

Ensure the cells are well-suspended and evenly distributed in the medium.

9. Remove an aliquot of cells to a centrifuge tube

10. Micro-pipette cells onto hemocytometer for manual counting with light microscope

11. Calculate dilution required to give desired concentration

12. Remove calculated volume of cells from original flask to a new culture vessel

13. Add the calculated volume of fresh growth medium to the new culture vessel

14. Incubate at 37°C

***Invitro* Cell Survival Curve**

Survival curves are fundamental to understanding experimental radiobiology. A cell survival curve plots the relationship between radiation dose received by cells exposed to a source of ionizing radiation and the proportion of cells that survive. Reproductive cell death, or survival, is a common end point measured with cells cultured *in vitro*. Cell death is defined as having lost reproductive integrity, the ability to divide indefinitely and generate a large number of progeny. A surviving cell is defined as having retained its reproductive integrity and, consequently, its capacity for sustained proliferation. The ability of a single cell to produce a large colony is a cell culture characteristic that is used as a marker for reproductive integrity.

Subcultures of cells seeded from an actively growing stock culture will repopulate the new culture vessel to confluence. Once a cell is seeded and begins to grow, each completed cycle results in a cellular division—a progeny cell. This process is repeated until a colony is formed. Each colony is formed from the progeny of a single ancestor cell. Consequently, the number of cells seeded corresponds to the number of colonies counted—parameters from which the plating efficiency can be calculated. Ideally, if 100 cells were plated, the number of colonies counted would also equal 100. However, this does not reflect the intrinsic nature of cell growth patterns. Due to several factors such as suboptimal growth conditions, uncertainties in cell culture technique and naturally occurring cell death, the plating efficiency will not equal 100 percent. Rather, for a nominal 100 cells seeded, the number of colonies counted may be expected to be in the range of fifty to ninety³.

$$\text{Plating Efficiency (PE)} = \frac{\text{Colonies counted}}{\text{Cells seeded}} \times 100 \quad (1)$$

If a parallel culture is exposed to an experimental treatment, the effect of the treatment on the cell culture can then be observed by comparison. In radiobiological studies, the causative agent of potential cell damage is radiation. Survival curves for mammalian cells are typically rendered with radiation dose plotted on a linear scale and surviving fraction on a logarithmic scale.

$$\text{Surviving fraction} = \frac{\text{Colonies counted}}{\text{Cells seeded} \times (\text{PE}/100)} \quad (2)$$

Although survival curves allow for a relatively simple and convenient quantitative assessment of direct radiation exposure effects on cells, they do not provide a specific, biological explanation accounting for the intricate physiological events which have occurred. Nevertheless, cell survival curves are a widely used analytical tool in radiobiological experiments.

In this study, an HT-29 cell survival curve was generated to provide assessment of cell survival over a range of ^{137}Cs γ -ray doses with clonogenic survival assessed following a 10 days incubation period. Irradiated cell cultures were placed symmetrically on the rotating turntable within the irradiator cavity and, thus, each flask was exposed to the same dose rate of 1.7 Gy/min.

Plating Efficiency Protocol

1. Split stock cells—refer to cell culture protocol

Desired concentration is 200 cells per 5 mL of growth medium.

Final dilution = 40 cells per mL

2. Remove 5 mL of final dilution and add to a new T25 cell culture flask
3. Repeat previous step, plating a total number of 4 flasks
4. Incubate T25 flasks for 10 days at 37°C
5. After 10 days, remove flasks from incubator
6. Aspirate medium from the cell monolayer
7. Add 2 mL of 70% ethanol to each flask

This “fixes” cells to prevent further growth.
8. Allow 15 minutes to pass
9. Dispose of ethanol
10. Add ~1 mL staining dye to each flask
11. Allow 15 minutes to pass
12. Dispose of dye
13. Rinse out each flask with tap water
14. Using a counter and a lab marker pen, count each visibly stained colony per flask
15. Calculate plating efficiency

Cell Survival Curve Protocol

1. Label 20 T25 flasks according to group—each group consisting of 4 flasks

Group 1 = 0 Gy

Group 2 = 2.5 Gy

Group 3 = 5 Gy

Group 4 = 10 Gy

Group 5 = 15 Gy

2. Split stock cells—refer to cell culture protocol

Desired concentrations are as follows:

Group 1 (x4 flasks) = 200 cells per 5 mL

Group 2 (x4 flasks) = 200 cells per 5 mL

Group 3 (x4 flasks) = 600 cells per 5 mL

Group 4 (x4 flasks) = 2,000 cells per 5 mL

Group 5 (x4 flasks) = 20,000 cells per 5 mL

3. Remove calculated concentrations and add to labeled T25 cell culture flasks

4. Incubate plated T25 flasks at 37°C overnight

5. The following day, calculate exposure times required for each group to be irradiated in

MARK I ¹³⁷Cs irradiator in order to achieve specified doses

Place flasks on rotating turntable so as to provide even dose distribution.

6. Incubate flasks for 10 days post-irradiation

7. Stain cells and count colonies formed—refer to plating efficiency protocol, steps 5-14

8. Calculate surviving fraction

9. Plot cell survival curve

HT-29 Cell Survival Curve

Cell survival data are generally plotted as the logarithm of surviving fraction versus dose. Hypothetical mathematical models based on the known mechanisms of lethality are applied to curves for ease of standardized interpretation, comparison, and analysis. Though no model exists that can truly account for the complex biological mechanisms that define the curve., the linear-quadratic model is currently the most popular model used to qualitatively describe the shape of survival curves.

The linear quadratic model has evolved from formulas having roots in target theory and assumes there are two components to cell killing by radiation. The first being proportional to dose ($e^{-\alpha D}$) with a linear shape on the curve representing a single lethal event and is proportional to dose. The second component is proportional to the square of the dose ($e^{-\beta D^2}$) with a curved quadratic shape representing the dual action of radiation in which two hits result in one lethal event.

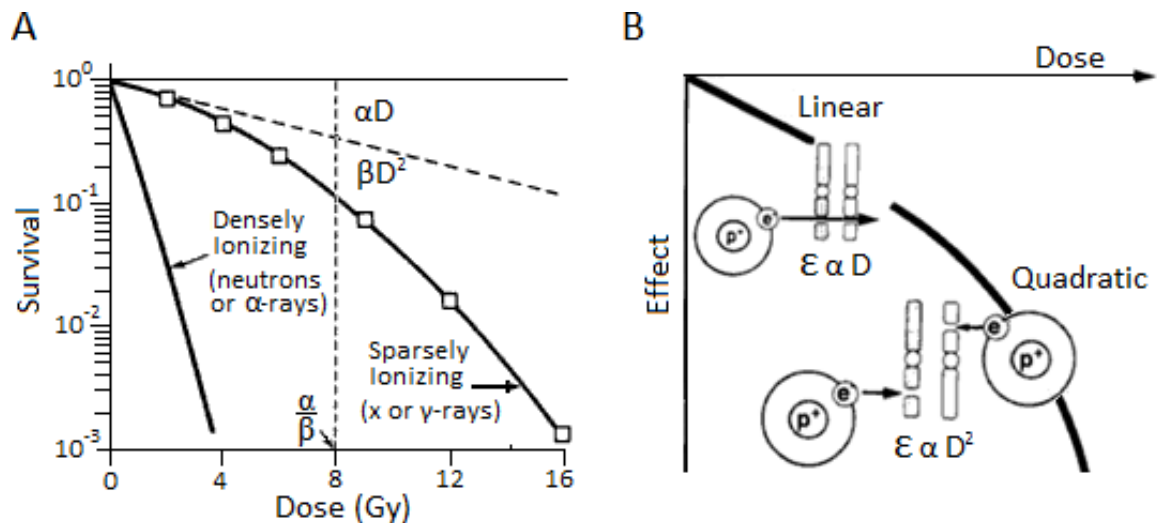


Figure 28^a. Shape of mammalian cell survival curve A) after exposure to radiation; B) relationship between chromosome aberrations (radiation dose) and cell survival

^a Adapted from Hall. ³. Radiobiology for the Radiologist (2006).

The overall survival curve of an asynchronous cell population is often described by two parameters—the α and β coefficients. Linear-quadratic analyses of survival data for asynchronous human tumor cells exhibit a wide variation in alpha coefficients with much less range between beta coefficients. For example, one study reported values for HT-29 (colon), OVAR10 (ovary), and A2780 (ovary) tumor cells with alpha coefficients of 0.03, 0.16, and 0.47 Gy⁻¹, respectively, and $\sqrt{\beta}$ coefficients of 0.23-0.27 Gy⁻¹ for asynchronous populations. The differences in interphase radiosensitivities has been shown to be determined primarily by the single-hit mechanism, indicating a dominant role for the single-hit inactivation, α , in the determination of intrinsic radiosensitivity of human tumor cells to ¹³⁷Cs γ radiation—especially at doses of 2 Gy and less¹⁰⁰.

Survival curves have been well established for many cell lines with the most radioresistant having shoulders with broad curves while the most radiosensitive cell lines have a linear appearance. The results of this study are in agreement with previously published HT-29 cell survival curves^{3,100} in which HT-29 cells are reported to be radioresistant—as displayed by the characteristic broad shoulder. Thus, according to the survival curve model illustrated in Figure 28, asynchronous HT-29 cell cultures exposed to lethal doses of ¹³⁷Cs γ radiation primarily die a mitotic death.

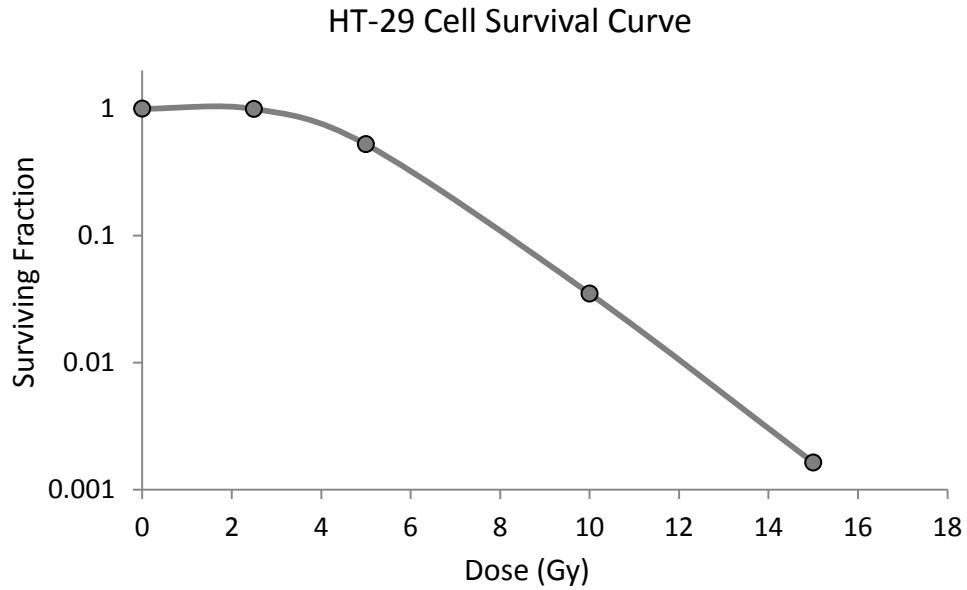


Figure 29. Survival curve of HT-29 cells exposed to ^{137}Cs γ radiation

MARK I ^{137}Cs Irradiator

The Shepherd Mark I Cesium-137 Irradiator Model 68 is a self-shielded, self-contained irradiation device designed primarily for biomedical research applications. Its purpose is to provide laboratory investigators with a convenient, accurate and reliable source of ionizing radiation in a controlled experimental environment—serving as a useful research tool for those studying the effects of radiation on biological samples, such as *in vitro* cell culture or small animals. The Mark I ^{137}Cs Irradiator was used for all irradiations performed in this study.



Figure 30. Shepherd MARK I model 68 ¹³⁷Cs irradiator

Vanderbilt University, Radiation Biology Laboratory, Nashville, TN; 21 Apr 2012.

¹³⁷Cs has a half-life of 30.04 years¹⁹ and decays by beta emission. It decays from a metastable nuclear isomer of barium-137: barium-137m. ^{137m}Ba decays by isomeric transition with the emission of a 662 keV photon at approximately ninety percent frequency¹⁹. The other five percent directly populates the ground state, which is stable. ^{137m}Ba has a half-life of about 153 seconds and is responsible for the γ -ray emissions—ultimately providing the source of external irradiation to the biological samples placed inside the ¹³⁷Cs irradiator.

The MARK I Irradiator was installed in the Vanderbilt radiation biology lab in September 1981 with a ^{137}Cs source activity of 1.85×10^{14} Bq (5,000 Ci). At the time of this study, almost exactly thirty years had passed since its installation—equivalent to one half-life of ^{137}Cs . Therefore, the activity contained within the source during the irradiations performed in this study was approximately 9.25×10^{13} Bq (2,500 Ci). Samples placed within the internal cavity are irradiated on a turntable adjacent to a ^{137}Cs rod source. The radioactive source in the irradiator is encased within two stainless steel tubes with a total thickness of 3.8 mm; therefore, no beta radiation can penetrate through the source encapsulation—ensuring the dose delivered to the sample is by γ -ray emission only²⁰. The turntable inside the irradiation cavity measures 30 cm in diameter, however, the total depth of the cavity measures approximately 35.5 cm along the center from the door to the source encapsulation. Therefore, a space of about 5.5 cm separates the edge of the turntable and the source encapsulation. The height of the cavity is approximately 30 cm. The irradiator was operated according to the guidelines indicated in the operating manual.

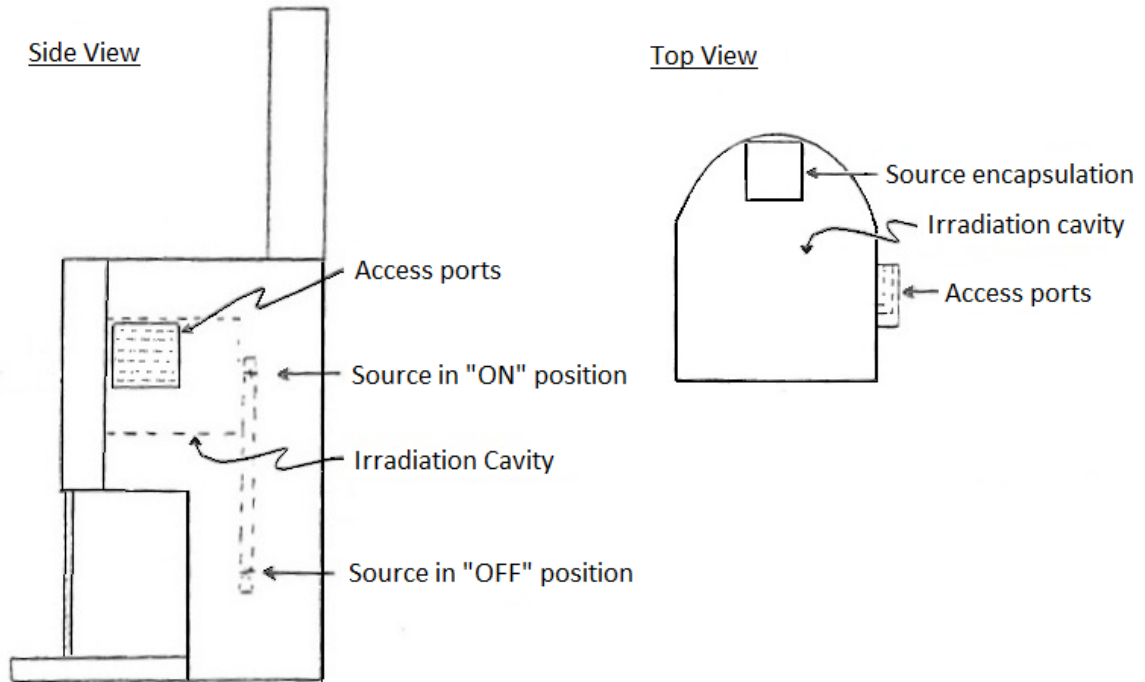


Figure 31^a. Schematic of Shepherd MARK I model 68 ¹³⁷Cs irradiator

^a Adapted from MARK I ¹³⁷Cs irradiator [operating manual]. ²⁰. JL Shepherd (1983).

¹³⁷Cs Irradiator Dose Profile

In order to characterize the dose and dose rate profiles within the irradiation cavity, a series of measurements were taken with an ionization chamber along the center line of the cavity beginning at contact with the source encapsulation and concluding at the far edge of the turntable closest to the door. As measurements of this nature were not provided by the manufacturer, a unique experimental setup was constructed for this purpose. A T25 flask was filled with 50 mL of water to simulate the growth medium environment in which cell cultures are subjected during irradiation. The ionization chamber was placed mid-way down the center of the flask in contact with the exposed wall's surface. As the flask's cap had to be removed to allow for the ion chamber's wiring, electrical tape was used to both hold the ion chamber in place and to prevent

water spillage. To hold the flask upright and provide stabilization, a stand was fashioned by attaching the bottom of the flask to a square piece of acrylic. The wiring was then run out of the irradiator through the access port and connected to the electronic detector.

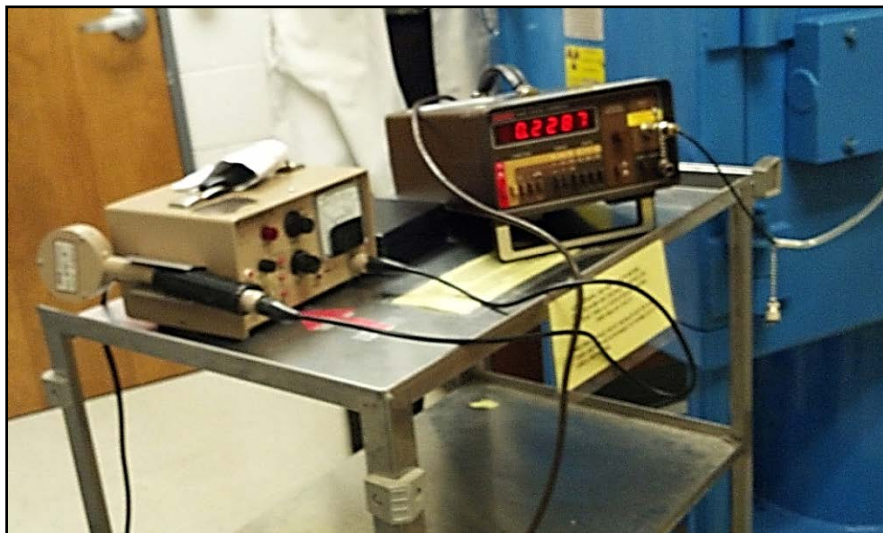


Figure 32. Ionization chamber setup for ^{137}Cs dose profile measurement

Vanderbilt University, Radiation Biology Laboratory, Nashville, TN; 13 Jan 2012.

A series of measurements were taken at seven positions. The distances were measured from the exposed T25 flask wall to the source encapsulation tube. The first position was at zero distance in which the flask and tube were placed in contact. The total number of measurements taken at each position was determined by the variability between the readings. If there was less than 5 % error between the values, no further measurements were taken at that position and the readings were averaged. The ionization chamber was then calibrated, and the raw data was converted from measurements of electric charge to units of absorbed dose.

Table 2. Ionization Chamber Measurements of ^{137}Cs Irradiator

Position	Source Distance (cm)	Average Reading (C)	Dose Rate (Gy/min)
1	0	0.8038×10^{-8}	25.29
2	2.5	0.3437×10^{-8}	10.85
3	5.0	0.2173×10^{-8}	6.86
4	12.5	0.09485×10^{-8}	2.99
5	20.0	0.05720×10^{-8}	1.81
6	28.0	0.03835×10^{-8}	1.21
7	33.0	0.03045×10^{-8}	0.96

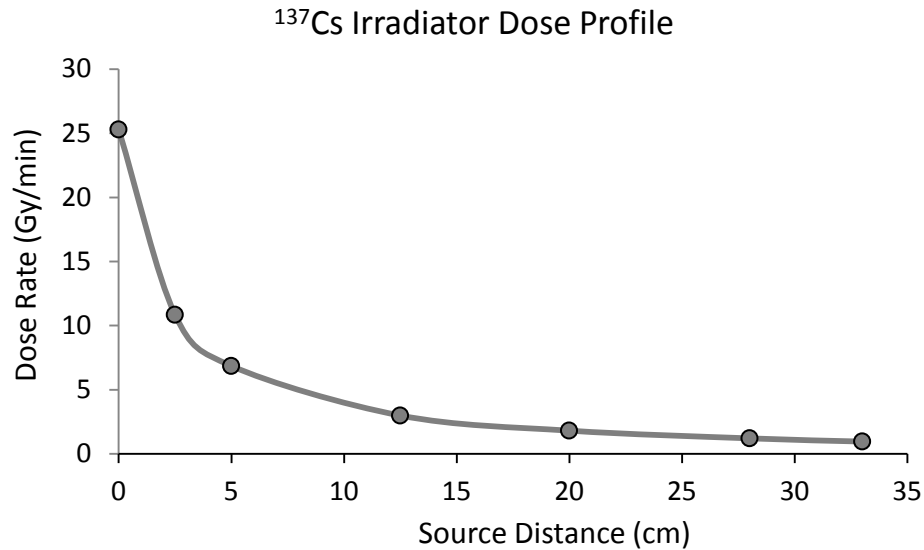


Figure 33. Dose profile of ^{137}Cs irradiator

Microtetrazolium (MTT) Assay

The effects of radiation on cell culture as a function of dose can be quantitatively determined using a number of different assay techniques. The measurement of cell growth is an essential tool used in cell-based experimental research studies. Specific indicators of cell survival within a sample population—such as cell proliferation and viability—can be evaluated by assaying for vital functions characteristic to healthy or growing cells.

The predictive assay most extensively used for *in vitro* radiobiological experiments is the clonogenic—or colony formation—assay. This technique is based on the ability of a single cell to grow into a colony. After being subjected to an experimental treatment that has the potential to cause lethally damaging effects—such as radiation exposure—this assay detects cells in the sample which have retained their reproductive integrity and multiplied to produce a large number of progeny. While the colony

formation assay is generally considered the premium experimental test system for *in vitro* radiation studies, problems do exist with this technique including a low assay success rate, technical difficulties of the assay which limit clinical usefulness, and the long period of time required to generate a result²⁵.

The microtetrazolium (MTT) colorimetric assay measures the metabolic activity of viable cells in culture and can be used as an estimation of cell survival. It is less labor intensive than the clonogenic assay and overcomes the need for cells to grow into colony formations because it measures the reduction of tetrazolium salts to a formazan end-product. The MTT assay has been widely used in previous studies measuring *in vitro* drug cytotoxicity and has also been successful in radiosensitivity experiments²².

The MTT assay is a rapid colorimetric analysis that quantitates viable cell number in a population by measuring mitochondrial enzyme activity through the reduction reaction of the soluble yellow 3-(4,5-dimethylthiazol-2-yl)-2,5-diphenyltetrazolium bromide salt by mitochondrial succinate dehydrogenase. Thus, tetrazolium salts, such as MTT, measure the activity of various dehydrogenase enzymes²³. MTT enters a viable cell and passes into the active mitochondria where the tetrazolium ring is cleaved and reduced to an insoluble, dark purple-colored formazan product. The cells are then solubilized with an organic solvent—or buffer—and the released solubilized formazan reagent is quantified in units of absorbance by use of a scanning multi-well spectrophotometer. The absorbance measured is directly proportional to the degree of activation in cells. Because this process requires active mitochondrial function, the reaction only occurs in living cells.

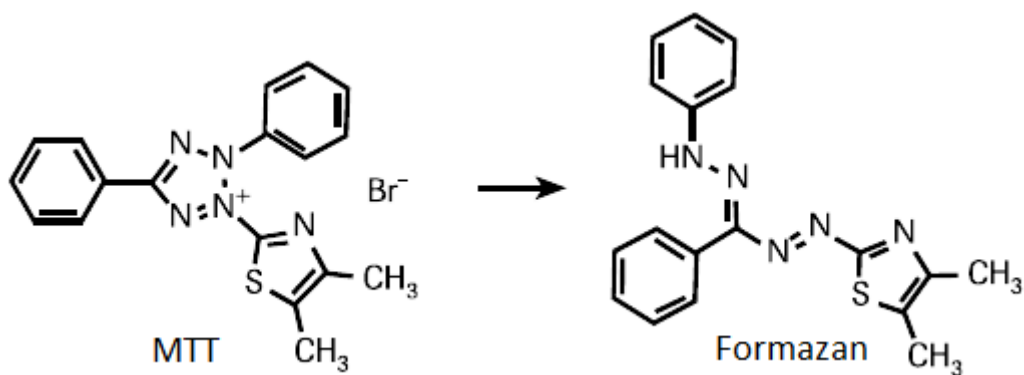


Figure 34^a. Chemical metabolization of MTT to a formazan salt by viable cells

^a Reprinted from Cell Proliferation Kit I (MTT) [package insert].²⁴ Roche (2005).

When the amount of purple formazan produced by cells treated with an assaulting agent is compared with the amount of formazan produced by untreated control cells, the effectiveness of the assaulting agent can be deduced and a dose-response curve can be generated. Absorbance values that are lower than the control cells indicate a reduction in the metabolic rate of the cellular population. Conversely, a higher absorbance value indicates an increase in cellular metabolic activity.

Unlike traditional colony formation techniques, the MTT assay is sensitive to low cell numbers. However, absorbance readings are non-linear at excessively high cell numbers. Consequently, if cell cultures are allowed to grow past confluence, the absorbance measurement will not be an accurate correlation—which is why it is essential to first perform a preliminary optimization assay to determine the best range of plating densities. MTT assay results can also be affected by variables in the cell culture environment such as pH level and glucose depletion—which can alter cellular metabolic processes. The MTT assay is also dependent on the substrate incubation period, as the formazan end-product can degenerate over time²².

Cell viability studies provide an evaluation of healthy cells within a sample but cannot distinguish between actively dividing and quiescent cells. An increase in viability denotes cell growth, while a decrease in viability may be interpreted as either the result of toxic effects caused by the assaulting agent or suboptimal culture conditions¹¹. Unlike cell viability, cell proliferation analysis provides a measurement of actively dividing cells within a sample.

Most viability assays are based on one of two characteristic parameters: metabolic activity or cell membrane integrity of healthy cells¹¹. Metabolic activity of cell populations is typically assessed via incubation with a tetrazolium salt that is cleaved into a colored formazan product by metabolically active cells. Cell viability studies can also be performed by use of staining methods—sometimes referred to as dye-exclusion assay. However, these protocols include washing steps which inherently increase processing time and sample variation, unlike MTT assay which does not require washing. Consequently, MTT analysis provides a significant advantage to that of staining methods for determination of cell viability. In this study, an MTT colorimetric assay was used to assess the early metabolic responses of HT-29 cell populations to factors and external stimuli present in the ICCM.

MTT Assay Optimization

A preliminary optimization study was first necessary in order to determine the most optimal cell plating number to use for each assay. A range of cell seeding densities were plated in a 96-well plate, and following the 24 hour incubation period, the MTT assay was carried out according to protocol. After establishing the optimal cell plating

density, a level of control was provided over the experiment by ensuring the plated cells did not reach confluency and, instead, remained within the range of linear response.

Based on these findings, as shown in Figure 35, the number of cells plated within all 96-well microplates used throughout this study was chosen to be 5,000 cells/well.

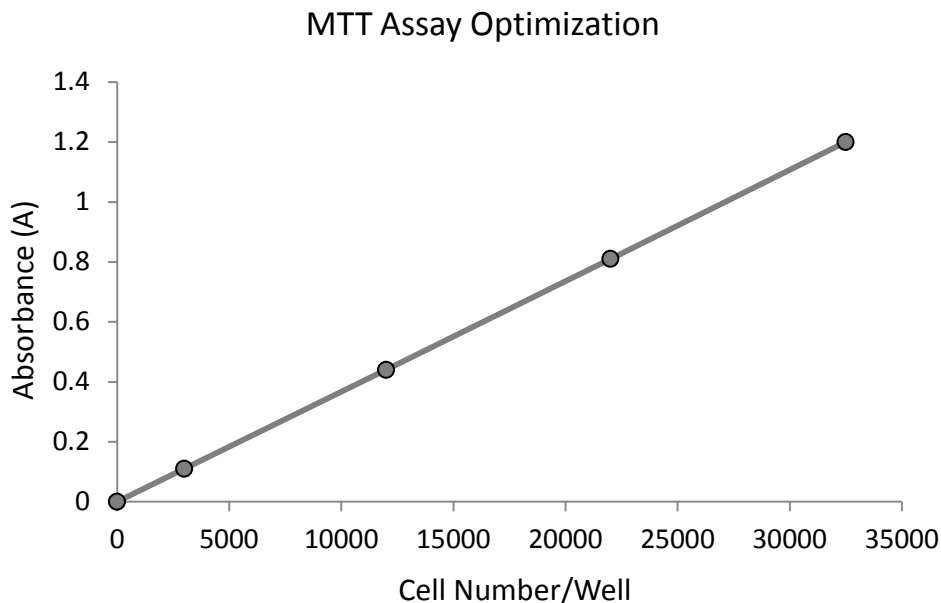


Figure 35. MTT assay optimization; determination of optimal cell plating density

Caspase-3/7 Assay

In cancer treatment, apoptosis is a well-recognized cell death mechanism through which cytotoxic agents kill tumor cells. It has been recently reported that dying tumor cells use the apoptotic process to generate potent growth-stimulating signals after exposure to radiation¹. These findings are of great importance to radiotherapeutic applications as they imply the possibility of stimulated cancer cell growth and tumor repopulation after radiation treatments. It was further reported that activated caspase 3—

historically known as the master executioner during apoptotic cell death—is also involved in cell death-mediated growth stimulation¹.

As caspases become activated, they cleave specific substrates—either by activating or inactivating them. Thus, an indication that caspase activation has occurred in a cell can be determined by the detection of caspase substrates. Inhibition of one cell death pathway—such as apoptosis—will mostly not restore clonogenic survival. Instead, a shift will occur from a particular mode of cell death to another phenotype²⁶. Therefore, it is crucial that cell death is measured by more than one means through the implementation of complementary methodologies²⁶. Thus, in addition to assessing the metabolic response of cells exposed to ICCM, the level of caspase-3 activation in responder cells was also measured.

In this study, a caspase-3/7 activation assay (Invitrogen, CellEvent Caspase-3/7 Green Detection Reagent) was used to investigate what role, if any, the caspase-3/7 signaling pathway plays in the observed bystander responses elicited in HT-29 cell culture through ICCM and to determine if the magnitude of caspase-3/7 activation correlates to the level of metabolic activity observed in correlating samples.

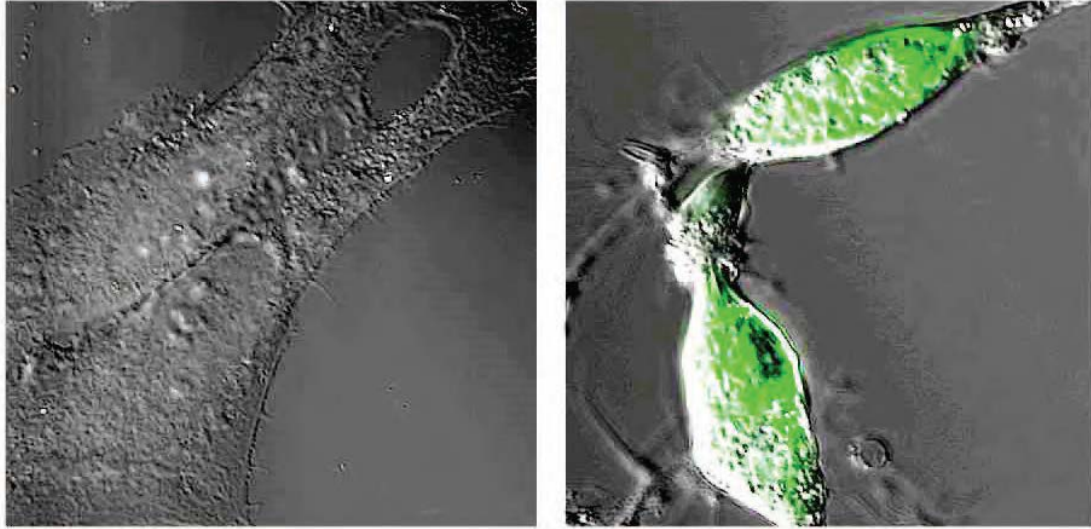


Figure 36^a. CellEvent Caspase-3/7 Green Detection Reagent expression; staurosporine-induced apoptosis in cells expressing activated caspase 3/7 fluoresce bright green (right), while control cells do not show any signal (left)

^a Reprinted from CellEvent Caspase-3/7 Green Detection Reagent [package insert].³⁰ Invitrogen (2011).

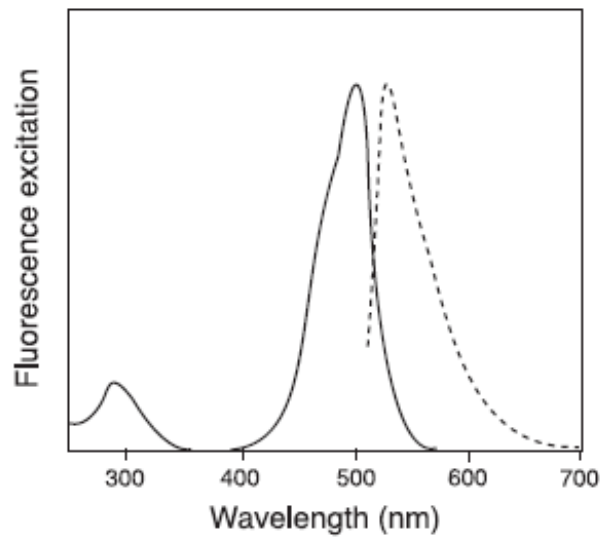


Figure 37^a. Fluorescent excitation and emission spectra of CellEvent Caspase-3/7 Green Detection Reagent after reaction with activated caspase-3 or 7, bound to DNA

^a Reprinted from CellEvent Caspase-3/7 Green Detection Reagent [package insert].³⁰ Invitrogen (2011).

Positive Control with Staurosporine Treatment

A positive control study was first conducted before experimental implementation of the caspase-3/7 detection reagent. Positive controls were required in order to demonstrate that a response could be induced and detected within the cells—thereby, providing a level of quality control to the experimental method. Staurosporine, obtained from Invitrogen, was used to induce apoptosis within HT-29 cell culture populations. A previous study reported that when HT-29 cells were incubated with staurosporine for twenty-four hours, apoptosis was first induced at a concentration of 0.1 μM and observed to progressively increase with higher staurosporine concentrations up to 1.0 μM —the maximum concentration that was studied in the experiment⁸⁸. At 1.0 μM concentration, apoptosis was induced in approximately forty-five percent of cells in a culture population. Cell plating densities were reported to be 500,000 cells per 100 cm^2 culture dish.



Figure 38. Staurosporine solubilization with DMSO

Vanderbilt University, Radiation Biology Laboratory, Nashville, TN; 12 Mar 2012.

Caspase-3/7 Assay Optimization

The purpose of this preliminary experiment was to establish the optimal caspase-3/7 detection reagent concentration with which to label the HT-29 responder cells. Based on earlier reports, the concentration of staurosporine was chosen to be 1.0 μM . HT-29 cells were plated in a 96-well clear black bottom microplate at 5,000 cells per well in 100 μL of growth medium and incubated for twenty-four hours. An aliquot of staurosporine solution was thawed and then diluted with growth medium to the desired concentration of 1.0 μM staurosporine in each well.

Next, medium transfer was performed—with each well receiving 100 μL of the staurosporine/growth medium dilution, and the plate was then incubated for twenty-four hours. At the end of this incubation period, the cells were labeled with the CellEvent caspase-3/7 detection reagent. In order to determine the optimal concentration of this reagent, four different dilutions were made—2.5 μM , 5 μM , 7.5 μM and 10 μM . Each dilution was adjusted in order to give each concentration within a volume of 50 μL —which was then pipetted into each respective well, giving a total volume of 150 μL /well for every sample data point. Following a one hour incubation period to uptake the fluorescent reagent, the samples were observed using an inverted fluorescence microscope. While all four concentration samples were fluorescing, those observed at 7.5 μM appeared brightest and most distinct. Therefore, 7.5 μM was the concentration of caspase reagent used to label all samples in which fluorescence was measured.

Table 3. Caspase-3/7 Reagent Concentration Optimization

Step	Description	Volume per Well	Incubation
1	Perform tissue culture using 96-well plate	100 μ L	24 h 37°C
2	Prepare staurosporine solubilization with DMSO (25 mg/mL) and dilute with growth medium (1 mM)	----	----
3	Perform medium transfer—add diluted staurosporine to cells and incubate in a humidified atmosphere	\pm 100 μ L	24 h 37°C
4	Prepare caspase-3/7 reagent dilution concentrations (2.5 μ M, 5 μ M, 7.5 μ M and 10 μ M)	----	----
5	Add caspase-3/7 reagent to cells and incubate in a humidified atmosphere	+ 50 μ L	1 hr 37°C
6	Evaluate with fluorescence microscopy (502 nm/530 nm)	150 μ L	----

Costar 96-well clear black bottom polystyrene microplates were used for all fluorescence assays. The opaque black-walled plates with optically clear bottoms offer the advantage of viewing the cells by microscopy during the course of the experiment—as opposed to those which have a solid black bottom. Black plates are used for fluorescent assays because they best absorb light while reducing background and well-to-well crosstalk between samples.

Effects of Radiation Dose and Dose Rate on Bystander Response

Cell Culture

A total of nine T25 flasks were plated and labeled as described in Table 4. In the dose rate study, two groups of T25 flasks were designated—each consisting of seven

flasks, as outlined in Table 5. In the dose and dose rate experiments, both MTT and caspase-3/7 assays were carried out in parallel to examine possible correlations that might exist between results gathered from two different endpoint measurements of the same system. Responder cells were plated in two separate 96-well microplates—a clear plate was used for the MTT assay and an opaque, black walled plate with optically clear well bottoms was used to plate the responder cells destined to undergo the fluorescent caspase assay. Both microplates were plated identically. One row in each plate—consisting of three individual wells—was assigned to each respective T25 flask. Each individual well within the row was plated with 5,000 cells in 100 μ L growth medium. All culture vessels were incubated for twenty-four hours in a humidified atmosphere at 37°C and 5% CO₂ in air.

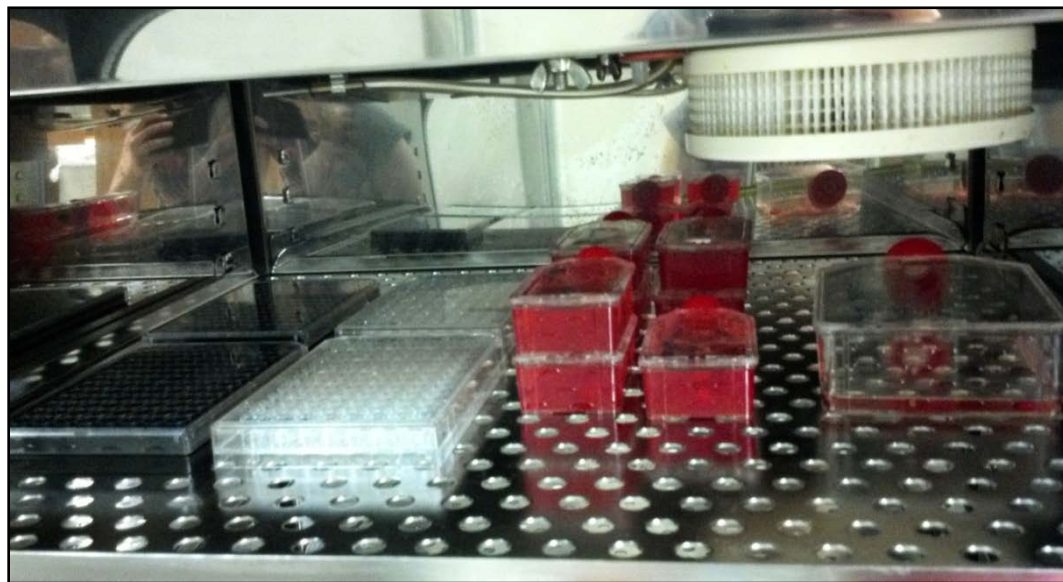


Figure 39. Plated cell cultures in incubator

Vanderbilt University, Radiation Biology Laboratory, Nashville, TN; 14 May 2012.

Irradiation

Immediately before irradiation, each T25 flask was filled with growth medium to a total volume of 50 mL. This step was done to ensure that the entire cell culture remained covered in growth medium during irradiation, as each T25 flask was placed in the irradiation chamber in an upright position with the plated flask wall facing toward the source—providing direct and even exposure across the entire monolayer of cells.

Twenty-four hours after plating, each flask was irradiated at room temperature using the MARK I ¹³⁷Cs Irradiator. For the dose effects study, all irradiated cell cultures were placed at the same location inside the irradiator cavity and, consequently, received the same dose rate of ~ 25 Gy/min, with total exposure time being the only variable throughout the experiment. Irradiation times were calculated based on the total radiation dose each flask was to receive. To avoid the occurrence of any attenuation or scatter effects within the irradiation cavity, the flasks were irradiated individually and, afterwards, immediately returned to the incubator.

Table 4. Dose Effect Study Irradiation Parameters

T25 Flask	Dose (Gy)	Dose Rate (Gy/min)	Source Distance (cm)	Time (min)
Control	0	0	----	----
#1	2	25.29	0	0.08
#2	5	25.29	0	0.20
#3	10	25.29	0	0.40
#4	20	25.29	0	0.79
#5	50	25.29	0	1.98
#6	100	25.29	0	3.95
#7	300	25.29	0	11.86
#8	500	25.29	0	19.77

The flasks used in the dose rate study were prepared and handled identically to those in the previous study—being irradiated at room temperature in a MARK I ^{137}Cs Irradiator twenty-four hours after plating. Each flask received the same total dose of 10 Gy, but at varied dose rates. To achieve a range of dose rates inside the ^{137}Cs irradiator, each flask was placed at a particular distance from the source along the center line of the cavity. Distances were calculated using previously measured dose values acquired with an ion chamber during the irradiator dose profile study. After irradiation, the flasks were returned to the incubator.

Table 5. Dose Rate Effect Study Irradiation Parameters

T25 Flask	Dose (Gy)	Dose Rate (Gy/min)	Distance (cm)	Time (min)
Control	0	0	----	----
#1	10	0.96	33.0	10.42
#2	10	1.81	20.0	5.53
#3	10	2.99	12.5	3.35
#4	10	6.86	5.0	1.46
#5	10	10.85	2.5	0.92
#6	10	25.29	0.0	0.40

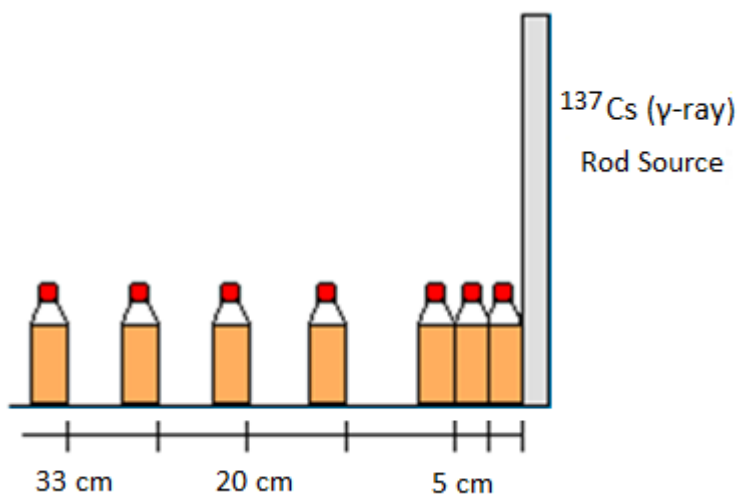


Figure 40. Illustrated experimental setup of dose rate study irradiation

Medium Transfer

All samples were handled separately throughout the entire medium transfer process to avoid cross-contamination. At six hours post-irradiation, 2 mL of ICCM was harvested from each T25 flask and passed through a 0.45 micron syringe filter in order to

remove any cells that may have been present in the sample. The filtrate from each flask was collected in a sterile disposable reagent reservoir. After the samples from each T25 flask were collected, the medium was aspirated from each well in the microplate and transference of the ICCM filtrate to the recipient cells was performed immediately after using an eight-channel pipette—each well receiving 100 μ L of ICCM. The 96-well plate was then incubated at 37°C for twenty-four hours in a humidified atmosphere of 5% CO₂ air.

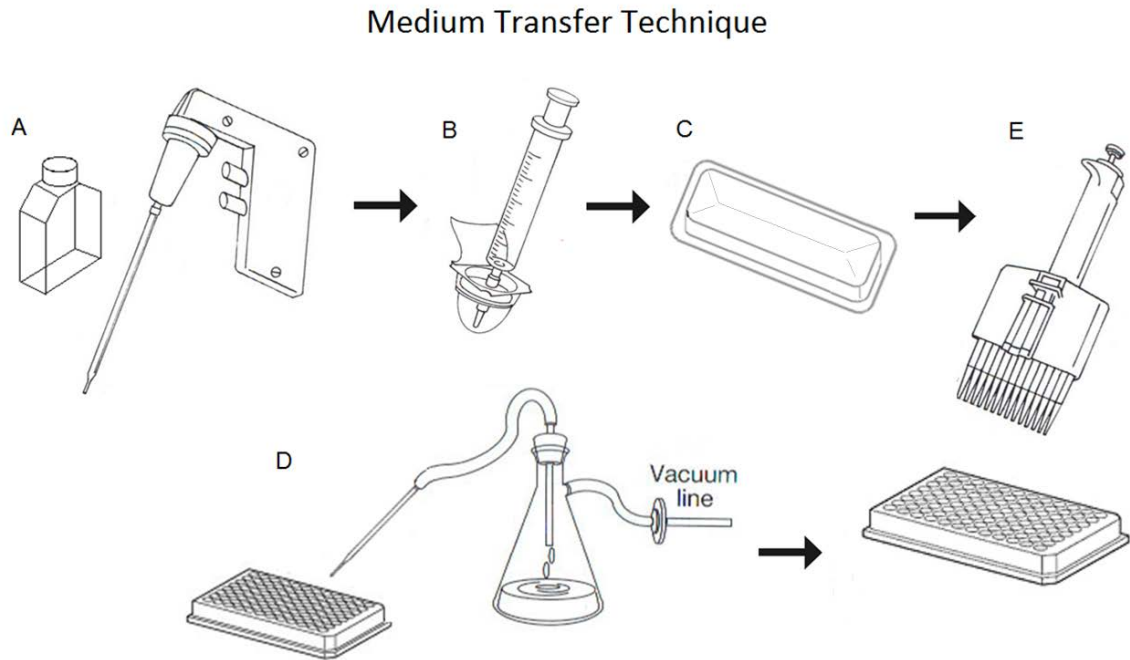


Figure 41. Medium transfer workflow; A) 2 mL of ICCM is removed from T25 flask via measuring pipette six hours post-irradiation; B) ICCM is filtered using a disposable 0.45 micron syringe filter; C) ICCM filtrate is collected in a disposable reagent reservoir, or “boat”; D) existing medium is aspirated from each well in microplate; E) using a multi-channel pipette, the ICCM filtrate is transferred to wells in microplate (100 μ L/well, 8 wells per T25 flask)



Figure 42. Experimental setup of medium transfer

Vanderbilt University, Radiation Biology Laboratory, Nashville, TN; 24 May 2012.

Liquid sterile filtration is a crucial part of the medium transfer process. Choosing which membrane to use can be critical to the integrity and overall success of the entire experiment. Factors such as pore size, media material, and membrane specifications must be considered in order to yield optimal results. In this experiment—and all medium transfer studies, in general—the filter serves a dual role. The membrane must act to remove extraneous material from the irradiated cell conditioned medium—such as any cells that may have detached from the wall of the flask—while simultaneously allowing safe passage of whatever secreted signaling factors which may be present in the sample.



Figure 43. Configuration of medium filtration system; Millex-HV syringe filter, 0.45 µm, PVDF, 13 mm, ethylene oxide sterilized

The 13 mm Millex-HV 0.45 µm syringe filter was used in this study. This particular unit employs a hydrophilic polyvinylidene fluoride (PVDF) Durapore membrane which has very low protein binding, providing sterility while enabling high flow rates and throughputs⁸⁹. The 13 mm Millex filter is used for processing volumes of 10mL or less and is sterilized by ethylene oxide.

MTT Assay

Metabolic activity of the responder cells was measured using the Roche Cell Proliferation Kit 1 (MTT) assay. The basic protocol as outlined in the package insert was followed for all MTT assays conducted in this study.

In this study, the Roche MTT Cell Proliferation Kit 1 (MTT) assay was used according to standard protocol as outlined in the package insert. All colorimetric assays were performed in clear, flat-bottom 96-well plates with cell cultures plated as described previously. Twenty-four hours following medium transfer, 10 µL of MTT reagent was

added to each well using a multi-channel pipette and the plate was incubated for four hours. After this incubation period, 100 μ L of solubilization solution was added to each well and the plate was incubated for eighteen hours. Absorbance was read at 595 nm on the BioTek Synergy HT Multi-Mode Microplate Reader—operated with BioTek Gen5 Data Analysis Software.

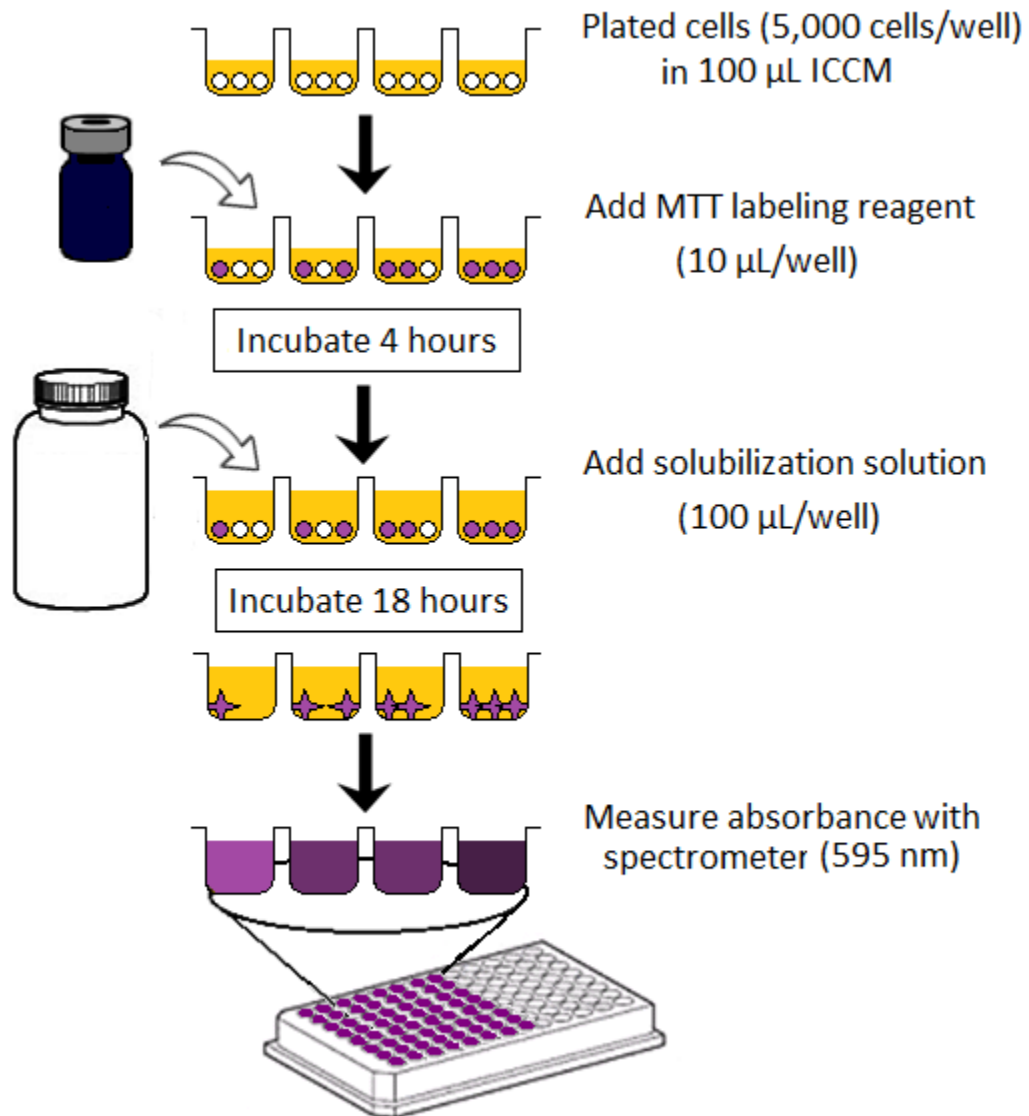


Figure 44. MTT assay workflow



Figure 45. BioTek Synergy HT multi-mode microplate reader

Vanderbilt University, Radiation Biology Laboratory, Nashville, TN; 5 Mar 2012.

Caspase-3/7 Assay

The assay used in this study was the CellEvent Caspase-3/7 Green Detection Reagent by Invitrogen—a novel fluorogenic substrate which is highly specific for caspase-3/7 activation. The reagent consists of a four amino acid peptide (DEVD) conjugated to a nucleic acid binding dye. This cell-permeant substrate is intrinsically non-fluorescent, because the DEVD peptide inhibits the ability of the dye to bind to DNA. After activation of caspase-3 or caspase-7 in apoptotic cells, the DEVD peptide is cleaved, enabling the dye to bind to DNA and produce a bright, fluorogenic response with an absorption/emission maxima of approximately 502/530 nm³⁰.

After positive controls were established using staurosporine, the caspase-3/7 assay was implemented in experimental protocols. For all experiments, an intermediate dilution

of the caspase-3/7 detection reagent was made in complete medium so that upon the addition of the fluorogenic substrate, the final concentration of the reagent on each cell culture was equal to 7.5 μM .

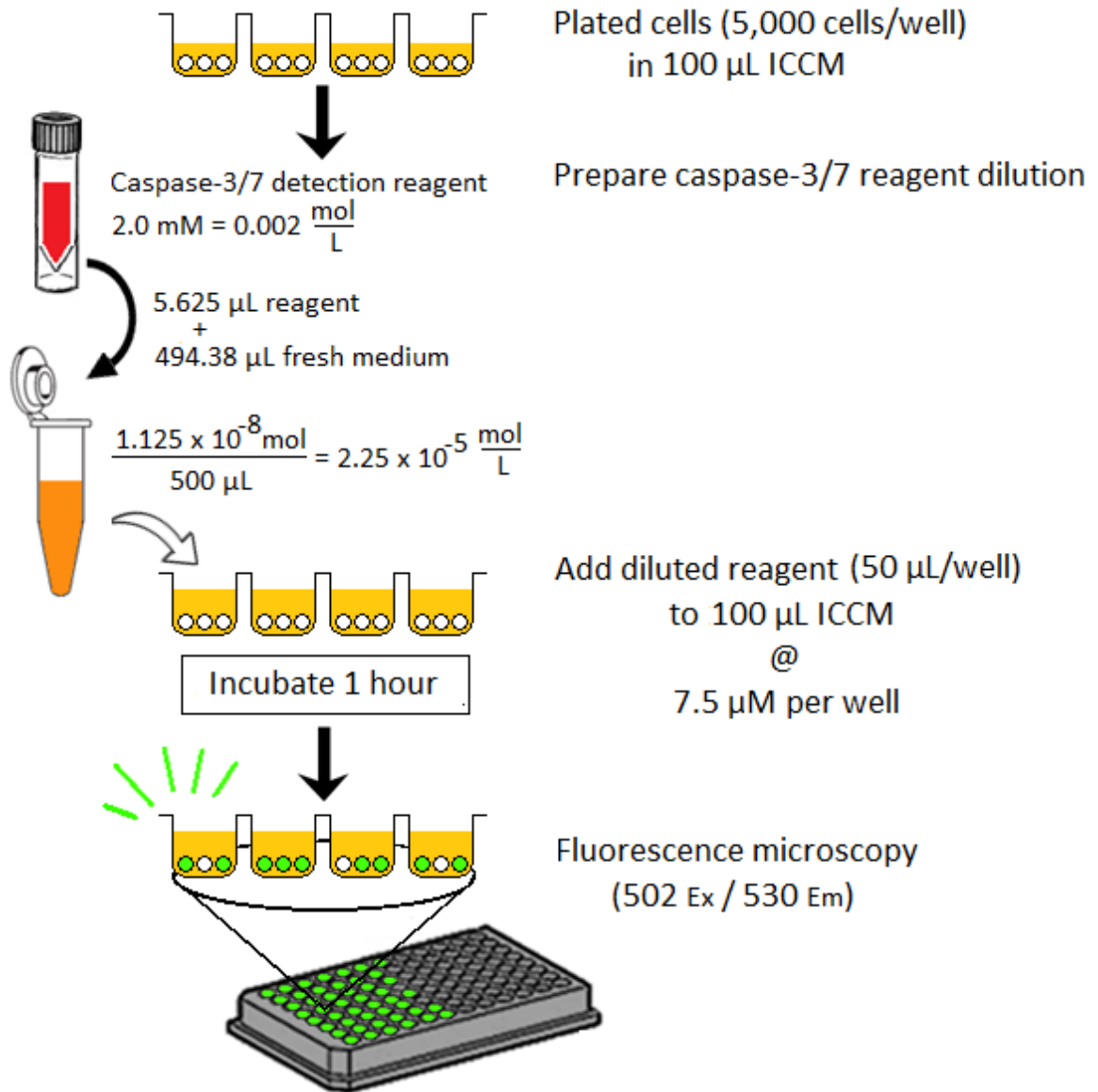


Figure 46. Caspase-3/7 assay workflow with example dilution calculation

Twenty-four hours following medium transfer, 50 μ L of the diluted reagent was added to each well in the microplate using a multi-channel pipette. The plate was then incubated in a humidified atmosphere at 37°C and 5% CO₂ in air for one hour to allow for optimal cellular uptake of the fluorescent reagent. After the incubation period, the plates were analyzed using the Olympus IX51 Inverted Microscope—which has both light and fluorescent capabilities.

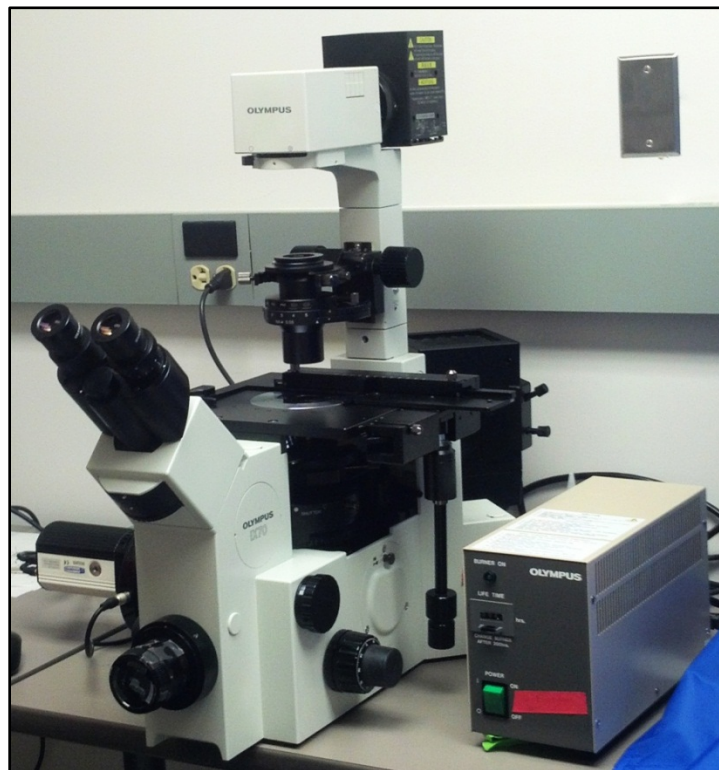


Figure 47. Olympus IX51 inverted fluorescence microscope

Vanderbilt University, Radiation Biology Laboratory, Nashville, TN; 24 May 2012.

Effect of Time Post-Irradiation of Medium Transfer

Cell Culture

The standard cell culture protocol outlined previously was followed throughout all experiments. Cells were washed with phosphate buffered saline (PBS) to remove traces of serum and then trypsinized using a solution of 0.05% trypsin-EDTA. When the cells had detached, they were resuspended in medium and syringed gently to produce a single cell suspension. An aliquot was removed for counting purposes. Cell numeration was performed manually using a hemocytometer under a light microscope. T25 flasks destined to be irradiated and become medium donors were plated with 500,000 cells in 5 mL growth medium—control flasks were included for each experiment but received no radiation exposure.

Responder cell cultures destined to be receive irradiated cell conditioned medium (ICCM) from the irradiated cultures were set up at the same time as the T25 flasks, but were plated in a 96-well microplate. One row—consisting of eight individual wells—was assigned to each respective T25 flask, resulting in eight measurements for every data point being investigated. Each individual well was plated with 5,000 cells in 100 μ L growth medium. All culture vessels were incubated for 24 hours in a humidified atmosphere at 37°C and 5% CO₂ in air.

For this experiment, a total of ten T25 flasks and one 96-well microplate were plated as previously described. Flasks were then divided into five groups, with each group consisting of one control.

CHAPTER IV

RESULTS AND DISCUSSION

Methods of Data Analysis

Where absorbance (A) was measured by MTT assay, eight replicates were counted for each experimental point in all studies. The data are presented as mean \pm standard error in all cases. Where significance was assessed, a paired Student's *t* test was used, and the differences were considered significant if $p < 0.05$.

Fluorescence images of caspase-3/7 activation were recorded from two independent experiments. Four images were taken of each data point using a microscopic camera and were analyzed using ImageJ processing software. Green fluorescent pixel number and area values were measured, with the final mean value for each sample point representative of the average of all images taken for each sample data point.

Effects of Radiation Dose and Dose Rate on Bystander Response

The aim of this study was to investigate the effect of dose and dose rate variation of ^{137}Cs γ radiation and its effect on the bystander response as observed using two end points—metabolic activity by means of MTT assay and caspase-3/7 activation by use of a fluorogenic substrate. For the dose experiment, all donor cell cultures were irradiated with a dose rate of ~ 25 Gy/min over several total doses ranging between 2 Gy and 500 Gy. As mentioned previously, this was achieved by varying the radiation exposure time

of each flask. As illustrated in Figure 48, the absorbance values of bystander response cells after treatment with the ICCM increased across all doses.

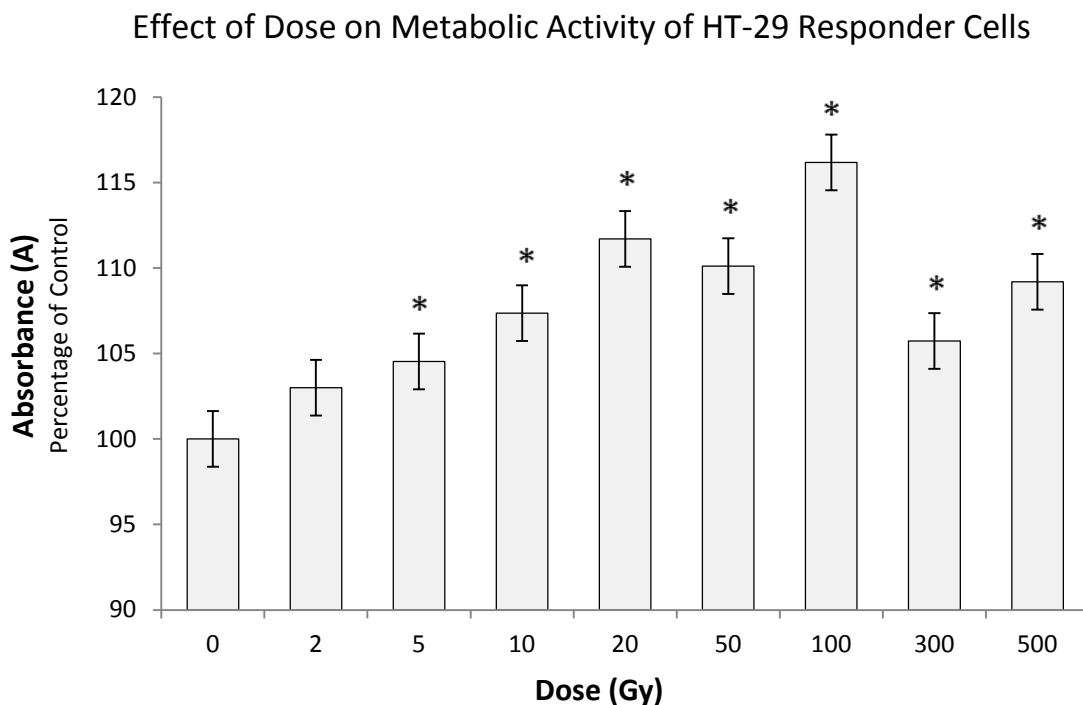


Figure 48. *In vitro* bystander effect induced in unirradiated responder cells by ^{137}Cs γ -ray exposure. Each cell culture flask received the same dose rate of 25.29 Gy/min. Medium transfers were performed six hours post-irradiation; Absorbance values are shown as a percentage of the control. Error bars represent mean \pm SEM ($n = 8$); * $P < 0.05$ by Student's t test.

For the dose rate experiment, cells were irradiated to a dose of 10 Gy over a wide range of dose rates which was achieved by varying the source-to-flask distance of the irradiated cell cultures. As illustrated in Figure 49, the absorbance values of bystander recipient cells after treatment with ICCM increased significantly across all dose rates—with 1.81 Gy/min, 2.99 Gy/min, 6.86 Gy/min, 10.85 Gy/min, and 25.29 Gy/min, all of which were statistically significant with $p < 0.02$.

Effect of Dose Rate on Metabolic Activity of HT-29 Responder Cells

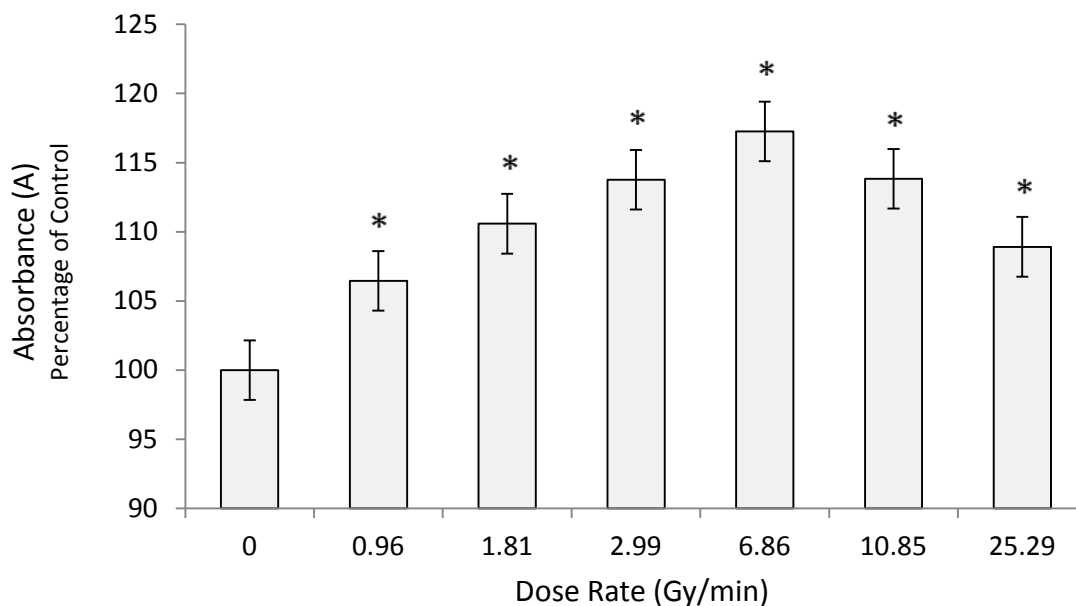


Figure 49. *In vitro* bystander effect induced in unirradiated responder cells by ^{137}Cs γ -ray exposure. Each cell culture flask received the same total dose of 10 Gy. Medium transfers were performed six hours post-irradiation; Absorbance values are shown as a percentage of the control. Error bars represent mean \pm SEM (n = 8); *P < 0.05 by Student's *t* test.

The primary source of cell stress and damage associated with ^{137}Cs γ radiation is primarily through production of free radicals and reactive oxygen species (ROS) by indirect action, as the incident γ -rays first produce Compton or photoelectrons which go on to produce radicals. As radiation dose increases, so does the production of free radicals and ROS⁹³. The increases in metabolic activity observed in this study may be indicative of a stress response to mitochondrial dysfunction occurring in the responder cells following exposure to reactive oxygen species (ROS) present in the ICCM. ROS have been shown to have a role in the perpetuation of bystander effects⁵⁸ and increases in ROS have been linked to increases in mitochondrial mass⁹⁹ in what appears to be a cellular response to compensate for reduced mitochondrial function. A decrease in

mitochondrial ATP production is often compensated for by increasing glycolysis, as is seen in most cancer cells, where OXPHOS is limited by hypoxic conditions⁹¹.

The primary function of mitochondria is the generation of ATP by oxidative phosphorylation. In addition to supplying cellular energy, mitochondria are involved in a range of other processes such as cellular differentiation, cell death, regulation of the cell cycle and growth, and are an integral part of multiple cell signaling cascades⁹⁴.

Mitochondria are the only other location of genetic material outside the nucleus. They contain a circular, double-stranded genome with no protective histone coat that is very compact and contains some over-lapping genes overlapping genes with only a small fraction of the genome being non-coding. There are approximately two to ten copies of the mitochondrial genome in each mitochondrion and tens to hundreds of mitochondria per cell—meaning that one cell may contain up to several thousand mitochondrial genomes.

The human mitochondrial genome encodes twenty-two tRNAs, two rRNAs, and thirteen polypeptides that are all subunits of enzyme complexes in the oxidative phosphorylation (OXPHOS) pathway⁹¹. This OXPHOS pathway consists of five enzyme complexes which are embedded within the inner mitochondrial membrane. The proximity of mitochondrial DNA (mtDNA) to this potential source of highly reactive species and its lack of any histone coat render it particularly susceptible to damage as electrons passing from complex to complex in the electron transport chain can be lost into the matrix, even under normal conditions.

However, due to the short half-life of ROS (10^{-9} - 10^{-10} s), it does not appear likely to be the direct factor mitigating the bystander response via medium transfer. Therefore, a

factor capable of activation or cleavage from irradiated donor cells via ROS is a more likely explanation. One possible candidate is the secreted transforming growth factor beta1 (TGF- β 1)⁹³. ROS have been shown to be a potent mediator of activation of TGF- β 1 from its latent complex⁹⁸ and that γ -irradiation increases the amount of active TGF- β 1 with increases in dose^{96,97}. TGF- β 1 serves many functions, with one of the most prominent being growth inhibition. What makes it a likely candidate responsible for the stimulatory phenomenon observed in this study is that excessive amounts of active TGF- β 1 have been shown to abolish its growth inhibitory effects, indicating that regulation is controlled via a negative-feedback mechanism⁹⁵.

One study⁹² has reported the existence of a dose threshold, or maximal response, for the bystander effect as low as 2 mGy—in which saturation occurs and above which no changes in the magnitude or nature of the bystander response occurs. Consequently, an overwhelming majority of bystander research has been within the area regarded as low dose radiobiology and typically does not investigate the effects of doses higher than 2 Gy. Furthermore, the bystander effect is largely assumed to be inhibitory in nature—often resulting in any observance of non-negative or stimulatory effects being looked over, much less further analyzed.

Though much of the literature does consist of reports on the negative or inhibitory nature of the bystander effect, there have been some accounts of stimulatory responses that are of particular relevance to the findings in this study. In one medium transfer study⁹⁰ where cloning efficiency was used as the endpoint, HT-29 cells were reported to have enhanced survival at doses of 0.5 Gy and 2 Gy. In another medium transfer study⁹³, radiation-induced bystander effects in HPV-G cell culture where clonogenic assay was

used as the endpoint measurement, the bystander survival fraction using two different sources— ^{60}Co γ -radiation and high energy electrons—resulted in typical decreases associated with doses of 0.5 Gy and 5 Gy and was shown to be independent of the dose rate given by either source. However, upon irradiation with a larger dose of 10 Gy, the bystander cell death associated with the lower doses was essentially abolished and, in fact, a proliferative response was observed. Furthermore, it was reported that by increasing doses of high energy electrons delivered by a medical linear particle accelerator, the proliferative effects were exaggerated further.

The data presented here does not support the existence of a low-dose threshold for bystander effects in cell culture and, instead, indicates a significant stimulatory bystander response across a wide range of doses from 2 to 500 Gy. Some have hypothesized that different cell lines induce different types of bystander responses through different mechanisms. Therefore, it is possible that even if bystander effects appear to saturate for a particular cell line, this may not be true when single large doses are used⁹³ and could be especially relevant in radiotherapy where large dose fractions are administered.

Caspase-3/7 Activation

The purpose of this set of experiments was to examine the hypothesis that lethally irradiated HT-29 cancer cells utilize the apoptotic pathway to generate stimulatory signals which are secreted into the surrounding medium and are capable of inducing bystander responses in unirradiated cell populations. For both dose and dose rate experiments, ICCM was transferred from irradiated flasks to unirradiated responder cells and incubated for 24 hours—corresponding to 24 hours of ICCM exposure. Caspase-3/7

reagent dilutions were prepared at 7.5 μM , added to each sample and incubated for 1 hour to allow for uptake of the fluorogenic substrate. Results were read with a fluorescence microscope. The average fluorescence of each sample was quantified by measuring the average number of green fluorescent pixels in each image—with an increase in fluorescence corresponding to an increase in pixel area and vice versa. All samples were compared against the control.

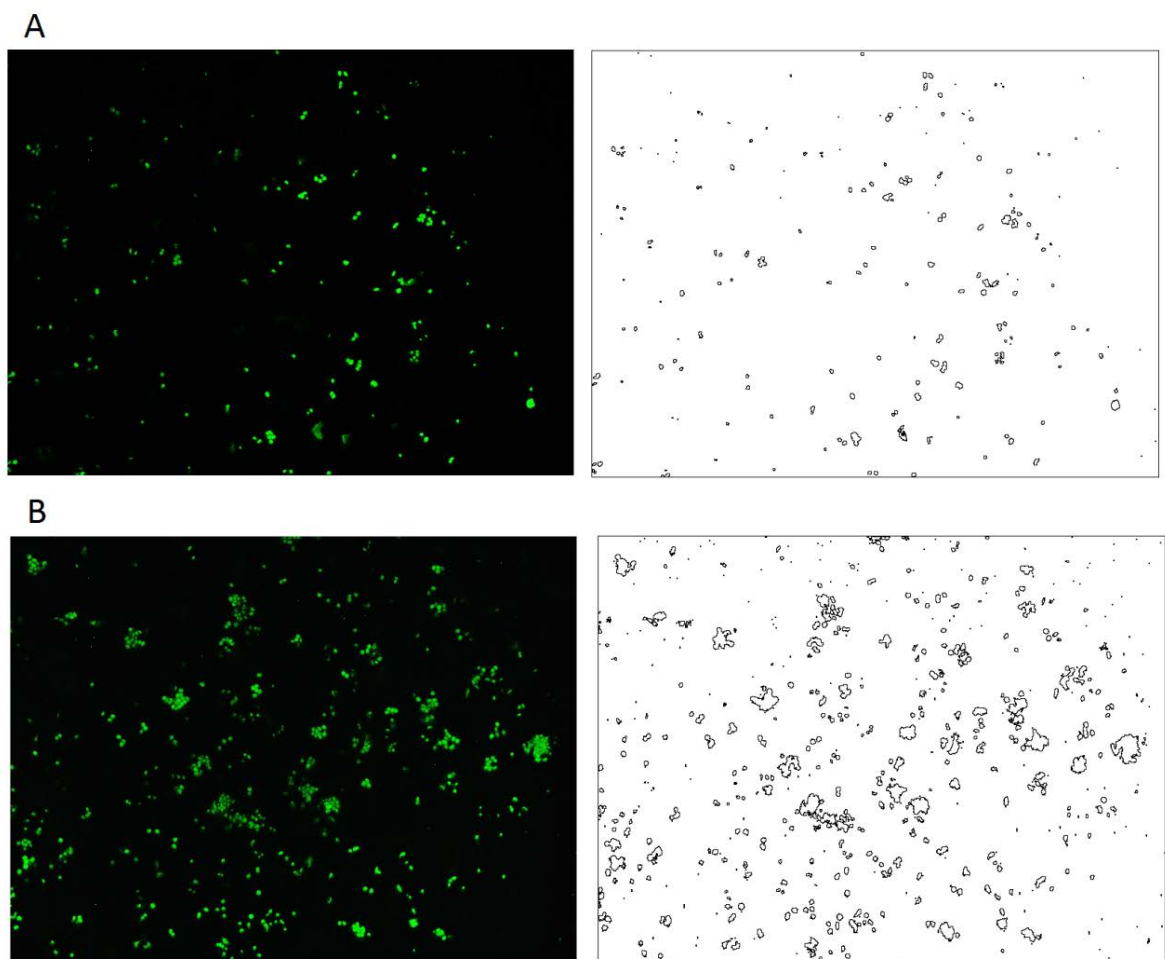


Figure 50. Fluorescence analysis with ImageJ software; raw fluorescence images taken with microscope camera displayed on left with corresponding particle area maps generated after ImageJ processing of samples A) control, and B) 6.68 Gy/min, 10 Gy total dose

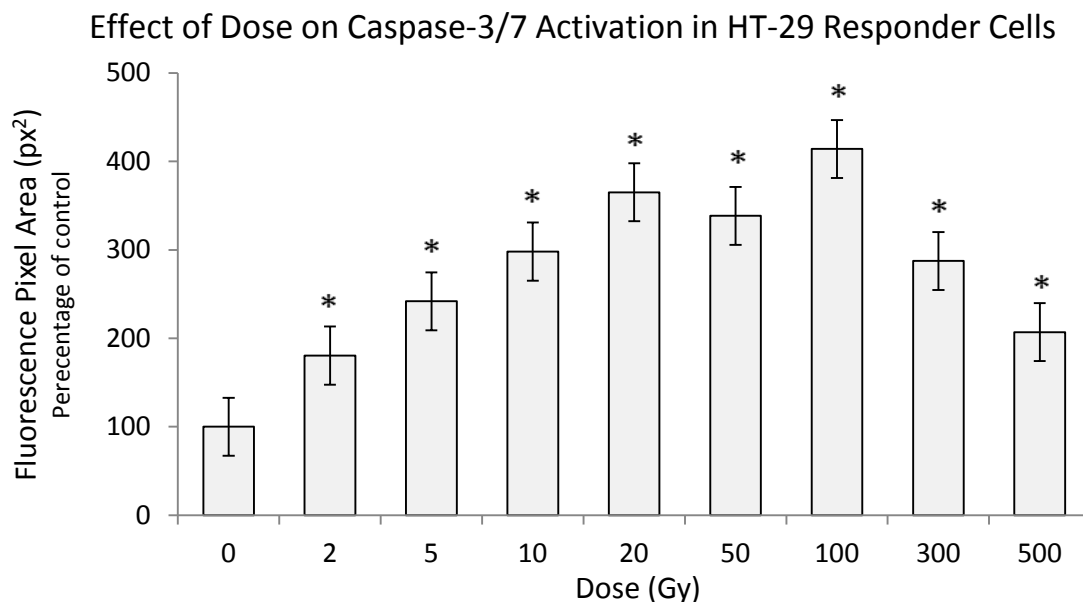


Figure 51. Caspase-3/7 activation bystander response induced in unirradiated cells by medium transfer from ¹³⁷Cs γ -irradiated cell cultures. All cell culture flasks irradiated at 25.29 Gy/min. Medium transfers were performed six hours post-irradiation. Fluorescence image processing with ImageJ; average fluorescent pixel area shown as a percentage of the control. Error bars represent mean \pm SEM (n = 4); *P < 0.05 by Student's t test.

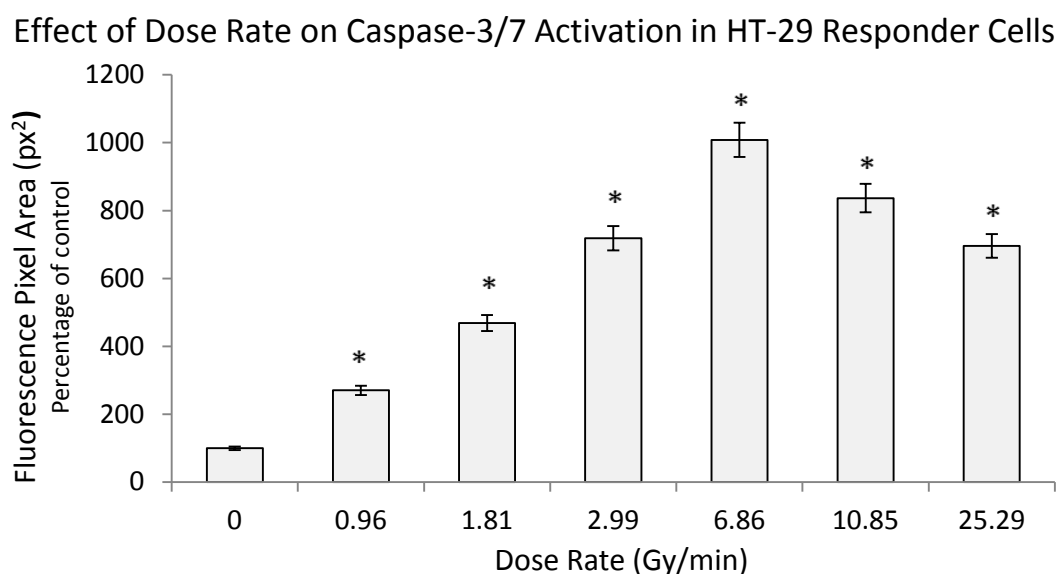


Figure 52. Caspase-3/7 activation bystander response induced in unirradiated cells by medium transfer from ¹³⁷Cs γ -irradiated cell cultures. All cell culture flasks irradiated to 10 Gy. Medium transfers were performed six hours post-irradiation. Fluorescence image processing with ImageJ; average fluorescent pixel area shown as a percentage of the control. Error bars represent mean \pm SEM (n = 4); *P < 0.05 by Student's t test.

The results of this study indicate that lethally irradiated HT-29 cancer cells do in fact release signaling factors into their immediate environment capable of inducing a stimulatory bystander effect in unirradiated responder cells. Furthermore, the caspase-3/7 signaling pathway, traditionally regarded as the apoptotic pathway, demonstrates significant activation in responder cells in what appears to be a linear fashion directly correlated to the level of metabolic activity expressed within these populations as measured in parallel MTT assay samples—the higher the absorbance value, the higher the caspase-3/7 activation and vice versa. Therefore, these results indicate that caspase 3 is involved in the stimulatory bystander responses observed in responder cell populations after exposure to ICCM.

The phenomenon reported here is in agreement with the findings of a previous *in vivo* study¹ in which deficiency of caspase 3 either in tumor cells or in tumor stroma was reported to cause substantial tumor sensitivity to radiotherapy in xenograft or mouse tumors. And in human subjects with cancer, higher amounts of activated caspase 3 in tumor tissues was correlated with a markedly increased rate of recurrence and death. Furthermore, Huang et al. found that cells could die in multiple ways after radiation exposure and the absence of caspase 3 shifted the mode of cell death from apoptosis to necrosis or autophagy¹. Thus, the hypothesis that different cell lines elicit different types of bystander responses through different mechanisms would appear to be correct. While there are undoubtedly other hypotheses, the results of this study suggest that at least one of the criteria in predicting the type and mechanism of bystander response expressed in irradiated cell populations is the level of caspase 3 presence. Therefore, the results of this study suggest the possibility of enhancing cancer radiotherapy through the inhibition of

caspase 3—which is in agreement with the previously reported *in vivo* study¹ which concluded that elevated tumor caspase 3 levels predict worse treatment outcomes in people with cancer.

Apoptosis-stimulated tissue regeneration has been observed in lower organisms such as *Drosophila* and hydra systems¹⁰⁴. While the mechanism of these phenomena are not entirely clear, it has been proposed that apoptotic cells elicit some form of compensatory proliferation for tissue regeneration—of which β -catenin–Wnt signaling has reportedly been involved in some instances of compensatory proliferation¹⁰³. Furthermore, PGE2 has been shown to stimulate the proliferation of colon cancer cells through activation of the β -catenin–Wnt pathway¹⁰². While it was beyond the scope of this study to further identify the expression of downstream factors of caspase 3, it is hypothesized that the caspase-activated iPLA2–arachidonic acid–PGE2 axis is involved in the generation of stimulatory bystander signals released from lethally irradiated cells.

One of the practical implications of this study, as first proposed by Huang et al¹ and further supported here, is a new and counterintuitive approach to enhancing cancer radiotherapy through caspase 3 inhibition. Another implication of this study is the potential use of activated caspase 3 as a biomarker tool in the assessment of tumor staging and radiation treatment response.

Effect of Time Post-Irradiation of Medium Transfer

Cells were plated at 5×10^5 cells per T25 flask and, after 24 hours of incubation, irradiated to a dose of 10 Gy at a dose rate of 25.29 Gy/min. After irradiation, the flasks were incubated for various times—30 min, 6 hr, 24 hr, 48 hr, and 72 hr—at which point a sample of ICCM was taken from each flask, filtered, and transferred to recipient cells

whose medium had been withdrawn immediately prior to the transfer. A total of four 96-well plates containing responder cells were plated new each day, 24 hours before each respective medium transfer time in order to avoid cellular multiplicity between the samples. Each was plated at 5,000 cells per well in 100 μ L. After medium transfer, each sample was incubated for 24 hours, after which the MTT assay was performed.

As illustrated in Figure 53, the absorbance values of bystander recipient cells after treatment with ICCM at 10 Gy increased rapidly in the first few hours post-irradiation, but slowly began to dissipate during the period of 24 to 72 hours. However, it is notable that at all time points, each sample exhibited significantly increased metabolic activity as measured in absorbance (A). Thus, the time point of 6 hours post-irradiation was used for all medium transfer experiments.

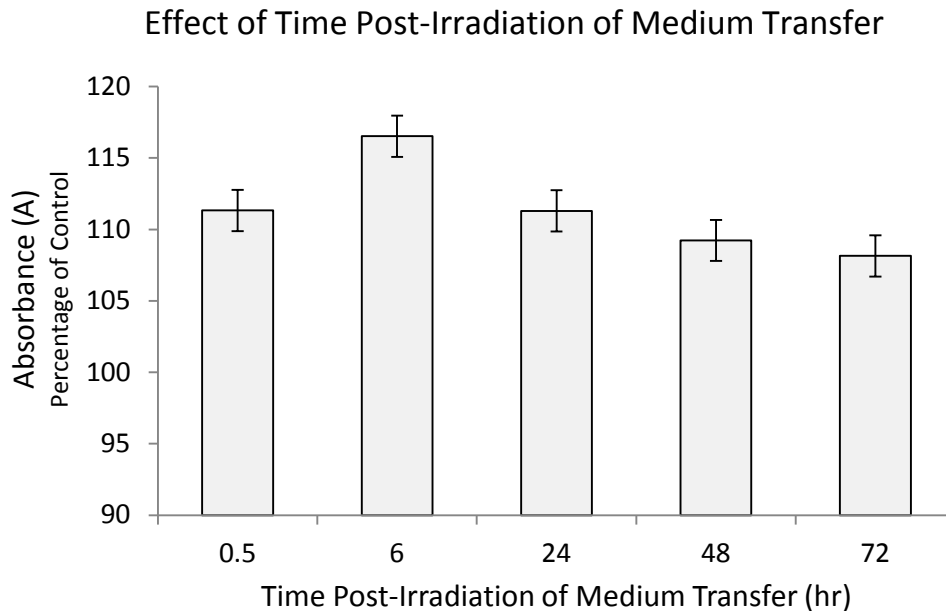


Figure 53. Effect of time post-irradiation of medium transfer on the magnitude of bystander response elicited in cell cultures receiving ICCM; Absorbance values are shown as a percentage of the control. Error bars represent mean \pm SEM (n = 8)

These findings are in agreement with a previous study that reported rapid increase in the bystander signal potency within the first few hours after irradiation using clonogenic assay as the endpoint. Though, because this previously reported study did not account for cellular multiplicity, it is difficult to compare their results at later time points. However, the results of this study clearly reveal a time-dependent response, suggesting that a factor is indeed secreted by the irradiated cells into the medium even after irradiation, as evidenced by the build-up of signal peaking at 6 hours post-irradiation. The slow dissipation in signal magnitude seen in the 24 to 72 hour period could represent possible rate of decay, or half-life, of the secreted factor within the medium. Another possibility is the increase of cell death among the irradiated cultures over this period resulting in progressively fewer donor cells by which to secrete a bystander signal—which would mean that the total number of cells targeted in irradiated cultures determines the magnitude of signal secreted into the medium and, likewise, the magnitude of bystander effect produced within responder cells.

Further Research

A PGE2 assay could be used to investigate the relationship between PGE2 expression and the magnitude of the bystander response to determine if the COX pathway is a critical signaling link utilized in the observed bystander phenomenon induced by exposure of HT-29 cells to ICCM. The PGE2 assay kit manufactured by Cisbio—which is based on HTRF (homogeneous time-resolved fluorescence) technology—would be a promising choice.

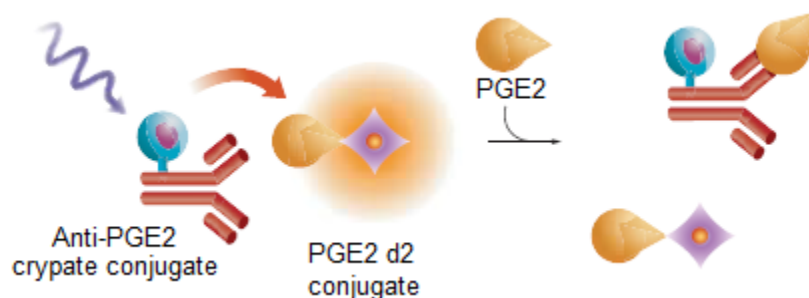


Figure 54^a. PGE2 assay principle; based on HTRF technology, this method is a competitive immunoassay in which native PGE2 produced by cells and d2-labeled PGE2 compete for binding to MAb anti-PGE2 labeled with cryptate.

^a Reprinted from Prostaglandin E2 Assay [package insert]. ⁸⁶. Cisbio (2008 Jul).

This technique uses a cryptate-linked antibody specifically recognizing PGE2 to bind a PGE2-d2 conjugate. When the two fluorophores are in close proximity, time-resolved fluorescence resonance energy transfer occurs. This detection method relies on competitive binding from free exogenous PGE2 to disrupt the donor-acceptor complex. Therefore, the observed HTRF signal decreases with increasing amounts of enzyme-produced PGE2. One benefit of using HTRF is the long lifetime of the donor fluorophores which minimize interfering fluorescence from the buffer and test compounds.

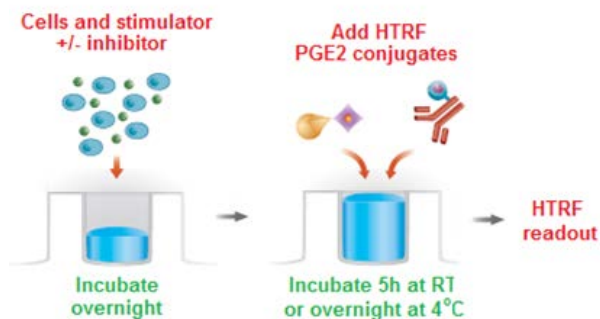


Figure 55^a. PGE2 assay protocol; the cell-based protocol is carried out in a single plate and allows the quantification of PGE2 directly on stimulated cells without any transfer steps.

^a Reprinted from Prostaglandin E2 Assay [package insert]. ⁸⁶. Cisbio (2008 Jul).

CHAPTER V

CONCLUSIONS

The results of this study support the existence of a cancer cell death-induced repopulation pathway in which caspase 3 has a major role. Though the properties of the bystander effect are becoming clearer, until the mechanistic nature of these non-targeted effects is more clearly defined and the signaling molecule is identified, it will ultimately remain unclear as to what relevance the phenomenon ultimately has on human carcinogenic risk. The fact that many of the effects associated with cellular exposure to radiation have the ability to manifest in non-targeted bystander cells has considerable implications in radiobiology, cancer therapy, and health physics applications as it suggests the target for biological responses to radiation might be greater than the volume exposed.

REFERENCES

1. Huang Q, Li F, Liu X, Li W, Shi W, Liu F, O'Sullivan B, He Z, Peng Y, Tan AC, et al. Caspase 3-mediated stimulation of tumor cell repopulation during cancer radiotherapy. *Nat Med.* 2011;17(7):860-867.
2. Blyth BJ, Sykes PJ. Radiation-induced bystander effects: what are they, and how relevant are they to human radiation exposures? *Radiat Res.* 2011;176(2):139-157.
3. Hall EJ, Giaccia AJ. Radiobiology for the radiologist. 6th ed. Philadelphia (PA): Lippincott Williams & Wilkins; 2006.
4. Hendee WR, Ritenour ER. Medical imaging physics. 4th ed. New York (NY): Wiley-Liss; 2002.
5. Mothersill C, Seymour C. Medium from irradiated human epithelial cells but not human fibroblasts reduces the clonogenic survival of unirradiated cells. *Int J Radiat Biol.* 1997;71(4):421-427.
6. Nagasawa H, Little JB. Induction of sister chromatid exchanges by extremely low doses of α -particles. *Cancer Res.* 1992;52:6394-6396.
7. Beiser A. Concepts of modern physics. 6th ed. Boston (MA): McGraw-Hill; 2003.
8. Hrabak M, Padovan RS, Kralik M, Ozretic D, Potocki K. Scenes from the past: Nikola Tesla and the discovery of X-rays. *Radiographics.* 2008;28:1189-1192.
9. Rayner-Canham MF, Rayner-Canham GW. A devotion to their science: pioneer women of radioactivity. Philadelphia (PA): Chemical Heritage Foundation; 1997.
10. Raff MC. Social controls on cell survival and cell death. *Nature.* 1992;356:397-400.
11. Roche. Cell proliferation and viability measurement: delicate tasks require precise solutions. *Biochemica* [Customer Journal]. 2003;3:26-28.
12. Goddu SM, Howell RW, Rao DV. Cellular dosimetry: absorbed fractions for monoenergetic electron and alpha particle sources and S-values for radionuclides uniformly distributed in different cell compartments. *J Nucl Med.* 1994;35:303-316.
13. Campbell NA, Reece JB. Biology. 6th ed. San Francisco (CA): Benjamin Cummings; 2002.

14. Kerr JFR, Wyllie AH, Currie AR. Apoptosis: a basic biological phenomenon with wide-ranging implications in tissue kinetics. *Brit J Cancer*. 1972;26:239-257.
15. Illidge TM. Radiation-induced apoptosis. *Clin Oncol*. 1998;10:3-13.
16. Puck TT, Morkovin D, Marcus PI, Cieciora SJ. Action of x-rays on mammalian cells: II. survival curves of cells from normal human tissues. *J Exp Med*. 1957;106(4):485-500.
17. Fogh J, Trempe G. New human tumor cell lines. In: Fogh J, editor. Human tumor cells in vitro. New York (NY): Plenum Press; 1975. p. 115-141.
18. ATCC catalog product description: HT-29 cell line [Internet]. American Type Culture Collection; 2012 [cited 2012 Jan 15]. Available from: <http://www.atcc.org/ATCCAdvancedCatalogSearch/ProductDetails/tabid/452/Default.aspx?ATCCNum=HTB-38&Template=cellBiology>
19. Radionuclide decay data: cesium-137 [Internet]. Health Physics Society; [cited 2012 Jan 15]. Available from: <http://hps.org/publicinformation/radardecaydata.cfm>
20. MARK I ¹³⁷Cs irradiators [operating manual]. JL Shepherd and Associates. Glendale (CA): 1983.
21. Lockshin RA, Williams CM. Programmed cell death: I. cytology of degeneration in the intersegmental muscles of the *pernyi* silkworm. *J Insect Physiol*. 1965;11:123-133.
22. Banasiak D, Barnetson AR, Odell RA, Mameghan H, Russell PJ. Comparison between the clonogenic, MTT, and SRB assays for determining radiosensitivity in a panel of human bladder cancer cell lines and a ureteral cell line. *Radiat Oncol Invest*. 1999;7:77-85.
23. Slater TF, Sawyer B, Straeuli U. Studies on succinate-tetrazolium reductase systems: III. points of coupling of four different tetrazolium salts. *Biochim Biophys Acta*. 1963;8(77):383-393.
24. Cell proliferation kit I (MTT): colorimetric assay (MTT based) for the non-radioactive quantification of cell proliferation and viability [package insert]. Version 17. Mannheim (Germany): Roche; 2005 Sep.
25. Roa W, Yang X, Guo L, Huang B, Khatibisepehr S, Gabos S, Chen J, Xing J. Real-time cell-impedance sensing assay as an alternative to clonogenic assay in evaluating cancer radiotherapy. *Anal Bioanal Chem*. 2011;400(7):2003-2011.

26. Schulze-Osthoff K. Apoptosis, cytotoxicity and cell proliferation manual. 4th ed. Mannheim (Germany): Roche; 2008.
27. Fischer U, Schulze-Osthoff K. New approaches and therapeutics targeting apoptosis in disease. *Pharmacol Rev.* 2005;57(2):187-215.
28. Melino G, Knight RA, Nicotera P. How many ways to die? how many different models of cell death? *Cell Death Differ.* 2005;12:1457-1462.
29. Kroemer G, El-Deiry WS, Golstein P, Peter ME, Vaux D, Vandenabeele P, Zhivotovsky B, Blagosklonny MV, Malorni W, Knight RA, et al. Classification of cell death: recommendations of the Nomenclature Committee on Cell Death. *Cell Death Differ.* 2005; 12:1463-1467.
30. CellEvent™ caspase-3/7 green detection reagent [package insert]. Carlsbad (CA): Invitrogen; 2011 Feb 7.
31. Linton OW. Medical applications of x rays. *Beam Line.* 1995;25(2):25-34.
32. Daniel J. The x-rays [letter]. *Science.* 1896;3(67):562-563.
33. Meggitt G. Taming the rays: a history of radiation and protection. Lulu.com; 2008.
34. Tesla N. Lecture before the New York Academy of Sciences: the streams of Lenard and Roentgen and novel apparatus for their production. Anderson LI, editor. Breckenridge (CO): Twenty-First Century Books; 1994.
35. Tesla N. On the Roentgen streams. *Electrical Review.* 1896;29(23):277.
36. Tesla N. On the source of Roentgen rays and the practical construction and safe operation of Lenard tubes. *Electrical Review.* 1897;31(4):67,71.
37. Assmus A. Early history of x rays. *Beam Line.* 1995;25(2):10-24.
38. Röntgen WC. Weitere beobachtungen über die eigenschaften der x-strahlen [Further observations on the characteristics of x-rays]. *Ann Phys-Leipzig.* 1898;300(1):18-37.
39. Blaufox MD. Becquerel and the discovery of radioactivity: early concepts. *Semin Nucl Med.* 1996;26(3):145-154.
40. Becquerel H. Sur les radiations émises par phosphorescence [On the radiation emitted by phosphorescence]. *C R Acad Sci.* 1896;122:420.

41. Tesla N. On hurtful actions of Lenard and Roentgen tubes. *Electrical Review*. 1897;30(18):207,211.
42. Historical timeline: important moments in the history of nuclear medicine [Internet]. Society of Nuclear Medicine; [cited 2012 Jan 25]. Available from: <http://interactive.snm.org/index.cfm?PageID=1107>
43. The Nobel Prize in physics 1906 [Internet]. Nobelprize.org; [cited 2012 Jan 25]. Available from: http://www.nobelprize.org/nobel_prizes/physics/laureates/1906/
44. The Nobel Prize in chemistry 1908 [Internet]. Nobelprize.org; [cited 2012 Jan 25]. Available from: http://www.nobelprize.org/nobel_prizes/chemistry/laureates/1908/
45. L'Annunziata MF. Radioactivity: introduction and history. Oxford (England): Elsevier; 2007.
46. The Nobel Prize in physics 1935 [Internet]. Nobelprize.org; [cited 2012 Jan 25]. Available from: http://www.nobelprize.org/nobel_prizes/physics/laureates/1935/
47. Lord CJ, Ashworth A. The DNA damage response and cancer therapy. *Nature*. 2012;481:287-294.
48. Podgorsak EB. Radiation oncology physics: a handbook for teachers and students. Vienna (Austria): International Atomic Energy Agency; 2005.
49. Weinberg RA. The biology of cancer. New York (NY): Garland Science; 2007.
50. Schwerk C, Schulze-Osthoff K. Non-apoptotic functions of caspases in cellular proliferation and differentiation. *Biochem Pharmacol*. 2003;66:1453-1458.
51. Brenner DJ, Raabe OG. Is the linear-no-threshold hypothesis appropriate for use in radiation protection? McDonald JC, moderator. *Radiat Prot Dosim*. 2001;97(3):279-285.
52. Stabin MG. Radiation protection and dosimetry: an introduction to health physics. New York (NY): Springer; 2007.
53. Lyng FM, Maguire P, McClean B, Seymour C, Mothersill C. The involvement of calcium and MAP kinase signaling pathways in the production of radiation-induced bystander effects. *Radiat Res*. 2006;165:400-409.
54. Mothersill C, Seymour RJ, Seymour CB. Bystander effects in repair-deficient cell lines. *Radiat Res*. 2004;161(3):256-263.

55. Mothersill C, Seymour C. Radiation-induced bystander effects, carcinogenesis and models. *Oncogene*. 2003;22:7028-7033.
56. Prise KM, Belyakov OV, Folkard M, Michael BD. Studies of bystander effects in human fibroblasts using a charged particle microbeam. *Int J Radiat Biol*. 1998;74(6):793-798.
57. Lyng FM, Seymour CB, Mothersill C. Production of a signal by irradiated cells which leads to a response in unirradiated cells characteristic of initiation of apoptosis. *Brit J Cancer*. 2000;83(9):1223-1230.
58. Lyng FM, Seymour CB, Mothersill C. Initiation of apoptosis in cells exposed to medium from the progeny of irradiated cells: a possible mechanism for bystander-induced genomic instability? *Radiat Res*. 2002;157(4):365-370.
59. Hickman AW, Jaramillo RJ, Lechner JF, Johnson NF. α -particle-induced p53 protein expression in a rat lung epithelial cell strain. *Cancer Res*. 1994;54:5797-5800.
60. Nagasawa H, Little JB. Unexpected sensitivity to the induction of mutations by very low doses of alpha-particle radiation: evidence for a bystander effect. *Radiat Res*. 1999;152(5):552-557.
61. Zhou H, Randers-Pehrson G, Waldren CA, Vannais D, Hall EJ, Hei TK. Induction of a bystander mutagenic effect of alpha particles in mammalian cells. *P Natl Acad Sci USA*. 2000;97(5):2099-2104.
62. Mothersill CE, Smith RW, Seymour CB. Molecular tools and the biology of low-dose effects. *Bioscience*. 2009;59(8):649-655.
63. Matsumoto H, Hamada N, Takahashi A, Kobayashi Y, Ohnishi T. Vanguard of paradigm shift in radiation biology: radiation-induced adaptive and bystander responses. *J Radiat Res*. 2007;48:97-106.
64. Feinendegen LE, Pollycove M, Neumann RD. Whole-body responses to low-level radiation exposure: new concepts in mammalian radiobiology. *Exp Hematol*. 2007;35(4 Suppl):37-46.
65. Hollowell JG Jr, Littlefield LG. Chromosome damage induced by plasma of x-rayed patients: an indirect effect of x-ray. *P Soc Exp Biol Med*. 1968;129(1):240-244.
66. Mothersill C, Seymour C. Radiation-induced bystander effects: past history and future directions. *Radiat Res*. 2001;155(6):759-767.

67. Berridge M. Cell signalling biology [Internet]. BJ Signal; [cited 2012 Feb 1]. Available from: <http://www.biochemj.org/csb/>
68. Barker K. At the bench: a laboratory navigator. Updated ed. Cold Spring Harbor (NY): Cold Spring Harbor Laboratory Press; 2005.
69. Cyberbridge: mitosis & meiosis [Internet]. Cambridge (MA): Harvard University; c2007. [cited 2012 Feb 1]. Available from: http://cyberbridge.mcb.harvard.edu/mitosis_5.html
70. Essential study partner: general & human biology [Internet]. Version 2.0. New York (NY): McGraw-Hill; c2001. [cited 2012 Feb 1]. Available from: http://www.mhhe.com/biosci/esp/2001_gbio/folder_structure/ge/m4/s1/index.htm
71. Protocols and applications guide: cell viability [Internet]. Madison (WI): Promega; c2012.
72. Li J, Yuan J. Caspases in apoptosis and beyond. *Oncogene*. 2008;27:6194-6206.
73. Mothersill C, Seymour CB. Cell-cell contact during gamma irradiation is not required to induce a bystander effect in normal human keratinocytes: evidence for release during irradiation of a signal controlling survival into the medium. *Radiat Res*. 1998;149(3):256-262.
74. Morgan WF, Sowa MB. Non-targeted bystander effects induced by ionizing radiation. *Mutat Res*. 2007;616:159-164.
75. Hei TK, Zhou H, Ivanov VN, Hong M, Lieberman HB, Brenner DJ, Amundson SA, Geard CR. Mechanism of radiation-induced bystander effects: a unifying model. *J Pharm Pharmacol*. 2008;60(8):943-950.
76. Zhou H, Ivanov VN, Gillespie J, Geard CR, Amundson SA, Brenner DJ, Zengliang Y, Lieberman HB, Hei TK. Mechanism of radiation-induced bystander effect: role of the cyclooxygenase-2 signaling pathway. *P Natl Acad Sci USA*. 2005;102(41):14641-14646.
77. Mothersill C, Stamato TD, Perez ML, Cummins R, Mooney R, Seymour CB. Involvement of energy metabolism in the production of 'bystander effects' by radiation. *Brit J Cancer*. 2000;82(10):1740-1746.
78. Dent P, Yacoub A, Fisher PB, Hagan MP, Grant S. MAPK pathways in radiation responses. *Oncogene*. 2003;22(37):5885-5896.
79. Wada T, Penninger JM. Mitogen-activated protein kinases in apoptosis regulation. *Oncogene*. 2004;23(16):2743-2975.

80. Greenhough A, Smartt HJM, Moore AE, Roberts HR, Williams AC, Paraskeva C, Kaidi A. The COX-2/PGE2 pathway: key roles in the hallmarks of cancer and adaptation to the tumour microenvironment. *Carcinogenesis*. 2009;30(3):377-386.
81. Chell S, Kaidi A, Williams AC, Paraskeva C. Mediators of PGE2 synthesis and signalling downstream of COX-2 represent potential targets for the prevention/treatment of colorectal cancer. *Biochim Biophys Acta*. 2006;1766(1):104-119.
82. Ivanov VN, Zhou H, Ghandhi SA, Karasic TB, Yaghoubian B, Amundson SA, Hei TK. Radiation-induced bystander signaling pathways in human fibroblasts: a role for interleukin-33 in the signal transmission. *Cell Signal*. 2010;22(7):1076-1087.
83. Kaidi A, Qualtrough D, Williams AC, Paraskeva C. Direct transcriptional up-regulation of cyclooxygenase-2 by hypoxia-inducible factor (HIF)-1 promotes colorectal tumor cell survival and enhances HIF-1 transcriptional activity during hypoxia. *Cancer Res*. 2006;66(13):6683-6691.
84. HTRF product and services catalog: PGE2 assay. Cisbio. Bedford (MA): c2009.
85. Shao J, Jung C, Liu C, Sheng H. Prostaglandin E2 stimulates the beta-catenin/T cell factor-dependent transcription in colon cancer. *J Biol Chem*. 2005;280(28):26565-26572.
86. Prostaglandin E2 assay [package insert]. Bedford (MA): Cisbio; 2008 Jul. Document reference: 62P2APEB rev01.
87. Hanahan D, Weinberg RA. The hallmarks of cancer. *Cell*. 2000;100(1):57-70.
88. Qiao L, Koutsos M, Tsai LL, Kozoni V, Guzman J, Shiff SJ, Rigas B. Staurosporine inhibits the proliferation, alters the cell cycle distribution and induces apoptosis in HT-29 human colon adenocarcinoma cells. *Cancer Lett*. 1996;107(1):83-89.
89. Millipore catalog: sterilizing-grade Durapore 0.1 μm and 0.22 μm hydrophilic cartridge filters. EMD Millipore. Billerica (MA): c2012.
90. Mothersill C, Seymour CB, Joiner MC. Relationship between radiation-induced low-dose hypersensitivity and the bystander effect. *Radiat Res* 2002;157(5):526-532.

91. Nugent SME, Mothersill CE, Seymour C, McClean B, Lyng FM, Murphy JEJ. Increased mitochondrial mass in cells with functionally compromised mitochondria after exposure to both direct γ radiation and bystander factors. *Radiat Res.* 2007;168(1):134-142.
92. Liu Z, Mothersill CE, McNeill FE, Lyng FM, Byun SH, Seymour CB, Prestwich WV. A dose threshold for a medium transfer bystander effect for a human skin cell line. *Radiat Res.* 2006;166(1):19-23.
93. Gow MD, Seymour CB, Byun SH, Mothersill CE. Effect of dose rate on the radiation-induced bystander response. *Phys Med Biol.* 2008; 53(1):119-132.
94. McBride HM, Neuspiel M, Wasiak S. Mitochondria: more than just a powerhouse. *Curr Biol.* 2006;16(14):R551-560.
95. Hashimoto K. Regulation of keratinocyte function by growth factors. *J Dermatol Sci.* 2000;24(1 Suppl):S46-50.
96. Barcellos-Hoff MH, Derynck R, Tsang ML, Weatherbee JA. Transforming growth factor-beta activation in irradiated murine mammary gland. *J Clin Invest.* 1994;93(2):892-899.
97. Ehrhart EJ, Segarini P, Tsang ML, Carroll AG, Barcellos-Hoff MH. Latent transforming growth factor beta1 activation in situ: quantitative and functional evidence after low-dose gamma-irradiation. *FASEB J.* 1997;11(12):991-1002.
98. Barcellos-Hoff MH, Dix TA. Redox-mediated activation of latent transforming growth factor-beta 1. *Mol Endocrinol.* 1996;10(9):1077-1083.
99. Lee CF, Liu CY, Hsieh RH, Wei YH. Oxidative stress-induced depolymerization of microtubules and alteration of mitochondrial mass in human cells. *Ann N Y Acad Sci.* 2005;1042:246-254.
100. Biade S, Stobbe CC, Chapman JD. The intrinsic radiosensitivity of some human tumor cells throughout their cell cycles. *Radiat Res.* 1997;147(4):416-421.
101. Baskerville C. Radium and radio-active substances: their application especially to medicine. Philadelphia (PA): Williams, Brown & Earle; 1905.
102. Castellone MD, Teramoto H, Williams BO, Druey KM, Gutkind JS. Prostaglandin E2 promotes colon cancer cell growth through a G_s-axin- β -catenin signaling axis. *Science.* 2005;310:1504-1510.

103. Chera S, Ghila L, Dobretz K, Wenger Y, Bauer C, Buzgariu W, Martinou JC, Galliot B. Apoptotic cells provide an unexpected source of Wnt3 signaling to drive hydra head regeneration. *Dev Cell*. 2009;17(2):279-289.
104. Fan Y, Bergmann A. Distinct mechanisms of apoptosis-induced compensatory proliferation in proliferating and differentiating tissues in the *Drosophila* eye. *Dev Cell*. 2008;14(3):399-410.
105. Lorimore SA, Kadhim MA, Pocock DA, Papworth D, Stevens DL, Goodhead DT, Wright EG. Chromosomal instability in the descendants of unirradiated surviving cells after alpha-particle irradiation. *P Natl Acad Sci USA*. 1998;95(10):5730-5733.
106. Sawant SG, Randers-Pehrson G, Geard CR, Brenner DJ, Hall EJ. The bystander effect in radiation oncogenesis: I. transformation in C3H 10T $\frac{1}{2}$ cells in vitro can be initiated in the unirradiated neighbors of irradiated cells. *Radiat Res*. 2001; 155(3):397-401.
107. Seymour CB, Mothersill C. Delayed expression of lethal mutations and genomic instability in the progeny of human epithelial cells that survived in a bystander-killing environment. *Radiat Oncol Invest*. 1997;5(3):106-10.
108. Kishikawa H, Wang K, Adelstein SJ, Kassis AI. Inhibitory and stimulatory bystander effects are differentially induced by Iodine-125 and Iodine-123. *Radiat Res*. 2006;165(6):688-94.
109. Seibert JA, Boone JM. X-ray imaging physics for nuclear medicine technologists: part 2. x-ray interactions and image formation. *J Nucl Med Technol*. 2005;33(1):3-18.